*Response to Reviewers:*

# Impacts of physical parametrization on prediction of ethane concentrations for oil and gas emissions in WRF-Chem

Maryam Abdi-Oskouei[1], Gabriele Pfister[2], Frank Flocke[2], Negin Sobhani[2], Pablo Saide[3], Alan Fried[4], Dirk Richter[4], Petter Weibring[4], and James Walega[4], Gregory Carmichael[1]

[1] Center for Global and Regional Environmental Research (CGRER), University of Iowa, Iowa City, Iowa, USA
[2] National Center for Atmospheric Research (NCAR), Boulder, Colorado, USA
[3] Department of Atmospheric and Oceanic Sciences, University of California Los Angeles (UCLA), Los Angeles, California, USA
[4] Institute of Arctic and Alpine Research, University of Colorado, Boulder, CO, USA

*Correspondence to*: Maryam Abdi-Oskouei (maryam-abdioskouei@uiowa.edu)

Dear Dr. Heini Wenli,

We thank you and the reviewers for the insightful comments, which have substantially improved the manuscript. We have revised the manuscript and addressed all comments raised by the reviewers. A version of the manuscript with highlighted modifications has been uploaded. Below you find our responses to the reviewer's comments. The reviewer's comments are shown in blue *italic*, our responses are shown in plain text, and the modified section of the manuscript is shown in **boldface**.

We do respect the comments raised by reviewers that there is a lack of conclusion on the best WRF-Chem configurations for this region. We highlighted the configurations we used for further emission sensitivity analysis in the conclusion section. However, we wanted to point out that the main goal of this paper is not to find an optimal WRF-Chem configuration but to quantify the sensitivity of modeled fields to different model configurations with significant implications for e.g. inverse modeling studies. We clarified this in the revised manuscript. Overall, changing one WRF-Chem model configuration may improve the performance of the model in some aspect of atmospheric chemistry and transport and may adversely impact another aspect. Thus, the "best configuration" can depend on the goal of the study. We have updated some of the figures and tables following the reviewers' comments to reduce clutter and convey information more effectively.

We appreciate your time and comments and look forward to your decision.

Best Regards,
Maryam Abdi-Oskouei, on behalf of all co-authors

Reviewer 1

General Comments

*R1:*
*In this article the authors test the influence of different configuration of the WRF-Chem model on the modeled ethane concentration. More specifically, they test three boundary layer schemes, two different dynamical boundary conditions, a scaling of the emission inventory, the effect of a free running simulation versus a re-initialised one and the impact of the horizontal resolution (12 km vs. 4 km). Investigation of the influence of different model configurations on the simulation results is an important issue, specificially for chemistry simulations where ensemble simulations can not be performed due to limitations in computing power and storage space. Unfortunately, the article stays at the surface of such investigations, solely comparing the differences of the simulations. Neither the authors go into the detail where these differences come from, nor do they draw any conclusions on the configuration, which should be chosen in future simulations.*
*This article requires at least major revisions. From my point of view a re-submission after a thorough revision would be the better way, as the article needs to provide much more substantial information to the reader.*

Response:
We highly appreciate the thorough review and helpful comments, which helped improve the quality of our manuscript. We revised the paper based on suggestions and comments. We have added more analysis and more detailed discussions throughout the text. A detailed reply to individual comments can be found below.

Major Points:
Sect. 2.2:
*R1:*
*With the horizontal resolution of 4 km x 4 km the smaller domain is well within the gap between the horizontal resolution where convection parametrisations are fully applicable and the convection resolving scale. The information, which convection parametrisations are still active in the 4 km domain (all or only deep convection) needs to be added to the model description. Note, that the influence of the choice of the convection parametrisation on the simulation result needs to be discussed (at least in the section where the influence of the horizontal resolution is investigated).*

Response:

We appreciate the point. We used the Grell-Freitas convective parametrization in all the simulations discussed in the paper. We have added information in text and in Table 1 regarding this scale-aware convective parametrization.
We have compared using Grell-Freitas convective parametrization with resolved convection in the inner (4 km x 4 km) domain but did not see significant impact on meteorology or ethane transport when we resolved convection in the inner domain compared to using a parameterized scheme. We did not include this analysis in the paper which focuses on physical parametrizations and set-ups with larger impacts on meteorological variables and ethane fields for in this study. Figure 1 shows measured and simulated diurnal cycles of meteorological variables at BAO averaged from August 1 to 15, 2014. The performance of the simulation with the Grell-Freitas convective parametrization is very similar to the simulation with resolved convection especially for temperature and RH (Similar results for 10m and 300m). Modeled ethane values along the flight paths are also very close for both simulations (Figure 2)

Text:
**The Morrison double-moment scheme was selected as the microphysics option and Goddard shortwave (Chou and Suarez, 1999) and RRTMG longwave radiation schemes (Iacono et al., 2008) were used as shortwave and longwave radiation parametrizations, respectively. The Grell-Freitas convection scheme (Grell and Freitas, 2014) was used as convective parametrization for both outer and inner domain. The inner domain falls into the "grey-scale" which means many of the assumptions used in convective parametrization will no longer be valid at this resolution. Grell-Freitas convection scheme is a stochastic scale dependent convective parametrization based on the method proposed by Arakawa et al. (2011) and is designed for domains with horizontal resolution up to a few kilometers. Comparisons between a simulation with resolved convection in the inner domain and a simulation using the Grell-Freitas convective parametrization showed similar performance in capturing transport (not shown). Thus, we used the Grell-Freitas convective scheme for both domains in all simulations to reduce the computation costs.**

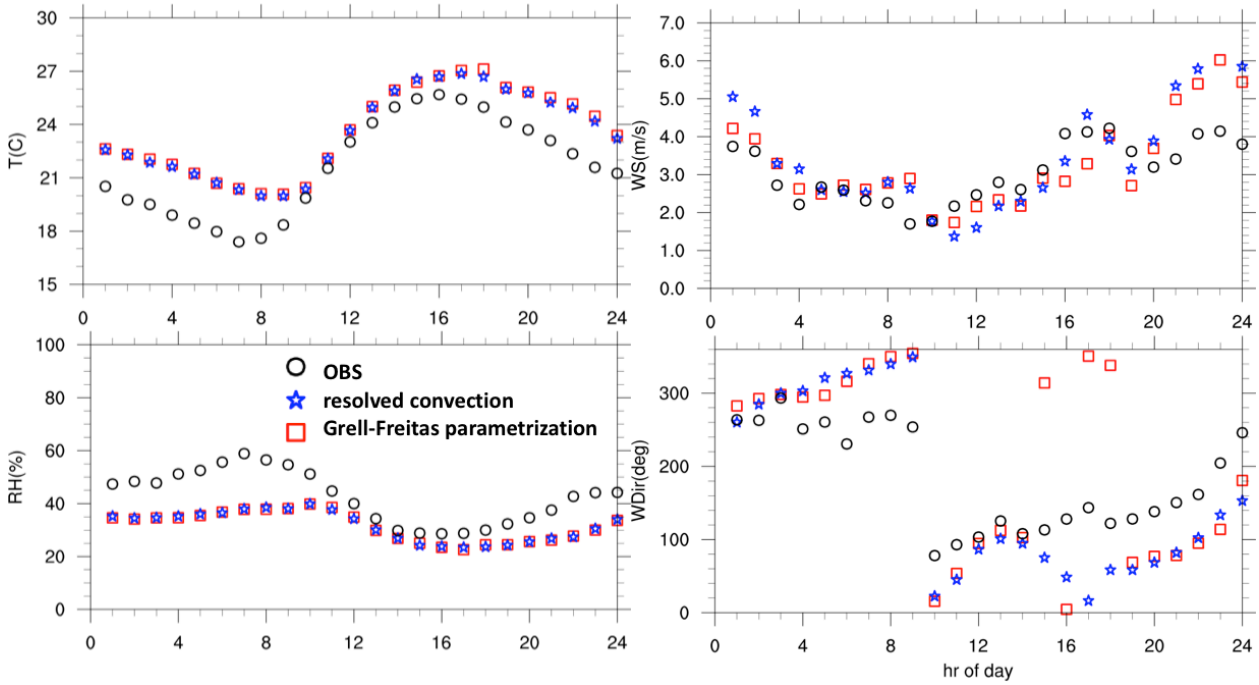


*Figure 1 Average diurnal cycle of meteorology variables for observation at BAO 100m, simulation with resolved convection and simulation with Grell-Freitas convective parametrization. Averages are calculated for August 1 to 15, 2014.*

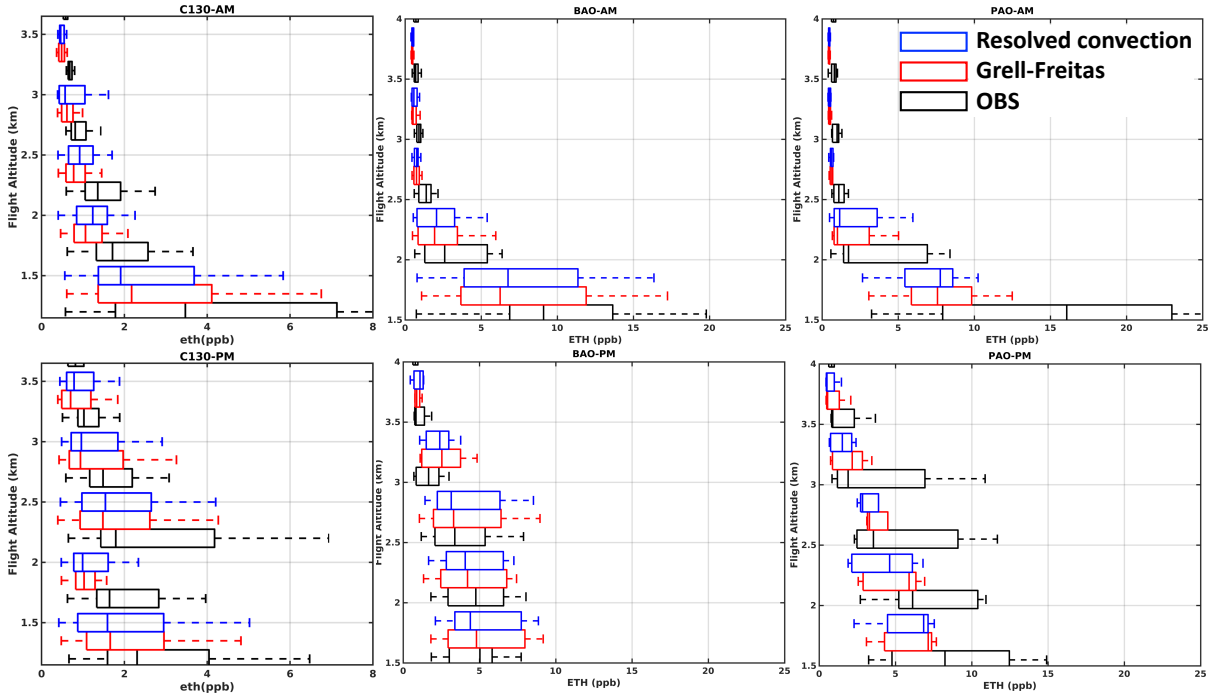


*Figure 2 measured and modeled (Grell-Freitas convective parametrization and resolved convection) ethane along C130 and P3-BAO and P3-PAO flights averaged for August flights.*

R1:
*Many informations on the chemical initial and boundary conditions (IC/BC) is missing: In which time interval are new BC data applied? Are the IC/BC data provided for this specific time interval/date? If yes, how do they fit to the two different dynamical boundary conditions used?*

Response:
Thank you. We have added more details regarding chemical IC/BC to the text.

Text:
Chemical boundary conditions from Monitoring Atmospheric Composition and Climate reanalysis (MACC**), available every 3 hours**, (Inness et al., 2013) and model output from RAQMS**, available every 6 hours,** (Natarajan et al., 2012; Pierce et al., 2007) were used as chemical boundary and initial conditions **in the simulations. The model outputs from these global models are specific to the simulation time (24 July 2014 and end on 18 Aug 2014) and are interpolated to the WRF-Chem domain and temporal resolution prior to starting the simulations.**

*R1:*
*How many species are included in the used chemical mechanism?*

Response:
We have added more information on the hydrocarbon lumped groups. Because of complexity of chemical mechanism, we ask the readers to refer to Stockwell (1997) for details on species and reactions in the RACM chemistry mechanism.

Text:
We selected the Regional Atmospheric Chemistry Mechanism chemistry using Earth System Research Laboratory (RACM-ESRL) (Stockwell, Kirchner, Kuhn, & Seefeld, 1997) coupled to the Modal Aerosol Dynamics Model/Secondary Organic Aerosol Model (MADE/SORGAM). **RACM includes 17 stable inorganics, 4 inorganic intermediates, 32 stable organic species, and 24 organic intermediates**. RACM_ESRL (Kim et al., 2009) is an updated version of the RACM mechanism and includes 23 photolysis and 221 chemical reactions (Ahmadov et al., 2015). **To reduce the computational costs, hydrocarbons with similar behavior are lumped together. For example, "HC3" in the RACM_ESRL mechanism includes alkanes such as propane, n-butane, isobutane, and acetylene (ethyne), and alcohols such as methanol and ethanol and "TOL" includes toluene and benzene. Ethane and methane are treated exclusively in the RACM_ESRL mechanism. More details regarding the reactions and lumping groups can be found in Stockwell et al., 1997.**

Sect. 3:

*R1:*

*The title of the section is wrong. So far it provides only a listing of differences between the sensitivity simulations (results), but almost always neither an explanation for the differences is provided, nor is discussed, what the consequences for future simulations are (discussion).*

Response:

We have added more discussions in this section and replaced some of figures to provide better explanations for each sensitivity test.

R1:

*Table SM4 (maybe SM3) should become part of the main paper.*

Response:

Thank you for the comment. However, we decided to only point out the important differences between 10m and 100m and 300m in the text and keep10m and 300m figures in the SM. This is mainly due to similarities between these three figures.

R1:

*Figure 2 might provide a nice overview over all simulations, but it does not provide enough information for the comparison of the respective sensitivity simlations. Simply because of the number of lines (different symbols) not all simulations are identifyable. Here the supplement could be used to pro- vide a figure 2 like figure individually for each of the tested parametrisations (one for the PBL schemes, one for (re-)init, one for IC/BC, one for horizontal resolutions and on for the different emission scenarios).*

Response:

Thank you. We have added figures with separated sub-figures for each test in the supplement (Figure SM 1 to 3)

R1:

*Figures SM1 / SM2: some as for Fig. 2 add individual panels for those comparisons referring to SM2 (PBL and re-init). Maybe add reference to SM 2 also for the other tested parametrisations?*

Response:

Thank you. We have added references. We have added figures with separated sub-figures for each test in the supplement (Figure SM 1 to 3)

R1:
*Figure 3 and Figure 4: Same as for Fig. 2. Use the supplement to provide the plots individually for each sensitivity study, where the lines are hardly distinguishable otherwise.*

Response:
We have changed Figures 3 and 4 to whisker plots to be more distinguishable.

R1:
*Figure 3/4: dashed and solid lines are not distinguishable in the legend.*

Response:
We have added figures with separated sub-figures for each test in the supplement (Figure SM 1 to 3)

R1:
*Why are the tables for the model performance only provided for BAO station? It would be nice to be able to compare the so far provided statistics to the other stations listed in the introduction.*

Response:
We focused mostly on BAO because we had measurements not only at the surface but also at two higher altitudes (100m and 300m). However, we have used wind measurements from stations across the domain in other figures (Figure 7 and Figure SM 4).

R1:
*Tab. (4/SM3/SM4)(3/SM2)Why do you show observations in a row? In this way you have to repeat the value for the observations for each simulation. Just show obs in an additional column! In this way you could easily combine Tables 4, SM 3 and SM 4 and Tables 3 and SM 2 in one landscape table, respectively.*

Response:
Thank you. We have added a column with the observations in Tables 3 and 4 and Tables SM 1, 2, 3, and 4. We still believe that adding BAO 10 and 300m to the tables and figures in the main text is not necessary.

R1:
*p. 7, 26./27.: Here I disagree, not "all" simulations show better skill at daytime. Better change "all simulations" to "most simulations".*

Response:
Thank you. We changed the text "all simulations" to "most simulations".

Text:
Overall, **most** simulations show skill in capturing diurnal cycles of wind speed and direction with better agreement with observations for daytime

R1:
*p.8, l. 15 / l. 29: I am missing any information why the AM and PM flights are different and any suggestions, why the modeled concentrations are off by such a hugh amount. If these points would be sufficiently discussed in the following subsections, it would be ok to refer to the following analysis, but so far, they are not discussed in the further analysis either.*

Response:
As mentioned in the paper the differences in AM and PM measured and modeled ethane is because of lower PBL height in the AM flight. We have added more details regarding the differences in subsection 3.1 and in each sensitivity test subsection.

Sect. 3.1
R1:
*as already mentioned, the difference between the PBL simulations hardly visible in Fig. 2. It would be good to have a figure showing only the three simulations and the observations in the supplement.*

Response:
Thank you. We added figures separated by the sensitivity test to the supplement (Figure SM 1-3)

R1:
*Why do you use different chemical initial and boundary conditions for the PBL sensitivity studies (MACC) in contrast to all other sensitivity studies (Table 2)? This courses additional differences you never discuss.*

Response:
Thank you. We highlighted in the text that we only saw negligible differences in ethane concentrations when comparing MACC and RAQMS boundary conditions. Simulations using MACC and RAQMS IC/BC predicted similar ethane values thus we did not include it as one of the sensitivity tests in the discussion. Figure 3 illustrates the measured and modeled (MACC and RAQMS IC/BC) ethane concentrations along C130, P3-BAO, and P3-PAO August flights.

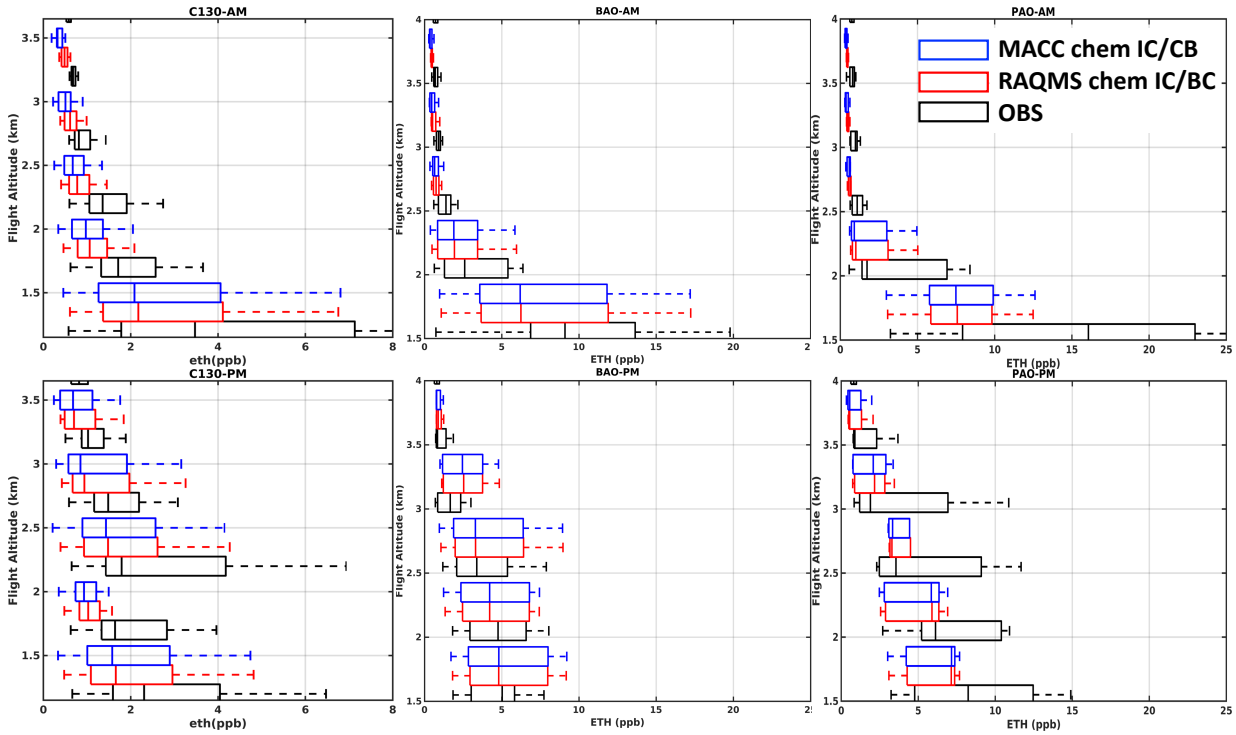


*Figure 3 measured and modeled (MACC and RAQMS Initial and Boundary Conditions) ethane along C130 and P3-BAO and P3-PAO flights averaged for August flights.*

Text:

**… Ethane concentrations showed no strong sensitivity to the two different chemical initial and boundary conditions (i.e., RAQMS and MACC) and is not discussed further.**

R1:

*p.9, l.16: Cite Figure SM1.*

Response:

Thank you. We cited the figure.

R1:

*Fig. 6: Article Text states "Fort-Collins-West (FCW)" , figure shows "FT".*

Response:

Noted

Thank you. We used "FC" throughout the paper

R1:

*p.9, l.26: For a non-specialist for boundary height measurements: Why is a quantitative comparison not possible?*

Response:

We removed the argument from the paper and only stated the different algorithm was used to estimated PBLH in the measurement.

Text:
Observed PBLH at the PAO, Fort Collins (FC), and Golden-NREL sites were retrieved from micro-pulse Lidar backscatter profiles **using Covariance Wavelet Transform (CWT)** (Compton et al., 2013).

R1:
*end of section: What are the consequences? Does the choice of PBL scheme matter or not? Which PBL scheme will you pick in future?*

Response:
We provide details on the impact of PBL scheme on NMB of ethane concentrations and the configurations we used for emission analysis in the conclusion section of the revised manuscript. As stated in the cover letter the main goal of this paper is not to find an optimal WRF-Chem configuration but to quantify the sensitivity of modeled fields to different model configurations with significant implications for e.g. inverse modeling studies.

Sect 3.2
R1:
*You change here from simulations driven by NCEP and MACC data, to simulations driven by ERAinterm and RAQMS data. Some information, why not the same driving data is used is missing here.*

Response:
Thank you for your comment. The simulations discussed in this section are based on the same meteorological and chemical IC/BC. The performance of NCEP and ERA-interim meteorological IC/BC is discussed in the section 3.4 Sensitivity to meteorological initial and boundary condition. As discussed in Figure 3 in this reply, we did not see a significant impact of chemical IC/BC on ethane fields. We added a sentence referring to Table 2 for details on model set-ups.

Text:
**Physical configurations and meteorological and chemical initial and boundary conditions are kept the same for these two simulations (Table 2).**

R1:
*p.10, l.28.: "in addition, Init 4 predicted higher wind speeds compared to Init5." And compared to Observations?*

Response:
Thank you. We changed the sentence.

Text:
In addition, Init4 predicted higher wind speeds compared to **BAO measurements (Figure 2) and** Init5.

R1:
*p.10, l.28.: Any suggestion, which simulation is more realistic?*

Response:
We provide details on the configurations we used for emission analysis in the conclusion. As stated in the cover letter the main goal of this paper is not to find an optimal WRF-Chem configuration but to quantify the sensitivity of modeled fields to different model configurations with significant implications for e.g. inverse modeling studies.

R1:
*p.10, l. 30/31 and 34 : Why does Init4 show the by far lowest ethane concentrations for C130-AM and all P3 flights? I thought the chemistry is not re-initialised in the same way as the meteorology?*

Response:
The difference is most likely due to higher wind speed in Init4. We added figure 8 to show the higher wind speed in Init4 across the domain.

Text:
When compared to C130-AM ethane concentrations (Figure 4), Init4 predicted the lowest ethane concentrations (a bias of -3.3 ppb and NMB of -63%) among all the simulations. **This is likely due to the high bias in wind speed in this simulation which resulted in lower concentrations of ethane (Figure 8).**

Sect. 3.3:
R1:
*The evaluation how much the simulation changes with respect to the meteorological initial and boundary data is meaningless without a comparison of the differences in the driving data themselves. How close are the reanalyses of ERA-Interim and NCEP-NFL to the observations in the area of interest?*

Response:

Thank you. We have compared WRF intermediate files prepared with ERA-Interim and NCEP-FNL model outputs in figure SM 6 and added discussion to the text.

Text:
**To prepare meteorological initial and boundary conditions from global models, WRF interpolates these outputs to the designed domains. Figure SM5 illustrates the differences between ERA-interim and NCEP-FNL model outputs interpolated to the outer domain at the lowest model level and averaged over August 1 to 15, 2014. Overall, the wind speed predictions by these two global models are very similar with slightly (less than 1 m/s) higher predictions by NCEP-FNL. ERA-interim and NCEP-FNL had larger discrepancies in temperature and relative humidity throughout the domain. Comparison with BAO observations (not shown) indicates similar performance for both models with somewhat lower temperature and higher relative humidity in ERA-interim compared to NCEP-FNL. These discrepancies did not have a large impact on temperature and relative humidity in the WRF-Chem simulation, however.** Figure 2 and Figure SM1-3 indicate that the performance of the two WRF-Chem simulations is comparable in capturing temperature and relative humidity **and better agreement with measurements during the day. This is because WRF-Chem only uses the global values as the initial and boundary values and resolves for atmospheric variables such as temperature and relative humidity in high resolution based on physical parametrizations set for the simulation**

R1:
*p. 11, l. 7-9: as far as I can deduce the correct lines from Fig. 2 and SM 1, both simulations overestimate temperature and underestimate moisture, where the ERA-Interim simulations is more off than the NCEP simulation.*

Response:
We modified the sentence for clarification to:

Text:
**Figure 2 and Figure SM1-3 indicate that the performance of the two simulations is comparable in capturing temperature and relative humidity with a better agreement with measurements during the day. Met5 had slightly higher temperature and lower relative humidity compared to Met6 and compared better to measurements especially during the night.**

R1:
*p.11, l. 14/15: I do not understand, I thought the Denver cyclone was not part of the analysis (top page 7). If this is just another "feature" and not the explanation of the huge differences in Met6*

*simulation for P3-PAO add this explanation and indicate by a line break, that you are talking about some- thing new.*

Response:
We removed the Denver cyclone discussion from the text to not deviate from the main goal and focus. Our analysis is focused on the time period Aug 1-15, 2014 and there were no occurrences of a Denver Cyclone during these two weeks.

R1:
*p. 11, l.19/20: Why do the simulations miss the event?*

Response:
We removed the Denver cyclone discussion from the text.

R1:
*p. 11, l.22 / SM4: Please show the absolute values (at least of one of the simulations) as well, otherwise absolute differences do not provide the full picture. This Figure should be part of the main paper. If you want to discuss the Denver cyclone, figure SM4 should be part of the main paper. But in this case, the analyses should go beyond the mere stating of the differences.*

Response:
Thank you. We removed the Denver cyclone discussion from the text

Sect 3.4:
R1:
*p. 11, l. 27: No, the domains are not run "independently" as the 4x4 km2 domain depends on the 12x12 km2 domain.*

Response:
We added details to clarify.

Text:
**This means that while the outer domain provides the boundary conditions to the inner domain, the higher resolution fields from the inner domain do not alter the outer domain fields.**

R1:
*p.11, l. 28./29.: What about temperature and relative humidity at PAO and WC tower?*

Response:
We have added more information on model performance in capturing wind in other stations across the domain because of its larger impact on ethane.

R1:
*p. 11, l. 28 /31: The different labels are hard to detect in the Figure 2 / SM2.*

Response:
Thank you. We added figures separated by the sensitivity test to the supplement (Figure SM1-3).

R1:
*p. 11, l. 31. This is only true at nighttime (Tab. 4 / SM 4). Cite the tables in the text.*

Response:
Thank you. We changed the sentence.

Text:
At 100m and 300m altitudes at BAO, the coarse domain predicted higher **nighttime** wind speed compared to the fine domain **and the measurements**.

Sect. 3.5:
R1:
*p. 12, l. 16: According to caption, Fig. 8 shows measurements. How can it be seen, that the model does not match the measurements? This is seen from Fig. SM 5, therefore this figure belongs in the article, not in the supplement. The phrase "as shown in Fig. 8a" is very irritating. It belongs in front of the "which", i.e., after the statement about high values of ethane.*

Response:
Thank you. We merged Figure 8 and Figure SM 5 and changed the sentence.

Text:
**Figure 10a and b illustrate** high values of ethane concentrations in the vicinity of oil and NG facilities which were not captured by the model resulting in low biases.

R1:
*as the comparison of the two emission scenarios is the topic of this subsection, SM 6 also belongs into the main paper. However, Fig. 9 could be part of the Supplement.*

Response:

Thank you for your comment. We agree that Figure SM 8 includes important information regarding the sensitivity of ethane to oil and gas emission. However, we believe that Figure 9 can provide more information about the background values and magnitude of underestimation. To keep the paper short, we had to put this figure in the supplement material.

R1:
*p.13, l.18/19: I do not think that you need an indicator for low emission rates. These are input by the emission inventory, thus this is aprior knowledge.?*

Response:
Thank you. Yes, emission rates are fed into the model through the emission inventory and the emission inventory is amongst the largest sources of uncertainties in the model. Here, we find a pronounced low model bias for xylene and toluene concentrations in the vicinity of oil and gas facilities. The model performance was not improved in the simulation with doubled oil and gas emission. This likely due to lower emission rates for these species compared to the measurements.

R1:
*Discussion of Fig. 10: Say more about the best fit lines (meaning of differences in intercepts and slope).*

Response:
We added more information about the differences between intercepts and slops.
Text:
Figure 10 illustrates the HC3 to TOL ratio measured along the C130 PM **limited to NFR region and altitudes below 2000m** and the corresponding model values. Figure 10a shows oil and NG influenced points with enhanced measured ethane (concentrations greater than 2 ppb). HC3 to TOL ratios in oil and NG influenced locations show inconsistency between measured **(HC3/TOL = 68)** and Em7 modeled ratios **(HC3/TOL = 22)** which was improved in the Em8 **(HC3/TOL = 40.9)**. However, doubling oil and NG emission still resulted in underestimations of HC3, TOL, and their ratios in this region. Figure 10b shows urban influenced points with low measured ethane (concentrations less than 2 ppb). Modeled HC3 to TOL **ratios (7.3 for Em7 and 8.9 for Em8)** in the urban influenced locations did not show large sensitivity to oil and NG emissions and agreed well with the measurements **(10.2). In both oil and NG and urban influenced regions models predicted lower than measured Y-intercepts which was not improved in Em8. Figure9c also confirms the low bias (about -2ppb) in background HC3 in the model. One reason for this offset can be underestimation in HC3 concentration in the boundary condition fields or leakage from the NG distribution system which was not captured in the model.**

R1:
*p. 13, l. 31/32: Where do I see these low biases (cite respective table / figure)*

Response:
Thank you. We have added reference to figure 9.

Text:
The low model bias for these species is more pronounced compared to the low model bias in ethane **(Figure 11).**

R1:
*What about cross evaluation? What changes with different chemical IC/BC? What is the influence of the PBL scheme for the higher emission scenario?*

Response:
Modeled ethane concentrations were not sensitive to the chemical IC/BC (Figure 3). Running all the sensitivity simulations with doubled oil and gas emissions is computationally very expensive and not much can be gained from these simulations. A simulation with doubled oil and gas emissions was conducted to assess the sensitivity of ethane to oil and gas emissions and will be later used to perform a variational inversion algorithm with the goal to find an optimal scaling factor for oil and gas emissions. If significant improvement is achieved with this method, we will use simulations discussed in this work to calculate the confidence level around optimal scaling factor.

Conclusion
R1:
*p. 14, l.10-22: In this section "NMB" and "NMB variability" is falsely used synonymously. It might be true that the inter-simulation variability of NMB might be usable "as a proxy for variability in the model performance caused by model configuration". But the percentages listed below are only the NMBs and not the inter-simulation variability of the NMB.*
*However, this paragraph again only lists (new) results (not even a discussion). Therefore it does not belong in the conclusion section.*

Response:
Thank you. We made sure that we did not falsely use NMB and NMB variability synonymously. We added NMB variability for each sensitivity test and each flight to Table 5. We added a concluding sentence on which configuration we used for further emission sensitivity analysis. We also made sure not to include any new results in the conclusion section.

Text:

**To further investigate the performance of the model in capturing oil and NG emissions in the NFR we used a similar domain set-up with 12 km x 12 km and 4 km x 4 km horizontal resolution for outer and inner domains, respectively, daily re-initialization of meteorological variables with ERA-interim model, and MYNN3 PBL scheme.**

R1:
*p. 14, l. 24 - p.15, l. 4: This section stays very in-concrete. All the species discussed here have a medium range lifetime. Nevertheless, the aspect of the influence of chemical initial and boundary conditions is completely left out.*

Response:
We added details regarding this issue in section 3.6.

Text:
Figure 10 illustrates the HC3 to TOL ratio measured along the C130 PM **limited to NFR region and altitudes below 2000m** and the corresponding model values. Figure 10a shows oil and NG influenced points with enhanced measured ethane (concentrations greater than 2 ppb). HC3 to TOL ratios in oil and NG influenced locations show inconsistency between measured **(HC3/TOL = 68)** and Em7 modeled ratios **(HC3/TOL = 22)** which was improved in the Em8 **(HC3/TOL = 40.9)**. However, doubling oil and NG emission still resulted in underestimations of HC3, TOL, and their ratios in this region. Figure 10b shows urban influenced points with low measured ethane (concentrations less than 2 ppb). Modeled HC3 to TOL **ratios (7.3 for Em7 and 8.9 for Em8)** in the urban influenced locations did not show large sensitivity to oil and NG emissions and agreed well with the measurements **(10.2). In both oil and NG and urban influenced regions models predicted lower than measured Y-intercepts which was not improved in Em8. Figure9c also confirms the low bias (about -2ppb) in background HC3 in the model. One reason for this offset can be underestimation in HC3 concentration in the boundary condition fields or leakage from the NG distribution system which was not captured in the model.**

R1:
*For me the final conclusion is missing: Based on this study, what has to be taken into account by setting up a WRF-Chem simulation? What would be the best WRF-Chem setup?*

Response:
We have added details regarding the WRF-Chem configurations we used for emissions sensitivity analysis. As stated in the cover letter the main goal of this paper is not to find an optimal WRF-Chem configuration but to quantify the sensitivity of modeled fields to different model configurations with significant implications for e.g. inverse modeling studies. Overall, changing one WRF-Chem model configuration may improve the performance of the model in

some aspect of atmospheric chemistry and transport and may adversely impact another aspect. Thus, the "best configuration" can depend on the goal of the study.

Minor points:

R1:

*From my point of view WRF-Chem is not a Chemical Transport Model (CTM). The term "transport" includes the fact, that the chemical substances are transported, but they do not feed back to the dynamics. WRF-Chem is a fully featured regional atmospheric chemistry model (RACM) which very well includes e.g., radiation and cloud feedback. Therefore I recommend to omit the term CTM with respect to WRF-Chem. I know that whole communities use this term wrongly, but this did not change the misconception of it.*

Response:

We removed the term CTM.

Text:

High resolution three-dimensional **atmospheric chemical transport models** can better capture the variability in meteorology and chemistry in different domains. **Paired with observations, these models** help evaluate the performance of emission inventories on high temporal and spatial scales and allow assessments of the impact of oil and NG activities on regional air quality.

R1:

*As this article is very WRF-Chem specific, it would be apropriate to name the model in the title of the article, e.g. "Impacts of physical parametrizations on pre- diction of ethane concentrations for oil and gas emissions a case study with WRF- Chem v3.6.1" or 'Impacts of physical parametrizations of WRF-Chem (v3.6.1) on prediction of ethane concentrations for oil and gas emissions"*

Response:

We changed the title.

Text:

Impacts of physical parametrization on prediction of ethane concentrations for oil and gas emissions **in WRF-Chem**

R1:

*Sect. 2.3: Add more information on how the emissions of 76 species are mapped to the species of the chemical mechanism used.*

Response:

Thank you. We have added Table SM 5 to the supplemental material. This table is copied from the subroutine (Fortran code) provided by NOAA to convert species in the NEI-2011 emission inventory to RACM and MADE/SORGAM chemical and aerosol mechanism.

Text:
**Table SM 5 includes details on the mapping table used to convert NEI-2011 species to RACM and MADE/SORGAM chemical and aerosol mechanism.**

R1:
*p.7, ll. 5-17: add the information, that these results will be discussed in more detail in the following subsections.*

Response:
Thank you. We have added subsection 3.1. Evaluation of overall model performance to better address this issue.

R1:
*p.7, ll. 19-34: add the information, that these results will be discussed in more detail in the following subsections.*

Response:
Thank you. We have added subsection 3.1. Evaluation of overall model performance to better address this issue.

R1:
*p. 10, l. 10: cite Table 5*

Response:
Thank you. We cited Table 5.

Text:
**Table 5 summarizes the mean and NMB for all simulations using C130 and P3 ethane measurements.**

R1:
*p. 10, l. 11: cite Fig. 4.*
Response:
We cited Figure 4.

Text:
**Similar to the C-130 comparison, Figure 4, the simulations did not capture the high ethane values measured during P3-BAO and P3-PAO spirals.**

R1:
*S1: Sums over i without any "i"s in the equations? What is "n"? IOA is introduced (also in the article) but never referenced.*

Response:
Thank you for your comment. We fixed the problem in equations. We removed IOA from tables.

Typos & CO
R1:
*p.4, l. 26: remove "Tables and Figures"*
Response:
We removed "Tables and Figures"

*p.5, l. 8: Did you consciously choose an abbreviation (4-MnERi) which is not included in Table 2 ?*
Response:
Thank you for your comment. No, this was a typo. We changed the example to 5-MnERi

*• p.5, l. 9: The abbreviation of the PBL scheme is (MYNN3)*
Response:
Thank you. We fixed the typo.

*• Through out the article (and in the figures) inconsistent abbreviations for Fort- Collings West are used (FC, FCW ...). This should be uniform.*
Response:
Thank you. We used FC through the text.

*• Fig. 5: Whatisthemeaningofthelineat41N?*
Response:
That is a state line between Colorado and Wyoming.

*It's the state line*
*• p. 9. l. 11: Cite SM 3/4 at end of sentence.*
Response:
Thank you. We cited the figures.

*• p. 9. l. 11: Fig. 5 does not "compare" anything, it "visualises", "shows", "depicts" ...*
Response:
We changed "compares" to "shows"

*• p. 9, l. 30 / 31: use full sentences: "PBL1, non-local PBL scheme" → " PBL1 using a non-local PBL scheme".*
Response:
We updated the sentence:
Text:
**The local PBL schemes (i.e.** PBL2 and PBL3) predict cooler and moister climates and lower PBLH, which indicates less vertical mixing.

*• p. 11. l. 20: A figure does not "compare" anything, it "visualises", "shows", "depicts" ...*
Response:
We changed "compares" to "shows"

*• p. 12, l. 14, Fig. 8: Limited to 200agl or 1500 m ?*
Response:
Thank you for the comment. We updated the sentence.
Text:
… the C130 PM measurements and bias limited to altitudes below **2000m.**

*• Fig. 8.: If these are measurements, what does "grids with more than 4 measurement points" mean?*
Response:
Thank you. We updated the caption.
Text:
Figure 8. Mean and mean bias for ethane concentrations (a and b), CO (c and d), HC3 (e and f), and TOL (g and h) along the C130 PM flights are limited to measurements below 2000m agl **and grids with more than 4 measurement points**. The outline of Denver county and the locations of BAO and PAO are marked on the underlying terrain map.

*• Fig. 10: Improve caption. The second sentence sound as if model vs. measure- ments are plotted.*
Response:
Thank you. We updated the caption.
Text:

Figure 10. Scatter plot of HC3 vs. TOL concentrations along the C130 PM flights limited to measurements in the NFR and below 2000m altitude. Plot (a**) shows HC3 vs. TOL (when measured ethane is greater than 2ppb) for measurements and the corresponding model values. Plot (b) shows HC3 vs. TOL (when measured ethane is less than 2ppb) for measurements and the corresponding model values**. Grey circles represent measurements, red diamonds represent the Em7 (base emissions), and blue circles represent Em8 (perturbed emissions). Grey, Red and Blue lines show the best fit using least square linear regression method for observations, Em7 and Em8, respectively.

*• Fig. 10 : give parameters of best fit line.*
Response:
We added parameters to the figure

*• Tab. 5: Is the NMB for PBL3 P3-BAO really 0 ?*
Response:
Yes, with 1 decimal point of ethane (ppb).

*• SM2: caption: state that "surface winds" are shown.*
Response:
We added information regarding the height of the measurement.

*• Table SM4: omit line breaks for init5*
Response:
We updated the Table.

*• Fig. SM3: What is surface ethane: ethane in the lowest model layer?*
Response:
Yes, surface ethane concentrations are represented by ethane fields at the lowest model layer which ranges from about 0 to 20m altitude agl.

# Reviewer 2

Thank you very much for your helpful comments and suggestions. Please find replies to individual comments below.

## Major Comments

*R2:*
*Aim, approach and conclusions: The aims of the presented study are somewhat twofold. 1) evaluate the chemistry-transport model and 2) draw some preliminary conclusions on the emissions from oil and gas extraction in the Northern Front Range Metropolitan area (NFRMA). In general, I agree with the authors that a transport model needs to be validated before it can be used for inverse modelling purposes (here emission estimation). However, these two subjects are somewhat mixed together in the study, since one main evaluation parameter of the model system is the ethane concentration, which strongly depends on the emissions, which one finally would like to determine. The manuscript would gain in significance if these two subjects (transport model performance and emissions from oil and gas) could be separated more clearly in the presentation of the results. Instead of evaluating model performance for ethane another model tracer (e.g. carbon monoxide) should be given more attention during the evaluation part of the manuscript. Since carbon monoxide is largely unrelated to the oil and gas emissions and its emissions are otherwise relatively well know, one should be able to distinguish, which model configuration is best suited for tracer transport simulations. Only afterwards, the less well known ethane emissions should be discussed.*

Response:
We appreciate the comment on using another tracer to separate the discussion on transport from oil and gas emissions. However, we found ethane to be the best tracer to study the transport of oil and gas emissions in the region. Besides the complex transport patterns in the region, there are multiple emission sources which makes finding an effective tracer very complicated. For example, CO can be released from any combustion sources such as cars, power plants, and oil and gas extraction activities. Also, it is sensitive to the background value. As discussed in the paper, high concentrations of CO were measured downwind of Denver as of well as oil and gas facilities. Comparison with modeled CO showed overestimation of CO over Denver and underestimation over oil and gas facilities. The oil and gas sector is the only notable source for ethane in the NFR which can help us attribute the errors in emissions to this sector. Ethane concentrations in the NFR also do not show any notable influence from transport from outside the NFR.

*R2:*

*In this context another question arises concerning the application of the full chemistry version of WRF-CHEM in the sensitivity runs. A passive tracer setup (as available in WRF-CHEM) would have been sufficient to carry out the sensitivity runs as well. Only the discussion including shorter lived VOCs really grants running the complete model. This is more a comment for future sensitivity simulations than for the current manuscript. However, since the complete chemistry model was run, it would also be interesting to have a look at a secondary pollutant (e.g., ozone) and how it reacts to the emission variations in the final sensitivity experiments. Most likely ozone observations were available from all flight campaigns and additionally surface sites. The model-observation mismatch for ozone might deliver another hint towards the suspected underestimation of emissions from gas and oil extraction.*

Response:
The FRAPPÉ and DISCOVER-AQ dataset includes comprehensive ground-based and airborne measurements of ozone and ozone precursors. Discussion on ozone predictions and ozone production in the model is complicated by uncertainties in the anthropogenic and biogenic emissions estimates and the complexity of the transport in the region. We decided to focus in this paper on the meteorology and the/transport and magnitude of primary oil and gas emissions as trying to understand all uncertainties would be too large a topic for a single manuscript.

*R2:*

*Finally and coming back to the beginning, the conclusions of the paper should give more emphasise to the finally selected model configuration. Which is the best configuration, which parameters were most important to change, and why does the change make sense? Without such a recommendation (although not necessarily valid for other study areas or periods) the whole presentation of sensitivity results remains of no avail for the reader who wants to find concrete hints for setting up his/her own simulations. Right now the conclusion only summarises all sensitivity simulations together, although there were clear performance difference for some of the runs (PBL1 vs PBL3, free-run vs re-ini, etc). These are important details of the model setup that should be more easily accessible when browsing the paper.*

Response:
We have added conclusions on the model configurations we used for the emissions sensitivity analysis and highlighted the parameters we found most important. As we stated in the cover letter: The main goal of this paper is not to find an optimal WRF-Chem configuration but to quantify the sensitivity of modeled fields to different model configurations with significant implications for e.g. inverse modeling studies. We clarified this in the revised manuscript.

Overall, changing one WRF-Chem model configuration may improve the performance of the model in some aspect of atmospheric chemistry and transport and may adversely impact another aspect. Thus, the "best configuration" can depend on the goal of the study.

R2:
*Page 2, Line 9: From the context and my own knowledge of emissions from the oil and gas sector it remains unclear why NOx emissions should play a major role in the extraction process. Is it due to fossil-fuel operated machinery (compressors, pumps, etc) or due to flaring? In the discussion of the model results there is no more mentioning of NOx either. Was it not observed on-board the aircraft?*

Response:
Thank you for your comment. We have added details about the NOx emissions from the oil and gas sector. NOx was measured at ground level and on-board the aircraft during FRAPPÉ and DISCOVER-AQ. Because of the complexity in estimating NOx emissions due to its short life-time and having multiple sources other than the oil and gas sector we did not include it in this paper. However, we have included multiple references that studied NOx and ozone concentrations in the Northern Front Range during FRAPPÉ and DISCOVER-AQ.

Text:
With the rapid increase in the unconventional oil and NG production, higher than expected levels of greenhouse gases, specifically methane, and air pollutants such Non-Methane Hydrocarbons (NMHC) and NOx **(from compressors, pneumatic devices, trucks, and other equipment using fossil fuel (Allen, 2016; Olaguer, 2012))** have been observed in some places in vicinity of oil and NG facilities.

R2:
*P3, first paragraph: Others have used WRF-CHEM already for 'inverse modelling' of emissions from oil and gas extraction. The study by Barkley et al. (2017), which used WRF-CHEM for CH4 emission estimation (although not with full chemistry), should be mentioned as well. Either when mass balance approaches to estimate emissions are discussed or more general in the discussion of the results.*

Response:
Thank you. We added the reference on introduction.

Text:
**Paired with observations and using inverse modeling techniques, these models** help evaluate the performance of emission inventories on high temporal and spatial scales **(Barkley et al.,**

**2017; Cui et al., 2014, 2017)** and allow assessments of the impact of oil and NG activities on regional air quality.

R2:
*Subsection 2.1: The presentation of the observations is lacking any reference to the applied measurement techniques, data quality, etc. Some of this information is given later when the results are presented, but it should actually be presented in this subsection. For the more involved measurements (VOC concentrations) it would also be nice to learn a bit about observation uncertainties before comparing with model results.*

Response:
Thank you for your comment. We moved the information about the ethane measurements to subsection 2.1.

R2:
*P4,L30: The kind of VOC lumping used in RACM should be mentioned. Is ethane treated explicitly? How many chemical species are present?*
Response:
Thank you we added details on the VOC lumping to the text.

Text:
**To reduce the computational costs hydrocarbons with similar behavior are lumped together. For example, "HC3" in the RACM_ESRL mechanism includes alkanes such as propane, n-butane, isobutane, and acetylene (ethyne), and alcohols such as methanol and ethanol. "TOL" includes toluene and benzene. Ethane and methane are treated exclusively in the RACM_ESRL mechanism. More details regarding the reactions and lumping groups can be found in Stockwell et al., 1997."**

R2:
*P5,L21 and elsewhere: Since it was mentioned above (P5,L10) that the simulation ID according to table 2 would be used throughout the text to identify the sensitivity simulations, I see no need to give the simulation name here as well. All these abbreviations will only confuse. All figures also contain a mix of names and identifiers that are not according to the ID. This should be unified, so that the reader only has to follow one set of abbreviations.*
Response:
Thank you. We unified the IDs used in figures and in the text. Some of the simulations such as 5-MnERi were used in multiple sensitivity tests. To avoid confusion, we used IDs in all figures.

R2:
*P6, 1st paragraph: What is the rational for this re-initialisation? The model domain is relatively small. Shouldn't the BCs dominate anyway? In this context it should also be mentioned why no meteorological data assimilation was run for WRF, which probably would have reduced the spread in the sensitivity tests significantly.*

Response:
Thank you for your comment. The outer domain covers most part of the CONUS with 12 km x 12 km resolution and receives BC from the global re-analysis. The outer domain provides BCs for the inner domain (covering Colorado and Utah) with the inner domain not having any feedback on the outer domain. Thus, we believe that BC do not dominate at least in the inner domain. Data assimilation and measurements are used to produce global models used for re-initialization of the model. By re-initializing meteorological field every 24 hours using re-analysis products from global models we decided not to use any nudging (data assimilation) in our simulations. One can test and compare the model performance with different nudging systems vs. re-initialization. However, given the complex terrain in the NFR and the limited amount of measurements nudging may not necessarily add strong constrains.

R2:
*P7, L5: 'average error'. Should this be absolute error, which would actually fit the definition in the supplement.*
Response:
Thank you. We changed "averaged" to "absolute" in the text and in the supplemental material.
Text:
For quantitative comparison between the simulations, we used statistical measures including correlation coefficient (R), root mean square error (RMSE), mean **absolute** error (MAE), mean bias (MB), normalized mean bias (NMB), and index of agreement (IOA).

R2:
*P7, L6: Although the supplement provides the definition of the comparison parameter 'index of agreement', it would be nice to give a short interpretation of its benefits and expected value range for a well performing simulation. Furthermore, values of IOA are presented in a table, but never discussed in the text. Something that is true for other comparison parameters as well. If they are shown in the table a short description and interpretation in the text should also be given.*
Response:
Thank you. We removed IOA from tables to focus on statistics that was used in the text.

R2:
*P7, L9: I feel like one could start a new subsection here (after 'model values') that deals with the general results. Everything before is an introduction to the results, now the first real results are shown.*
Response:
Thank you for your comment. We added a subsection (3.1. Evaluation of overall model performance) in this section.

R2:
*P7, L25: Maybe I missed this somewhere else, but at which altitude were the measurements at WC tower and PAO taken?*
Response:
Altitudes were added.

R2:
*P8, L12 and 8ables or figures? If yes a cross-reference to the figure would be useful, if not this should also be mentioned (e.g. adding 'not shown'). Otherwise the reader will try to confirm this information in one of the figures.*
Response:
Thank you. We cited Table 5 here.

Text:
Lower concentrations of ethane were measured during the PM flights compared to AM flights because of the higher PBLH and stronger vertical mixing in the afternoon. **Table 5 summarizes the mean and NMB for all simulations using C130 and P3 ethane measurements.** In all simulations, the ethane concentrations are under-predicted by up to 3.3 ppb (NMB ranges between -63% to -42%) for the C130 AM flights and up to 1.7 ppb (NMB ranges between -47.6% to -29.5%) for the C130 PM flights.

R2:
*P8, L31ff: It is argued that the model 'represents the profile shape [...] well.' I don't agree with this completely and for all cases. For the afternoon observations, where C130 and BAO observations actually show relatively low values at the bottom of the profile, most model runs still show a smoothly increasing concentration towards the surface. What is the potential reason for the observed profile shapes and what does the model miss here?*
Response:
Thank you. We have changed Figure 3 and 4 to whisker plots at each altitude bin to convey more statistical information. We have changed the sentence discussing the vertical profile shape.

Text:
**While the model shows difficulty in representing the absolute magnitude in ethane concentrations in all simulations at lower altitudes, most simulations capture the changes in variance of ethane concentrations from lower to higher altitudes well especially for the C130 and P3 BAO flights.**

R2:
*P9, L26: It is argued that a 'quantitative comparison between model and measurement [of PBLH] is not possible'. I don't agree. It depends on the situation, but during the day the agreement between a lidar-derived PBLH and one derived from temperature profiles should actually be pretty good as long as you have an aerosol-laden PBL, which is most likely the case in the American South-West. See also Collaud Coen et al. (2014).*
Response:
We removed the argument from the paper and only stated the different algorithm was used to estimated PBLH in the measurement.

Text:
Observed PBLH at the PAO, Fort Collins (FC), and Golden-NREL sites were retrieved from micro-pulse Lidar backscatter profiles **using Covariance Wavelet Transform (CWT)** (Compton et al., 2013).

R2:
*Figure6: I suggest to extend this figure for all other sensitivity simulations as well. Next to wind speed, PBLH is the most important dispersion parameter on local to regional scale. The use of the same turbulence scheme in all other sensitivity runs will not necessarily lead to the same PBL heights. For example the two different BC runs are also likely to result in different PBL structures.*
Response:
Thank you. In Figure 3 we plotted cross sections of modeled ethane for all sensitivity tests at PAO averaged from Aug 1 to 10, 2014 and measured PBL height by Lidar backscatter. This figure can help us compare the diurnal variation of measured PBL height and its impact on ethane vertical distribution.

R2:
*P10,L7ff: This paragraph should include a short description of the changes in profile shape for the different PBL runs. The interesting part is that with PBL2 and PBL3 and although these runs are supposed to produce more realistic PBL heights, the increase in PBL concentrations compared to PBL1 is opposite to what the observations suggest (Fig 3 and 4). That is: afternoon concentrations increased from PBL1 to PBL2 and PBLE3 below a certain altitude, but the resulting profile shape is then even less in line with the observations.*

Response:
Thank you for the comment. We replaced figures 3 and 5 with whisker plots at each altitude bin. Figure 3 shows a faster growth in morning PBL in PBL1 compared to PBL2 and PBL3. This resulted in higher concentrations of ethane in the morning to noon period at higher altitudes (0.5 to 2 km). We added this discussion in the paper.
Text:
**On average PBL1 predicted higher ethane concentrations during AM flights at lower altitudes compared to PBL2 and PBL3 (Figure 3). Faster evolution of morning PBL and stronger vertical mixing in PBL1 lofted pollutants (including ethane) higher into the atmosphere in the morning (Figure 6). The rapid growth of morning PBL in PBL1 resulted in higher concentration of ethane at higher altitudes (0.5 to 2 km) compared to PBL2 and PBL3.**

R2:
*P11,L14ff: In the beginning of the results section it is mentioned that the Denver cyclone period was removed from the analysis. Why is it presented here again? Either this part should be moved to the beginning of the results section when justifying why the phase was excluded from the analysis or it should be mentioned here again which period is really contained in the figures.*

Response:
We removed the Denver cyclone discussion from the text to not deviate from the main goal and focus. Our analysis is focused on the time period Aug 1-15, 2014 and there were no occurrences of a Denver Cyclone during these two weeks.

R2:
*Section 3.5: Megan biogenic emissions are mentioned in the Table but not in the text. What is their significance for this sensitivity run and overall for this study? Did Megan predict significant emissions of ethane or HC3? Probably not!*

Response:
Thank you. We added a sentence to the text.

Text:
We used the Model of Emissions of Gases and Aerosols from Nature (MEGAN) for biogenic emission in all simulations (Guenther et al., 2012). **Ethane does not have a significant biogenic source (Yacovitch et al., 2014); thus, we did not assess the impact of biogenic emissions in this study.**

R2:

*P12,L27f: Not surprisingly, the measurements did not differ for the two different simulations! Should it be 'simulated CO'?*

Response:
Thank you. We corrected the sentence.

Text:
CO is mostly emitted from combustion processes and is released from many different source sectors. **Figure10.c shows CO enhancements over both Denver and oil and NG facilities.**

R2:
*P13,L21ff: In the discussion of Figure 10 it should be mentioned that for the longer-lived HC3 one should/could have removed a background concentration. The presentation is still valid if only the slopes/ratios are discussed and background did not change over the domain of interest. The latter should be commented on.*
*P13,L26f: Following up on the last comment, it most likely is not recently emitted HC3 that leads to elevated levels but background levels. The alkanes contributing to HC3 are relatively long-lived and the HC3 concentration at the domain boundaries is most likely a few ppb. This could be easily checked in the model fields. In contrast TOL is relatively short-lived, so BC concentration are probably close to zero.*

Response:
Thank you. We have added this to the discussion.

Text:
Figure 10 illustrates the HC3 to TOL ratio measured along the C130 PM **limited to NFR region and altitudes below 2000m** and the corresponding model values. Figure 10a shows oil and NG influenced points with enhanced measured ethane (concentrations greater than 2 ppb). HC3 to TOL ratios in oil and NG influenced locations show inconsistency between measured **(HC3/TOL = 68)** and Em7 modeled ratios **(HC3/TOL = 22)** which was improved in the Em8 **(HC3/TOL = 40.9)**. However, doubling oil and NG emission still resulted in underestimations of HC3, TOL, and their ratios in this region. Figure 10b shows urban influenced points with low measured ethane (concentrations less than 2 ppb). Modeled HC3 to TOL **ratios (7.3 for Em7 and 8.9 for Em8)** in the urban influenced locations did not show large sensitivity to oil and NG emissions and agreed well with the measurements **(10.2). In both oil and NG and urban influenced regions models predicted lower than measured Y-intercepts which was not improved in Em8. Figure9c also confirms the low bias (about -2ppb) in background HC3 in the model. One reason for this offset can be underestimation in HC3 concentration in the**

**boundary condition fields or leakage from the NG distribution system which was not captured in the model.**

Technical comment

R2:
*P2,L25: 'Thousand Cubic Feet' probably supposed to be 'Million Cubic Feet'. Also, I am not sure if ACP allows US customary units.*
Cubic meter was added to the text. MCF is short for thousand cubic feet.

R2:
*P9,L22 and elsewhere: 'Fried, 2000' is not the correct formatting. Please refer to the ACP guidelines.*
Response:
Thank you. We corrected the format.

# Impacts of physical parametrization on prediction of ethane concentrations for oil and gas emissions in WRF-Chem

Maryam Abdi-Oskouei[1], Gabriele Pfister[2], Frank Flocke[2], Negin Sobhani[2], Pablo Saide[3], Alan Fried[4], Dirk Richter[4], Petter Weibring[4], and James Walega[4], Gregory Carmichael[1]

[1] Center for Global and Regional Environmental Research (CGRER), University of Iowa, Iowa City, Iowa, USA
[2] National Center for Atmospheric Research (NCAR), Boulder, Colorado, USA
[3] Department of Atmospheric and Oceanic Sciences, University of California Los Angeles (UCLA), Los Angeles, California, USA
[4] Institute of Arctic and Alpine Research, University of Colorado, Boulder, CO, USA

*Correspondence to*: Maryam Abdi-Oskouei (maryam-abdioskouei@uiowa.edu)

**Abstract.** Recent increases in the Natural Gas (NG) production through hydraulic fracturing have called into question the climate benefit of switching from coal-fired to natural gas-fired power plants. Higher than expected levels of methane, Non-Methane Hydrocarbons (NMHC), and NOx have been observed in areas close to oil and NG operation facilities. Large uncertainties in the oil and NG operation emission inventories reduce the confidence level in the impact assessment of such activities on regional air quality and climate, as well as development of effective mitigation policies. In this work, we used ethane as the indicator of oil and NG emissions and explored the sensitivity of ethane to different physical parametrizations and simulation set-ups in the Weather Research and Forecasting with Chemistry (WRF-Chem) model using the U.S. EPA National Emission Inventory (NEI-2011). We evaluated the impact of the following configurations and parameterizations on predicted ethane concentrations: Planetary Boundary Layer (PBL) parametrizations, daily re-initialization of meteorological variables, meteorological initial and boundary conditions, and horizontal resolution. We assessed the uncertainties around oil and NG emissions by using measurements from the FRAPPÉ and DISCOVER-AQ campaigns over the Northern Front Range Metropolitan Area (NFRMA) in summer 2014. The sensitivity analysis shows up to 57.3% variability in normalized mean bias of the near-surface modeled ethane across the simulations, which highlights the important role of model configurations on the model performance and ultimately the assessment of emissions. Comparison between airborne measurements and the sensitivity simulations indicates that the model-measurement bias of ethane ranged from -14.9 ppb to -8.2 ppb (NMB ranged from -80.5% to -44%) in regions close to oil and NG activities. Under-prediction of ethane concentration in all sensitivity runs suggests an actual under-estimation of the oil and NG emissions in the NEI-2011. Increase of oil and NG emissions in the simulations partially improved the model performance in capturing ethane and lumped alkanes (HC3) concentrations but did not impact the model performance in capturing benzene, toluene, and xylene which is due to very low emission rates of these species from oil and NG sector in the NEI-2011.

## 1. Introduction

Recent advances in the unconventional Natural Gas (NG) production technology (hydraulic fracturing) have resulted in economical access to NG reserves in deep shale formations and a 36% rise in US NG production from 2005 to 2014 (Lyon, 2015). Increase in the NG production, decrease in the NG price, and environmental advantages of NG-fired power plants over coal-fired power plants have made NG an important competitor for coal in the electricity generation sector. In 2015, NG and coal each had a 33% share in the electricity generation in the US. It is predicted that NG's share in electricity generation will grow 1.5% every year (Energy information administration of US Department of Energy., 2016; U.S. Energy Information Administration, 2016). With the rapid increase in the unconventional oil and NG production, higher than expected levels of greenhouse gases, specifically methane, and air pollutants such Non-Methane Hydrocarbons (NMHC) and $NO_x$ (from flaring or compressors, reboilers, pneumatic devices, trucks, and other equipment using fossil fuel) (Allen, 2016; Olaguer, 2012) have been observed in some places in vicinity of oil and NG facilities. The high concentrations of these chemicals measured in many studies at different scales and regions suggest that official emission inventories (e. g. Greenhouse Gas Inventory (GHGI) and Emission Database for Global Atmospheric Research (EDGAR)) fail to capture the magnitude of emissions from unconventional extraction activities (Brandt et al., 2014). The underestimation of emission inventories has raised concerns regarding the climate implications of promoting NG as the "bridge fuel" (Alvarez et al., 2012; Howarth et al., 2011; Levi, 2013; McJeon et al., 2014), and its impacts on the air quality and public health (Halliday et al., 2016; McKenzie et al., 2012). Additionally, Methane and NMHC emitted from the oil and NG sector can degrade regional air quality and contribute to ozone formation on regional and global scales (Helmig et al., 2016). Outdated Emission Factors (EF), super-emitters in the production systems, and rapid growth in the production facilities are some of the reasons for the underestimation (Brandt et al., 2014; Lyon, 2015; Zavala-Araiza et al., 2015).

The Colorado Northern Front Range (NFR), including the Denver metropolitan area, is located between the Rocky Mountains and the High Plains with a total population of about 4.8 million. In 2007, a large region of the NFR was declared in nonattainment of the National Ambient Air Quality Standard (NAAQS) for 8h average ozone. Major sources of pollutants in this area are vehicle emissions, oil and NG operation, agriculture and feedlots, and power plants. In the past years, oil and NG development has increased drastically in the NFR. NG production in Weld County has increased from $55.8\times10^6$ $m^3$ ($1.97\times10^6$ Thousand Cubic Feet (MCF)) to $181.8\times10^6$ $m^3$ ($6.42\times10^6$ MCF) from 2004 to 2016. The Wattenberg gas field in Weld County is close to populated regions and has the highest well density in the NFR with more than 25,000 active NG wells (Colorado Oil and Gas Conservation Commission, 2017). In the NFR, measured NMHCs are 18-77 times greater than the regional background as determined from the NOAA flask network (Thompson et al., 2014). High levels of NMHC can cause health concerns at regional scales and can contribute significantly to the ozone pollution in the region (Cheadle et al., 2017; Gilman

et al., 2013; McDuffie et al., 2016; Pétron et al., 2012; Pfister et al., 2017b; Thompson et al., 2014). Using box models constrained with observations, McDuffie et al. (2016) estimated that NFR oil and NG activities contribute ~50% to the regional Volatile Organic Compound (VOC) OH reactivity and 20% to the regional photochemical ozone production.

Mass balance approach methods have been widely used to estimate the emissions from oil and NG activities (Conley et al., 2016; Karion et al., 2015; Peischl et al., 2016; Pétron et al., 2012; Smith et al., 2015). This method cannot provide details on the spatial and temporal variability of emissions and has limitations in domains with complex atmospheric transport such as the NFR. High resolution three-dimensional atmospheric chemical transport models can better capture the variability in meteorology and chemistry in different domains. Paired with observations and using inverse modeling techniques, these models help evaluate the performance of emission inventories on high temporal and spatial scales (Barkley et al., 2017; Cui et al., 2014, 2017) and allow assessments of the impact of oil and NG activities on regional air quality. Ahmadov et al. (2015) used the Weather Research and Forecasting Model with Chemistry (WRF-Chem) to study high ozone episodes and emission reduction scenarios in the Uintah Basin. Their results show a strong underestimation of methane and VOC emissions in the National Emission Inventory 2011 (NEI-2011).

WRF-Chem provides users with different dynamical, physical, and chemical schemes (Grell et al., 2005; Skamarock et al., 2008). These choices can impact the performance of the model, specifically in regions with complex transport patterns (Saide et al., 2011). In order to assess the performance of emission inventories, it is critical to address the uncertainties derived from model configurations on simulated concentration fields. The goal of this study is to quantify the impact of WRF-Chem configurations on predicting the oil and NG emissions in the NFR. VOCs in the NFR have shown a clear source signature associated with oil and NG activities (Gilman et al., 2013; Pétron et al., 2014). Diverse air pollution sources and complex metrological patterns due to mountain-valley circulation, high elevation, and harsh terrain are some of the challenges for air quality modeling in this area. We use ethane, which has a simple chemical cycle and a lifetime of about two months, as a tracer for oil and NG (Helmig et al., 2016). The model and emission inventory performance are evaluated by comparing meteorological parameters as well as ethane and VOC concentrations to surface and airborne measurements. We explore the sensitivity of the modeled transport and ethane concentrations to different WRF-Chem physical parametrizations and set-ups. This work will be followed by development of an inverse modeling technique to constrain the oil and NG emission rates by calculating optimal scaling factor for the emission inventory. Simulations discussed in this study will be used to calculate the variability of the optimal scaling factor. To inform not only about the absolute magnitude in the ethane emissions but to further explore the feasibility to constrain other trace gas oil and NG emissions, we investigate CO and VOC emission estimates from oil and NG sector and VOC ratios in the observations and the model.

## 2. Method

### 2.1. Aircraft and ground-based observations

The National Science Foundation/National Center for Atmospheric Research (NSF/NCAR) Front Range Air Pollution and Photochemistry Éxperiment (FRAPPÉ) and National Aeronautics and Space Administration (NASA) Deriving Information on Surface Conditions from COlumn and VERtically Resolved Observations Relevant to Air Quality (DISCOVER-AQ) campaigns were conducted in July and August 2014, in the NFR Colorado. These two campaigns provide detailed and coherent airborne and ground-based measurements in this area, which can assist in evaluation and improvement of chemical transport models and emission inventories. The NSF/NCAR C130 collected extensive airborne measurements of various atmospheric constituents during the FRAPPÉ campaign. A total of 15 flights (~80 flight hours) were conducted in the NFR with the goal of mapping the emissions and their transport and chemistry in this region. During the DISCOVER-AQ campaign, the NASA P3B aircraft performed approximately 20 flights containing spiral ascents or descents over six key sites in the NFR to capture the vertical profiles of the atmospheric constituents and their diurnal variation. Ethane was measured on board of C130 and P3 aircrafts. On C130 aircraft, ethane was measured by the University of Colorado's CAM instruments with detection sensitivity of 15 ppt, details for which are discussed in Richter et al. (2015). Aerodyne Ethane-Mini spectrometer on P3 was used to measure ethane concentration (Yacovitch et al., 2014). Fried (2015) compared CAMS ethane measurements with sub-ppb precision with the Aerodyne measurements during wing tip comparisons and the agreement was within 9%, corresponding to differences of less than 55 ppt.

The National Oceanic and Atmospheric Administration (NOAA), the Colorado Department of Public Health and Environment (CDPHE), and the National Park Services (NPS) operated numerous ground-level measurement sites during these two campaigns. In this work, we present ground-level measurements from the NOAA Boulder Atmospheric Observatory (BAO; 40.05°N, 105.01°W, 1584 m above sea level (asl)), the NOAA Platteville site (PAO; 40.18°N, −104.73°W, 1523 m asl), Fort Collins (FC; 40.89°N, -105.13°W, 1572 m asl), NREL-Golden (Golden; 39.74°N, -105.18°W, 1833 m asl), and CDPHE wind measurements at Weld County tower (WC-Tower; 40.39°N, -104.73°W, 1483 m asl), Rocky Flats N (RF-N;39.91°N, -105,19°W, 1803 m asl), Welch (39.64°N, -105.14°W, 1743 m asl), Chatfield (39.53°N, -105.07°W, 16756 m asl), and Aurora-East (39.64°N, -104.57°W, 1802m asl). BAO and PAO are located north of Denver and close to the Wattenberg Gas Field in Weld County (Figure 1). Measurements of temperature, relative humidity, wind speed and direction at 10m, 100m, and 300m were recorded at BAO. Surface wind measurements from PAO (3m) and WC-Tower (4m) were used in this study. The planetary Boundary Layer (PBL) height was measured and calculated at PAO, Fort Collins (FC), and NREL-Golden using micro-pulse Lidar backscatter during the daytime (Compton et al., 2013).

### 2.2. WRF-Chem model

We used WRF-Chem 3.6.1 (Grell et al., 2005; Skamarock et al., 2008), a fully coupled online air quality and transport model, to investigate the sensitivity of modeled PBL, winds, temperature, relative humidity, and ethane concentrations to different

physical parametrizations and configurations. Figure 1 illustrates the location of the two nested domains and the underlying terrain map. We used one-way nesting (i.e., the outer domain ran independently of the inner domain). The outer domain has a 12 km × 12 km horizontal resolution, and the inner domain has a 4 km × 4 km horizontal resolution. Both domains have 53 vertical levels with the domain top at 50 hPa (~11 layers below 1km). The outer domain is designed to capture the emission from the Western US, and the inner domain includes Colorado and Utah. Sensitivity simulations start on 24 July 2014 and end on 18 Aug 2014. Table 1 shows a summary of the WRF-Chem configurations for this study, used in all sensitivity simulations. The Morrison double-moment scheme was selected as the microphysics option and Goddard shortwave (Chou and Suarez, 1999) and RRTMG longwave radiation schemes (Iacono et al., 2008) were used as shortwave and longwave radiation parametrizations, respectively. The Grell-Freitas convection scheme (Grell and Freitas, 2014) was used as convective parametrization for both outer and inner domain. The inner domain falls into the "grey-scale" which means many of the assumptions used in convective parametrization will no longer be valid at this resolution. The Grell-Freitas convection scheme is a stochastic scale dependent convective parametrization based on the method proposed by Arakawa et al. (2011) and is designed for domains with horizontal resolution up to few kilometers. Comparisons between a simulation with resolved convection of inner domain and a simulation using the Grell-Freitas convective parametrization in the inner domain showed similar performance in capturing transport (not shown). Thus, we used the Grell-Freitas convective scheme for both domains in all simulations to reduce the computation costs.

We selected the Regional Atmospheric Chemistry Mechanism chemistry using Earth System Research Laboratory (RACM-ESRL) (Stockwell et al., 1997) coupled to the Modal Aerosol Dynamics Model/Secondary Organic Aerosol Model (MADE/SORGAM). RACM includes 17 stable inorganics, 4 inorganic intermediates, 32 stable organic species, and 24 organic intermediates. RACM_ESRL (Kim et al., 2009) is an updated version of the RACM mechanism and includes 23 photolysis and 221 chemical reactions (Ahmadov et al., 2015). To reduce the computational costs, hydrocarbons with similar behavior are lumped together in the chemical mechanisms. For example, "HC3" in the RACM_ESRL mechanism includes alkanes such as propane, n-butane, isobutane, and acetylene (ethyne), and alcohols such as methanol and ethanol. "TOL" includes toluene and benzene. Ethane and methane are treated exclusively in the RACM_ESRL mechanism. More details regarding the reactions and lumping groups can be found in Stockwell et al., 1997. Chemical boundary conditions from Monitoring Atmospheric Composition and Climate reanalysis (MACC), available every 3 hours, (Inness et al., 2013) and model outputs from RAQMS, available every 6 hours, (Natarajan et al., 2012; Pierce et al., 2007) were used as chemical boundary and initial conditions in the simulations. The model outputs from these global models are specific to the simulation time (24 July 2014 tp 18 Aug 2014) and are interpolated to the WRF-Chem domain and temporal resolution prior to starting the simulations. Ethane concentrations showed no strong sensitivity to the two different chemical initial and boundary conditions (i.e., RAQMS and MACC) and is not discussed further.

#### 2.2.1. WRF-Chem sensitivity tests

WRF-Chem provides users with a number of different dynamical, physical, and chemical schemes. Users can select schemes based on the physical properties of the domain of interest, goals of the study, and computational limitations. We evaluated the

sensitivity of WRF-Chem to different physics options, such as the PBL parametrization, and configurations including daily re-initialization of meteorological fields, different meteorological initial and boundary conditions, and varying horizontal resolution. Table 2 shows details on the sensitivity runs and lists the meteorological and chemical boundary conditions used for each run. The naming system for the simulations is based on the different settings (e.g. simulation 5-MnERi represents the simulation number (5), PBL Scheme (MYNN3), meteorological initial and boundary condition (ERA-interim), chemical initial and boundary condition (RAQMS), and daily re-initialization of meteorological fields (i)). Simulation ID in Table 2 has been used when discussing sensitivity tests in the paper.

An accurate simulation of air pollution is dependent on a precise description of transport processes, meteorological conditions, and the PBL height (PBLH) (Cuchiara et al., 2014; Hu et al., 2010). Transport of pollutants within the domain depends on turbulent motions and vertical mixing within the PBL. WRF-Chem (3.6.1) has eleven different PBL schemes to address the closure problem in the simulation of turbulent motions. In general, PBL schemes can be classified into two main groups; local and non-local. A local PBL scheme estimates the turbulent fluxes of heat, momentum, and moisture from local mean and gradient flux values. In a non-local PBL scheme, non-local fluxes can influence fluxes in each grid, hence they are expected to better capture large-size eddies in the simulation (Stull, 1988). We tested one non-local and two local PBL schemes to understand the sensitivity of the model to PBL parameterization in a domain with high elevation and complex terrain. We used Yonsei University (YSU) first order (Hong et al., 2006) as the non-local PBL scheme in the PBL1 (1-YFM) simulation. The local schemes used in PBL2 (2-MjFM) and PBL3 (3-MnFM) simulations were Mellor–Yamada–Janjic (MYJ) 1.5 order (2.5 level) (Janjic, 2001; Janjic et al., 2000) and Mellor-Yamada-Nakanishi-Niino (MYNN3) 3$^{rd}$ level (Nakanishi and Niino, 2009).

WRF-Chem is a mesoscale model and requires initial and boundary conditions from a larger-scale model. Usually, these initial and boundary conditions are taken from re-analysis products of larger-scale models optimized using assimilation techniques and observations. The choice of initial and boundary condition products can impact the model performance (Angevine et al., 2012; Saide et al., 2011). We tested two different meteorological initial and boundary conditions, European Reanalysis (ERA-interim) by European Center for Medium-Range Weather Forecasts (ECMWF) in Met5 (5-MnERi) simulation and NCEP's Global Forecast System (GFS) in Met6 (6-MnFRi) simulation. ERA-Interim reanalysis is produced with 80km by 80km horizontal and 6-hour temporal resolution (European Centre for Medium-Range Weather Forecasts (ECMWF), 2009), and NCEP FNL (final) operational global analysis is produced using GFS with 1-degree by 1-degree horizontal and 6-hour temporal resolution (National Centers for Environmental Prediction, National Weather Service, NOAA, 2000).

Simulations were performed for 24 days from 24 July 2014 to 18 August 2014. Initializing the meteorological fields in the simulation at the first time step with the larger-scale model values and running it for 24 days without any nudging will result in deviations from the larger scale re-analysis products. On the other hand, the lower resolution of the larger-scale models can lower the accuracy of WRF-Chem high-resolution simulations. To investigate this impact, we tested two different set-ups for

WRF-Chem. In Init4 (4-MnER) simulation, we initialized the meteorological fields at the first time step with larger-scale model values and ran the simulation freely for 24 days ("free run"). In Init5 (5-MnERi) simulation, the meteorological fields were re-initialized every day at 18 UTC (12pm local time) and run for the next 30 hours. The first 6 hours of the simulation (18 UTC to 00 UTC) were discarded to allow for the model to spin up. In this set-up, chemistry fields were recycled from previous cycles of simulations.

The sensitivity of the model to the horizontal resolution was examined by comparing the performance of the outer domain (12 km × 12 km) to the inner domain (4 km × 4 km) in Hor5 (5-MnERi) simulation. In one-way nesting, the outer domain runs independently of the inner domain; thus, comparing the performance of the outer and inner domains is valid.

### 2.3. Emission inventory

NEI-2011 version 2 is a bottom-up emission inventory of U.S. anthropogenic emissions. While we cannot expect the year 2011 inventory to fully represent the model year 2014, it was the only inventory available to the WRF-Chem user community at the time of this study. Emissions in this inventory are calculated based on fuel consumption, source activity, and emission factors reported by state, tribal, and local governing agencies (U.S. Environmental Protection Agency, 2015). WRF-Chem provides a processed version of NEI-2011 to the users, which includes emission of 76 species (50 speciated VOC compounds, 19 PM2.5 aerosol species, and 7 primary species). NEI-2011 and emissions for only oil and NG sector in the NEI-2011 were provided to us by Dr. Stuart McKeen (NOAA Earth Systems Laboratory, Boulder, CO). Table SM 1 includes details on the mapping table used to convert NEI-2011 species to RACM and MADE/SORGAM chemical and aerosol mechanism. The separate oil and NG emission information was used to conduct an additional sensitivity simulation with perturbed oil and NG emission, which we used to study the sensitivity of modeled ethane concentrations as well as concentrations of VOCs and CO to the oil and NG emission sector. We used the Model of Emissions of Gases and Aerosols from Nature (MEGAN) for biogenic emission in all simulations (Guenther et al., 2012). Ethane does not have a significant biogenic source (Yacovitch et al., 2014); thus, we did not assess the impact of biogenic emissions in this study. Wildfire emissions were not included in the simulations, but this will have a negligible impact on the results as wildfires did not significantly influence the air quality in the NFR during the FRAPPÉ campaign (Valerino et al., 2017).

## 3. Results and Discussion

We start with an evaluation of the overall performance of all simulations and later provide a detailed discussion on the different sets of sensitivity simulations. To evaluate the sensitivity of WRF-Chem to different physical parametrizations, we compared the simulated meteorological variables, such as temperature, relative humidity, wind fields, and PBLH, with measurements. 27 July 2014 and 28 July 2014 were reported as Denver cyclone episodes (Dingle et al., 2016; Valerino et al., 2017; Vu et al., 2016), and neither simulation captured the cyclone pattern and enhancements accurately on these two days. Thus, we only

included the period of 1 August 2014 to 15 August 2014 in our analysis to avoid skewing the results because of large model errors during the Denver cyclone episode. For quantitative comparison between the simulations, we used statistical measures including correlation coefficient (R), root mean square error (RMSE), mean absolute error (MAE), mean bias (MB), and normalized mean bias (NMB). Definitions of these metrics can be found in the supplement. We used NMB as a proxy for model sensitivity to quantify the impact of model configuration on different variables. Variability of NMB (calculated by subtracting minimum NMB from maximum NMB) in sensitivity tests can provide a range for uncertainties in the model cases independent of the model values.

### 3.1. Evaluation of overall model performance

Table 3 includes the statistical measures for temperature and relative humidity in all the simulation tests at 100m altitude at BAO. Figure 2 compares the diurnal cycles of measured temperature, relative humidity, wind speed, and wind direction at 100m altitude at BAO with corresponding model values for all the simulation tests. While Figure 2 provides an overview of all sensitivity tests, Figure SM 2 separates each sensitivity test to provide a clearer test by test comparison. Similarly, Table SM 2 to 5 includes statistical measures and Figure SM 1 and Figure SM 3 show diurnal cycles of temperature, relative humidity, wind speed, and wind direction at BAO 10m and 300m. All model simulations capture the overall daily cycle in temperature and relative humidity well (Figure 2 and Table 3). The variability across different sensitivity runs can be large, with modeled temperature varying by up to 6°C and the model-measurement NMB ranging from -3.9% to 11.1%. Relative humidity has larger variability among the simulations during nighttime compared to daytime. The NMB of relative humidity ranges from -29.7% to 52.6%.

Wind patterns vary significantly from daytime to nighttime. During the day, wind primarily blows from the east towards the Rocky Mountains with a slight southerly component. During the night, this pattern switches to predominantly westerly winds bringing cooler air to lower terrain. Wind measurements at the BAO at different altitudes (10m, 100m, 300m) can help us better understand the wind pattern at higher model levels. Table 4 includes mean and standard deviation of daytime and nighttime wind fields in the simulations and the observations at 100m. Results for the 10m and 300m level at BAO during 1 August 2014 to 15 August 2014 are included in Table SM 4 and Table SM 5, respectively. In addition to BAO, we investigated the wind sensitivity to physical parametrizations at two other sites that are close to oil and NG operations, WC tower and PAO (Figure SM 5). At BAO, higher wind speeds were measured at higher elevations which is captured by the model. Overall, most simulations show skill in capturing diurnal cycles of wind speed and direction with better agreement with observations for daytime (Table 4, Table SM 4, and Table SM 5). Overall, the model runs show fairly good performance in capturing temperature, relative humidity, and wind fields, especially for daytime. A higher sensitivity to the physical parametrization was observed for nighttime.

Ethane is predominantly emitted from oil and NG production sites (Helmig et al., 2016; Xiao et al., 2008) and is a valuable chemical tracer to study the transport patterns of oil and NG emissions. To evaluate the impact of vertical mixing intensity on the distribution of pollutants, we compared the vertical distribution of ethane concentrations between the simulations. Figure 3 shows the diurnal cycle of averaged vertical cross section of ethane concentrations at PAO with measured PBL height for each simulation.

Complex local topography can cause localized transport patterns in the domain, which cannot be resolved at the model's 4 km x 4 km horizontal resolution. Pfister et al. (2017) discuss the impacts of the complicated wind patterns in the NFR and the limitations of WRF-Chem simulations in capturing the transport during FRAPPÉ campaign in details. To reduce the impact of localized influences on the sensitivity analysis we use airborne measurements which better represent the regional picture. Evaluation of modeled ethane concentrations with aircraft data provides information on the impact of different configurations on the transport of oil and NG emissions. Whisker plots of ethane concentrations at different elevations along the C130 morning and afternoon flights are shown in Figure 4. This plot limits the C130 observation to the NFR region (east of -105.2 longitude) to reduce transport errors, and it separates observations collected during 9:00 to noon (AM flights) and noon to 18:00 (PM flights) to account for the diurnal changes in PBLH. For this comparison, hourly model output has been interpolated to the time and location of each 1-minute average observation. Lower concentrations of ethane were measured during the PM flights compared to AM flights because of the higher PBLH and stronger vertical mixing in the afternoon (Figure 3). Table 5 summarizes the mean and NMB of ethane concentration for all simulations using ethane airborne measurements. In all simulations, the ethane concentrations are under-predicted by up to 3.3 ppb (NMB ranges between -63% to -42%) for the C130 AM flights and up to 1.7 ppb (NMB ranges between -47.6% to -29.5%) for the C130 PM flights. Overall, measured ethane concentrations, absolute biases, and absolute NMBs are higher for C130 AM compared to C130 PM. However, the differences between variability in NMBs for C130 AM and C130 PM are small i.e., 21% and 18.1%.

Measurements from P3 spirals focus on smaller regions and can capture the impact of local emissions. Figure 5 compares the vertical distribution of measured ethane concentrations against the corresponding model values (interpolated to time and location of each 1-min average observation) for all the simulations at BAO and Platteville (PAO) spirals. Both sites are located close to oil and NG sources (Figure 1), however urban emissions from Denver region can reach BAO (Pfister et al., 2017a). Similar to C130 observations, we illustrate the morning and afternoon data separately. Mean concentrations of up to 18.6 ppb (SD 2.8 ppb) were measured by P3 aircraft, but these high values were not captured by the model and resulted in biases up to -14.9 ppb (NMB of -80.5%) at PAO spirals and biases up to -7.16 ppb (NMB of -57.8%) at BAO spirals. Similar to C130 flights, higher measured ethane concentrations, absolute biases, and NMBs are observed for P3 AM flights compared to PM flights. Higher absolute biases and larger variance at lower altitude in AM flights and can be due to larger uncertainties in capturing morning evolution of PBL. Variability in NMBs across simulations are greater in the PM spirals (42.8% at PAO and 57.3% at BAO) compared to AM spirals (36.5% at PAO and 31.3% at BAO).

While the model shows difficulty in representing the absolute magnitude in ethane concentrations in all simulations at lower altitudes, most simulations capture the changes in variance of ethane concentrations from lower to higher altitudes well especially for the C130 and P3 BAO flights. The C130 flights covered a larger region with varying flight patterns across the NFR, thus less variability in the modeled ethane concentrations was observed compared to the P3, which flew a repetitive pattern and the repeated spirals over the key surface locations reflect a higher influence from localized emissions.

### 3.2. Sensitivity to Planetary Boundary Layer Parametrization

We evaluated the sensitivity of WRF-Chem meteorological fields and ethane concentrations to a non-local (YSU) and two local (MYJ and MYNN3) PBL schemes in PBL1, PBL2, and PBL3 simulation, respectively. Table 2 includes details on simulation configurations. Temperature at BAO changed little between the different PBL schemes and the model agrees with observations (Figure 2). At all three altitudes, PBL1 had a small positive bias (errors less than 1$^{o}$C) while PBL2 and PBL3 had a small negative bias (errors less than 1$^{o}$C) (Table 3 and Table SM 2). Relative humidity differed slightly between local and non-local PBL parametrizations. PBL1 captured relative humidity well, especially at lower altitudes (mean bias of 0.38%, 1.47%, and 4.93% for 10m, 100m, and 300m respectively). PBL2 and PBL3 both over-predicted relative humidity at all altitudes. The mean bias for PBL2 and PBL3 ranged between 11.12% to 14.78% and 6.61% to 9.55%, respectively.

At all altitudes of BAO, PBL1 predicted higher wind speeds than observed as well as PBL2 and PBL3 (Figure 2, Figure SM 1-3). Wind direction does not vary significantly between PBL1, PBL2, and PBL3 at BAO tower and the model missed the southerly component of afternoon winds. Figure SM 4 shows the 10m average wind speed (during 1-August to 11-August) in PBL1, PBL2, and PBL3 for daytime and nighttime and compares it with measurements. Higher daytime wind speed was predicted by PBL1 in the Colorado Eastern plains, especially north of Denver and close to oil and NG operations. Figure SM 5 shows the averaged diurnal cycle of wind speed and wind direction at WC Tower and PAO (sites close to oil and NG operation). At WC tower and PAO, PBL2 and PBL3 better captured the southerly component of afternoon winds compared to BAO.

Each PBL scheme in the WRF model uses different diagnostics to determine the PBLH. To have a consistent comparison of PBL height in the three simulations, we used the 1.5-theta-increase method to estimate PBL height. In this method, PBLH is the lowest altitude where the difference between minimum potential temperature and potential temperature is greater than 1.5 K (Hu et al., 2010; Nielsen-Gammon et al., 2008). Figure 6 shows the diurnal evolution of PBLH as calculated using the 1.5-theta-increase method in the simulations. Observed PBLH at the PAO, Fort Collins (FC), and Golden-NREL sites were retrieved from micro-pulse Lidar backscatter profiles using Covariance Wavelet Transform (CWT) (Compton et al., 2013). PBLH in the PBL1 simulation is greater than either PBL2, PBL3, or observations, and the bias is largest in the afternoon. Figure 3 (a, b, and c) shows PBL1 distributed ethane higher into the atmosphere and more dilution resulted in lower ethane

concentration within the PBL. Figure SM 6 shows, on average, up to 5 ppb higher surface ethane concentrations in simulations based on local PBL schemes (PBL2 and PBL3) compared to the simulation based on non-local PBL scheme (PBL1).

The high bias in temperature, wind speed, and PBLH in PBL1, non-local PBL scheme, suggests a strong vertical mixing that is more defined in the Colorado Eastern plains and close to the oil and NG activities. The local PBL schemes (i.e. PBL2 and PBL3) predict cooler and moister climates and lower PBLH, which indicates less vertical mixing. This is consistent with previous works that compared local and non-local PBL schemes in the WRF model (Angevine et al., 2012; Hu et al., 2010).

The comparison between C130 airborne measurements and modeled ethane concentrations across the NFR, as illustrated in Figure 4, shows biases between -2.5 ppb and -2.3 ppb for AM flights and between -1.7 ppb and -1 ppb for PM flights. Lower NMB variability (4%) was observed in the C130 AM with NMB ranging from -43.1% to -47.1% compared to C130 PM with NMB variability of 18% and NMB ranging from -29.5% to -47.6%. Similar to the C-130 comparison, Figure 5, the simulations did not capture the high ethane values measured during P3-BAO and P3-PAO spirals. The sensitivity of modeled ethane profiles to the PBL scheme is larger in P3 flights compared to C130 flights, with NMB variability of 14.1% ranging from -58% to -44% for PAO AM flights and NMB variability of 32.4% ranging from -37.3% to -69.7% for the PAO PM flight. On average PBL1 predicted higher ethane concentrations during AM flights at lower altitudes compared to PBL2 and PBL3 (Figure 3). Faster evolution of morning PBL and stronger vertical mixing in PBL1 lofted pollutants (including ethane) higher into the atmosphere in the morning (Figure 6). The rapid growth of morning PBL in PBL1 resulted in higher concentration of ethane at higher altitudes (0.5 to 2 km) compared to PBL2 and PBL3.

### 3.3. Sensitivity to re-initialization

We investigated the impact of daily initialization of meteorological fields on the model performance in capturing the transport of pollutants. For this, we conducted a sensitivity simulation (Init5) in which each daily cycle started at 18 UTC from ERA-interim meteorological fields and ran for 30 hours. In the comparison free-running simulation, Init4, we initialized the model at the first time step using the ERA-interim model and ran the simulation from 24 July 2014 to 18 August 2014 freely. Physical configurations and meteorological and chemical initial and boundary conditions kept the same for these two simulations (Table 2). Figure 2 shows an up to 3$^{o}$C bias in nighttime temperature in Init5, but good agreement with the measured temperature during the day. Init4 showed better skill in capturing nighttime temperature compared to Init5, but predicted the lowest daytime temperature among all the simulations with a bias up to -3$^{o}$C. On average, the NMB of the temperature at BAO100m is between 8.6% in Init5 and -6.0% in Init4 (Table 3), which is the largest variability in NMB temperature across the simulations. Similar to the temperature, relative humidity showed a strong sensitivity to re-initialization. Init4 predicted the highest relative humidity, with NMB of 39.2% and Init5 predicted the lowest relative humidity, with an NMB of -26.5% among the simulations at BAO 100m (Table 3). Nighttime wind direction at BAO (Figure 2), PAO, and WC tower (Figure SM 2) had a strong southerly component in Init4 compared to Init5 and observations. In addition, Init4 predicted higher wind speeds compared to

BAO measurements (Figure 2) and Init5. Figure 7 shows on average higher wind speed at 10m altitude across the domain in Init4 compared to Init5 and measurements at both daytime and nighttime.

When compared to C130-AM ethane concentrations (Figure 4), Init4 predicted the lowest ethane concentrations (a bias of -3.3 ppb and NMB of -63%) among all the simulations. This is likely due to the high bias in of wind speed in this simulation which resulted in lower concentrations of ethane (Figure 7). The ethane bias is ~-2.5 ppb and NMB is -47.9% in Init5 during C130-AM. Concentrations during the C130-PM flights showed a weak sensitivity to re-initialization with NMB ranging from -37.8% (Init4) to -40.1% (Init5). For the P3-BAO and P3-PAO spirals in both AM and PM flights, Init4 had the lowest ethane values compared to all the other simulations and compared to observations (Figure 5). This resulted in the largest NMB variability across the simulations. During PAO AM, NMB ranges between -80.5% for Init4 and -53.2% for Init5 (NMB variability of 27.3%) and during PAO PM, NMB ranges between -72.9% for Init4 and -30.0% for Init5 (NMB variability of 43.9%).

### 3.4. Sensitivity to meteorological initial and boundary condition

We tested the performance of changing the meteorological initial and boundary conditions by comparing simulations using ERA-Interim (Met5) with simulations using NCEP-FNL (Met6). As was done for Met5, we initialized meteorological fields with the re-analysis fields every day allowing for a 6-hour spin-up. To prepare meteorological initial and boundary conditions from global models, WRF interpolates these outputs to the designed domains. Figure SM 7 illustrates the differences between ERA-interim and NCEP-FNL model outputs interpolated to the outer domain at the lowest model level and averaged during August 1 to 15, 2014. Overall, the wind speed predictions by these two global models are very similar with slightly (less than 1 m/s) higher prediction by NCEP-FNL. ERA-interim and NCEP-FNL had larger discrepancies in temperature and relative humidity throughout the domain. Comparison with BAO observations (not shown) indicates similar performance for both models with somewhat lower temperature and higher relative humidity in ERA-interim compared to NCEP-FNL. These discrepancies did not have a large impact on temperature and relative humidity in the WRF-Chem simulation, however. Figure 2 and Figure SM 1-3 indicate that the performance of the two simulations is comparable in capturing temperature and relative humidity with a better agreement with measurements during the day. Met5 had slightly higher temperature and lower relative humidity compared to Met6 and compared better to measurements especially during the night. This is because WRF-Chem only uses the global values as the initial and boundary values and resolves for atmospheric variables such as temperature and relative humidity in high resolution based on physical parametrizations set for the simulation.

Comparison of ethane measurements by the C-130 and P3 aircraft with Met5 and Met6, shown in Figure 4 and Figure 5, respectively, also reflects an overall low sensitivity of the model performance to meteorological initial and boundary condition for both AM and PM flights. High sensitivity was observed during P3-PAO PM flight with ethane NMB variability of 23.9% where Met5 had a bias of -2.6 ppb (NMB of -30%) and Met6 had -4.7 ppb (NMB of -53.9%).

### 3.5. Sensitivity to Horizontal resolution

The two nested domains in simulation Hor5 had a horizontal resolution of 12 km × 12 km (coarse) and 4 km × 4 km (fine). The one-way nesting method was used to prevent any feedback from the higher resolution inner domain on the outer domain. This means that while the outer domain provides the boundary conditions to the inner domain, the higher resolution fields from the inner domain do not alter the outer domain fields. To compare the impact of horizontal resolution, we compared the performance of the coarse domain with the fine domain in the same simulation (5Hor). Temperature and relative humidity did not show significant sensitivity to the horizontal resolution at BAO and PAO, as neither did surface winds at BAO (Figure 2), PAO, and WC tower (Figure SM 4). At 100m and 300m altitudes at BAO, the coarse domain predicted higher nighttime wind speed compared to the fine domain and the measurements.

Averaged ethane concentrations along the C130 flights (Figure 4) do not vary significantly with horizontal resolution. However, higher differences are observed for the P3 spirals. This might be due to the C130 flights covering a larger area and, in parts, averaging out the impact of horizontal resolution, whereas the P3 spirals capture small-scale transport patterns in the domain more effectively. For the P3 spirals (Figure 5), the ethane NMB during BAO PM is +11.6% for the fine domain and -21.6% for the coarse domain. These values are -30% and -55.1% during PAO PM flights, respectively.

### 3.6. Oil and NG emission in the NFR

We assessed the performance of the model in capturing oil and NG emissions by focusing on ethane, which is mostly emitted from oil and NG emission sources, and on species with multiple emission sources such as CO and other VOCs. To investigate the contribution of oil and NG emissions to NFR air quality, we ran two additional simulations: in the one, the emissions are based on the NEI-2011 as provided (base simulation or Em7), in the other we doubled the oil and NG emissions (perturbed simulation or Em8).

Figure 8 shows the C130 PM measurements and bias limited to altitudes below 2000m and Figure 9 displays scatterplots of measured to modeled species concentrations limited to NFR, below 2000m with measured ethane greater than 2ppb. Figure 8a and b illustrate high values of ethane concentrations in the vicinity of oil and NG facilities which were not captured by the model resulting in low biases. As can be expected, the simulated ethane concentrations show a high sensitivity to changes in the oil and NG emissions (Figure SM 8). The highest sensitivity was observed for measurements taken over regions close to oil and NG sources, such as the P3-PAO spirals. Ethane biases between Em7 and Em8 varied from -9.4 ppb to -1 ppb (NMB from -50.8% to -5.5%) during P3-PAO AM, and from -2.7 ppb to +2.8 ppb (-31.2% to +31.8%) during P3-PAO PM. Doubling oil and NG emissions lowered the absolute bias during the AM flights (NMB from -50.8% to -5.5%), but resulted in an overestimation of ethane concentrations during the PM flights (NMB from -31.2% to +31.8%). One possible reason for the

difference between AM and PM biases might be an incorrect representation of the diurnal variation of ethane emission rates in the NEI-2011. An inverse modeling technique, as will be subject of further studies, can be used to calculate optimal scaling factors for hourly ethane emissions with the goal to minimize the discrepancies between model and measurement.

CO is mostly emitted from combustion processes and is released from many different source sectors. Figure 8c shows CO enhancements over both Denver and oil and NG facilities. Biases along the C130 flight tracks (Figure 8d) show an over-prediction of CO over Denver and west of Denver and an under-prediction over the oil and NG facilities. The scatterplot in Figure 9b reflects an overall low bias in modeled CO can be partly due to errors in capturing background CO. Doubling oil and NG emissions in Em8 only marginally increased the slope of the regression line indicating a low sensitivity of CO in the NFR to oil and NG emissions. This suggests that the source of the low bias in CO likely is related to other source categories and/or the model boundary conditions.

In the RACM chemical mechanism, alkanes such as propane, n-butane, isobutane, and acetylene (ethyne), and alcohols such as methanol and ethanol are lumped under the "HC3" group (Stockwell et al., 1990). We compared the simulated HC3 concentrations with the sum of measured chemicals in the HC3 group during C130 flights. Similar to ethane, the highest values of HC3 were measured over oil and NG facilities (Figure 8c). These enhancements were not captured in the model and resulted in low model biases (Figure 7f). Comparison of measured HC3 with modeled values from Em7 and Em8, Figure 9c, confirms the low bias of HC3 and shows some increase in the slope of the regression line in Em8 albeit less pronounced compared to ethane.

Toluene and benzene are lumped together in the RACM chemistry under "TOL" (Stockwell et al., 1990). We compared simulated TOL with the sum of toluene and benzene concentrations observed during the C130 flights. The transport sector is a strong source of toluene and benzene in the NFR as well as oil and NG activities. TOL enhancements were observed over oil and NG facilities and Denver with higher values associated with oil and NG emissions (Figure 8g). The model did not capture the enhancements in regions influenced by oil and NG emissions, but well captured TOL values over Denver (Figure 7h). TOL showed very low sensitivity to perturbed oil and NG emissions as shown in Figure 9d. TOL emissions from oil and NG sector in the emission inventory used in this study (NEI-2011) were very low thus doubling oil and NG emissions did not increase TOL in the Em8. Similar to toluene and benzene, xylene enhancements were measured over oil and NG facilities and Denver. Model underestimated xylene enhancements over oil and NG activities and overestimated these enhancements over Denver. Em8 with doubled oil and NG emissions showed very similar performance to Em7 which indicates low emission rates of xylene from oil and NG sector in the NEI-2011 (not shown).

Figure 10 illustrates the HC3 to TOL ratio measured along the C130 PM limited to NFR region and altitudes below 2000m and the corresponding model values. Figure 10a shows oil and NG influenced points with enhanced measured ethane

(concentrations greater than 2 ppb). HC3 to TOL ratios in oil and NG influenced locations show inconsistency between measured (HC3/TOL = 68) and Em7 modeled ratios (HC3/TOL = 22) which was improved in the Em8 (HC3/TOL = 40.9). However, doubling oil and NG emission still resulted in underestimations of HC3, TOL, and their ratios in this region. Figure 10b shows urban influenced points with low measured ethane (concentrations less than 2 ppb). Modeled HC3 to TOL ratios (7.3 for Em7 and 8.9 for Em8) in the urban influenced locations did not show large sensitivity to oil and NG emissions and agreed well with the measurements (10.2). In both oil and NG and urban influenced regions models predicted lower than measured Y-intercepts which was not improved in Em8. Figure 9c also confirms the low bias (about -2ppb) in background HC3 in the model. One reason for this offset can be underestimation in HC3 concentration in the boundary condition fields or leakage from the NG distribution system which was not captured in the model.

The results suggest that HC3, toluene, benzene, and xylene from oil and NG sector are significantly underestimated in the NEI-2011. The low model bias for these species is more pronounced compared to the low model bias in ethane (Figure 9). The inconsistency between these biases implies that the NEI-2011 emission ratios might need to be changed and HC3, toluene, benzene, and xylene oil and NG emissions would need to be increased by a larger factor than ethane.

## 4. Conclusion

We used WRF-Chem to understand the sensitivity of pollutant transport at a high horizontal resolution to different model configurations with the focus on oil and NG emissions. By conducting a range of different sensitivity simulations, we assessed the variability of meteorological variables such as temperature, relative humidity, and wind fields as well as of ethane concentrations (used as a tracer for the oil and NG sector) to different model configurations and parameterizations. The overall daily cycle of temperature and relative humidity was captured well in the simulations with NMB ranging from -3.9% to 11.1% in temperature and from 29.7% to 52.6% in relative humidity. All simulations showed good skill in capturing daytime wind fields but showed higher biases for nighttime wind speeds.

Table 5 summarizes the mean and NMB for ethane concentrations from C130 and P3 airborne measurements below 2000m agl and the corresponding model values for all sensitivity tests. Significant underestimation of ethane in all simulations– especially in regions close to oil and NG activities – with biases up to -14.9 ppb (NMB up to -80.5%) suggest that the emission inventory used (NEI-2011) under-predicts oil and NG emissions. NMB variability (Table 5) was used as a proxy for variability in the model performance caused by model configurations. NMB of the near-surface ethane concentration for aircraft flight patterns across sensitivity simulations varied by up to 57.3% for P3-BAO, by up to 42.8% for P3-PAO and by up to 21.1% for C130 flights. The lower NMB variability during C130 flight can be due to the larger area coverage by this aircraft during the FRAPPÉ campaign and the irregular flight patterns. P3 spirals, covering smaller regions within the domain during repetitive flight patterns, focused more on the local emissions and smaller scale transport patterns and captured a larger ethane sensitivity to model configurations. The largest sensitivity occurred in the initialization test (comparing daily re-initialization with free-

run simulation) with ethane NMB variability up to 57.3%, followed by the horizontal resolution test (comparing horizontal resolution of 12 km × 12 km with 4 km × 4 km) and the PBL parametrization test (comparing local with non-local PBL schemes) with ethane NMB variability up to 33.3% and 32.4%, respectively. To further investigate the performance of the model in capturing oil and NG emissions in the NFR we used a similar domain set-up with 12 km × 12 km and 4 km × 4 km horizontal resolution for outer and inner domains, respectively, daily re-initialization of meteorological variables with ERA-interim model, and MYNN3 PBL scheme.

We compared measured ethane, CO, lumped alkanes (HC3), lumped toluene and benzene (TOL), and xylene to corresponding modeled values and assessed the changes in the model performance when doubling oil and NG emissions. The model showed under-prediction of ethane with the original inventory and a strong sensitivity of ethane concentrations to oil and NG emissions. Doubling oil and NG emissions resulted in an improvement during AM flights and an overestimation of ethane during the PM flights which suggests possible incorrect representation of the diurnal variation of ethane emission rates in the NEI-2011. The model tends to overestimate CO over the Denver region and underestimates CO over the oil and NG region. Low sensitivity of CO to oil and NG emissions indicates that CO in the region is predominantly emitted from sources other than oil and NG. Enhancements of HC3, TOL, xylene over oil and NG facilities were not fully captured in the model and resulted in low biases. Doubling emissions from oil and NG emissions improved the model performance in capturing HC3, but still resulted in a low model bias. Although high values of TOL and xylene were measured over oil and NG facilities, the model did not capture these enhancements in either the simulations with base NEI-2011 emissions or doubled oil and NG emissions. The inconsistency between the sensitivity of ethane, HC3, benzene, toluene, and xylene to the increase in oil and NG emissions and mismatch between VOC ratios in the model and measurement suggest that oil and NG emission rates in the NEI-2011 need to be scaled differently for these species. VOC ratios in the measurements can be used to update these ratios in the emissions inventory.

The presented results reflect the challenges that one is faced with when attempting to improve emission inventories by contrasting measured with modeled concentrations, either through simple direct comparisons or more advanced methods, such as inverse modeling. Any uncertainties that arise from the model configuration will translate into the derived emission constraints, and it is important to be aware of the uncertainties resulting from different model setups. The WRF-Chem simulations and knowledge gained from this study will be used to support inverse modeling studies aimed to improve estimates of emission from oil and NG sector in the NFR.

**Acknowledgements**

The authors would like to acknowledge the FRAPPÉ and DISCOVER-AQ science team. The authors acknowledge the use of WRF-Chem version 3.6.1 and the NCAR Command Language (UCAR/NCAR/CISL/TDD, 2017). We acknowledge Stuart

McKeen (NOAA) for providing NEI-2011 emission inventory, Bradley Pierce (NOAA) for providing RAQMS model outputs for chemical initial and boundary conditions, and Ravan Ahmadov (NOAA) for help with conducting WRF-Chem simulations. We thank Gordon Pierce (CDPHE/APCD) and Erick Mattson (CDPHE/APCD) for providing wind data at CDPHE site, Daniel Wolfe (NOAA) for providing meteorological data at BAO tower, William Brune (Pennsylvania State University) for providing meteorological data at PAO site. We further acknowledge Teresa Campos (NCAR/ACOM) for C130 CO measurements, Lisa Kaser (NCAR) for C130 PTR-MS VOC measurements, Eric Apel (NCAR/ACOM) for C130 TOGA VOC measurements, Don Blake (UC Irvine) for aircraft VOC WAS measurements. The University of Iowa group activities are partly funded by Regional Scale Modeling in Support of KORUS-AQ: Improving Predictions of Dynamic Air Quality using Aircraft, Ground Networks, and Satellite Data (Award No: NNX15AU17G) and Regional-Scale Analysis of Gas and Aerosol Distributions and the Development of Emissions in Support of the NASA SEAC4RS Mission (Award No: NNX12AB78G). This work was supported by computational resources provided by the University of Iowa.

**Reference:**


Ahmadov, R., McKeen, S., Trainer, M., Banta, R., Brewer, A., Brown, S., Edwards, P. M., De Gouw, J. A., Frost, G. J., Gilman, J., Helmig, D., Johnson, B., Karion, A., Koss, A., Langford, A., Lerner, B., Olson, J., Oltmans, S., Peischl, J., Pétron, G., Pichugina, Y., Roberts, J. M., Ryerson, T., Schnell, R., Senff, C., Sweeney, C., Thompson, C., Veres, P. R., Warneke, C., Wild, R., Williams, E. J., Yuan, B. and Zamora, R.: Understanding high wintertime ozone pollution events in an oil- and natural gas-producing region of the western US, Atmos. Chem. Phys., 15(1), 411–429, doi:10.5194/acp-15-411-2015, 2015.

Allen, D. T.: Emissions from oil and gas operations in the United States and their air quality implications, J. Air Waste Manage. Assoc., 66(6), 549–575, doi:10.1080/10962247.2016.1171263, 2016.

Alvarez, R. A., Pacala, S. W., Winebrake, J. J., Chameides, W. L. and Hamburg, S. P.: Greater focus needed on methane leakage from natural gas infrastructure., Proc. Natl. Acad. Sci. U. S. A., 109(17), 6435–40, doi:10.1073/pnas.1202407109, 2012.

Angevine, W. M., Eddington, L., Durkee, K., Fairall, C., Bianco, L. and Brioude, J.: Meteorological model evaluation for CalNex 2010, Mon. Weather Rev., 3885–3906, doi:10.1175/MWR-D-12-00042.1, 2012.

Arakawa, A., Jung, J. H. and Wu, C. M.: Toward unification of the multiscale modeling of the atmosphere, Atmos. Chem. Phys., 11(8), 3731–3742, doi:10.5194/acp-11-3731-2011, 2011.

Barkley, Z. R., Lauvaux, T., Davis, K. J., Deng, A., Miles, N. L., Richardson, S. J., Cao, Y., Sweeney, C., Karion, A., Smith, M., Kort, E. A., Schwietzke, S., Murphy, T., Cervone, G., Martins, D. and Maasakkers, J. D.: Quantifying methane emissions from natural gas production in north-eastern Pennsylvania, Atmos. Chem. Phys, 17, 13941–13966, doi:10.5194/acp-17-13941-2017, 2017.

Brandt, A. R., Heath, G. A., Kort, E. A., O'Sullivan, F., Petron, G., Jordaan, S. M., Tans, P., Wilcox, J., Gopstein, a M., Arent, D., Wofsy, S., Brown, N. J., Bradley, R., Stucky, G. D., Eardley, D. and Harriss, R.: Methane Leaks from North American Natural Gas Systems, Science (80-. )., 343(6172), 733–735, doi:10.1126/science.1247045, 2014.

Cheadle, L. C., Oltmans, S. J., Pétron, G., Schnell, R. C., Mattson, E. J., Herndon, S. C., Thompson, A. M., Blake, D. R. and Mcclure-begley, A.: Surface ozone in the Northern Front Range and the influence of oil and gas development on ozone production during FRAPPE / DISCOVER-AQ, Elem. Sci. Anthr., 6, doi:http://doi.org/10.1525/elementa.254, 2017.

Chou, M.-D. and Suarez, M. J.: Technical Report Series on Global Modeling and Data Assimilation A Thermal Infrared Radiation Parameterization for Atmospheric Studies Revised May 2003 i, Nasa Tech. Memo., 15(104606), 40, 1999.

Colorado Oil and Gas Conservation Commission: COGIS - Production Data Inquiry, [online] Available from: http://cogcc.state.co.us/data.html#/cogis (Accessed 1 January 2017), 2017.

Compton, J. C., Delgado, R., Berkoff, T. A. and Hoff, R. M.: Determination of planetary boundary layer height on

short spatial and temporal scales: A demonstration of the covariance wavelet transform in ground-based wind profiler and lidar measurements, J. Atmos. Ocean. Technol., 30(7), 1566–1575, doi:10.1175/JTECH-D-12-00116.1, 2013.

Conley, S., Franco, G., Faloona, I., Blake, D. R., Peischl, J. and Ryerson, T. B.: Methane emissions from the 2015 Aliso Canyon blowout in Los Angeles, CA, Science (80-. )., 2348(October 2015), 2–7, doi:10.1126/science.aaf2348, 2016.

Cuchiara, G. C., Li, X., Carvalho, J. and Rappenglück, B.: Intercomparison of planetary boundary layer parameterization and its impacts on surface ozone concentration in the WRF/Chem model for a case study in Houston/Texas, Atmos. Environ., 96, 175–185, doi:dx.doi.org/10.1016/j.atmosenv.2014.07.013, 2014.

Cui, Y. Y., Brioude, J., Frost, G. J., Peischl, J., Ryerson, T., Trainer, M., Wofsy, S. C., Santoni, G. W. and Kort, E. a.: Top-Down Estimate of Methane Emissions in California Using a Mesoscale Inverse Modeling Technique, 13th Annu. C. Conf., 1–6, doi:10.1002/2014JD023002, 2014.

Cui, Y. Y., Brioude, J., McKeen, S. A., Angevine, W. M., Kim, S. W., Frost, G. J., Ahmadov, R., Peischl, J., Bousserez, N., Liu, Z., Ryerson, T. B., Wofsy, S. C., Santoni, G. W., Kort, E. A., Fischer, M. L. and Trainer, M.: Top-down estimate of methane emissions in California using a mesoscale inverse modeling technique: The San Joaquin Valley, J. Geophys. Res. Atmos., 122, 3686–3699, doi:10.1002/2014JD023002, 2017.

Dingle, J. H., Vu, K., Bahreini, R., Apel, E. C., Campos, T. L., Flocke, F., Fried, A., Herndon, S., Hills, A. J., Hornbrook, R. S., Huey, G., Kaser, L., Montzka, D. D., Nowak, J. B., Reeves, M., Richter, D., Roscioli, J. R., Shertz, S., Stell, M., Tanner, D., Tyndall, G., Walega, J., Weibring, P. and Weinheimer, A.: Aerosol optical extinction during the front range air pollution and photochemistry Éxperiment (FRAPPÉ) 2014 summertime field campaign, Colorado, USA, Atmos. Chem. Phys., 16(17), 11207–11217, doi:10.5194/acp-16-11207-2016, 2016.

Energy information administration of US Department of Energy.: International energy outlook 2016-Natural gas, in International energy outlook 2016, pp. 37–60., 2016.

European Centre for Medium-Range Weather Forecasts (ECMWF): ERA-Interim Project, , doi:10.5065/D6CR5RD9, 2009.

Fried, A.: Fast Airborne Spectroscopic Measurements of Formaldehyde and Ethane During the 2014 Front Range Air Pollution and Photochemistry Éxperiment (FRAPPÉ), Color. Dep. Public Heal. Environ., 1–6, 2015.

Gilman, J. B., Lerner, B. M., Kuster, W. C. and De Gouw, J. A.: Source signature of volatile organic compounds from oil and natural gas operations in northeastern Colorado, Environ. Sci. Technol., 47(3), 1297–1305, doi:10.1021/es304119a, 2013.

Grell, G. A. and Freitas, S. R.: A scale and aerosol aware stochastic convective parameterization for weather and air quality modeling, Atmos. Chem. Phys. Discuss., 14(10), 5233–5250, doi:10.5194/acp-14-5233-2014, 2014.

Grell, G. A., Peckham, S. E., Schmitz, R., McKeen, S. A., Frost, G., Skamarock, W. C. and Eder, B.: Fully coupled "online" chemistry within the WRF model, Atmos. Environ., 39(37), 6957–6975, doi:10.1016/j.atmosenv.2005.04.027, 2005.

Guenther, A. B., Jiang, X., Heald, C. L., Sakulyanontvittaya, T., Duhl, T., Emmons, L. K. and Wang, X.: The model of emissions of gases and aerosols from nature version 2.1 (MEGAN2.1): An extended and updated framework for modeling

biogenic emissions, Geosci. Model Dev., 5(6), 1471–1492, doi:10.5194/gmd-5-1471-2012, 2012.

Halliday, H., Thompson, A. M., Wisthaler, A., Blake, D. R., Hornbrook, R. S., Mikoviny, T., Muller, M., Eichler, P., Apel, E. C. and Hills, A. J.: Atmospheric benzene observations from oil and gas production in the Denver-Julesburg Basin in July and August 2014, J. Geophys. Res. Atmos., 121(18), doi:10.1002/ 2016JD025327., 2016.

Helmig, D., Rossabi, S., Hueber, J., Tans, P., Montzka, S. A., Masarie, K., Thoning, K., Plass-Duelmer, C., Claude, A., Carpenter, L. J., Lewis, A. C., Punjabi, S., Reimann, S., Vollmer, M. K., Steinbrecher, R., Hannigan, J. W., Emmons, L. K., Mahieu, E., Franco, B., Smale, D. and Pozzer, A.: Reversal of global atmospheric ethane and propane trends largely due to US oil and natural gas production, Nat. Geosci., 9(July), 490–495, doi:10.1038/ngeo2721, 2016.

Hong, S.-Y., Noh, Y. and Dudhia, J.: A new vertical diffusion package with an explicit treatment of entrainment processes., Mon. Weather Rev., 134(9), 2318–2341, doi:10.1175/MWR3199.1, 2006.

Howarth, R. W., Santoro, R. and Ingraffea, A.: Methane and the greenhouse-gas footprint of natural gas from shale formations, Clim. Change, 106(4), 679–690, doi:10.1007/s10584-011-0061-5, 2011.

Hu, X. M., Nielsen-Gammon, J. W. and Zhang, F.: Evaluation of three planetary boundary layer schemes in the WRF model, J. Appl. Meteorol. Climatol., 49(9), 1831–1844, doi:10.1175/2010JAMC2432.1, 2010.

Iacono, M. J., Delamere, J. S., Mlawer, E. J., Shephard, M. W., Clough, S. A. and Collins, W. D.: Radiative forcing by long-lived greenhouse gases: Calculations with the AER radiative transfer models, J. Geophys. Res. Atmos., 113(13), 2–9, doi:10.1029/2008JD009944, 2008.

Inness, A., Baier, F., Benedetti, A., Bouarar, I., Chabrillat, S., Clark, H., Clerbaux, C., Coheur, P., Engelen, R. J., Errera, Q., Flemming, J., George, M., Granier, C., Hadji-Lazaro, J., Huijnen, V., Hurtmans, D., Jones, L., Kaiser, J. W., Kapsomenakis, J., Lefever, K., Leitão, J., Razinger, M., Richter, A., Schultz, M. G., Simmons, A. J., Suttie, M., Stein, O., Thépaut, J. N., Thouret, V., Vrekoussis, M. and Zerefos, C.: The MACC reanalysis: An 8 yr data set of atmospheric composition, Atmos. Chem. Phys., 13(8), 4073–4109, doi:10.5194/acp-13-4073-2013, 2013.

Janjic, Z.: Nonsingular Implementation of the Mellor-Yamada Level 2.5 Scheme in the NCEP Meso model, Natl. Centers Environ. Predict., 1–61, 2001.

Janjic, Z., Emanuel, K. and M., Z.-R.: Comments on "Development and Evaluation of a Convection Scheme for Use in Climate Models," J. Atmos. Sci., 57(21), 3686–3686, 2000.

Karion, A., Sweeney, C., Kort, E. A., Shepson, P. B., Brewer, A., Cambaliza, M., Conley, S. A., Davis, K., Deng, A., Hardesty, M., Herndon, S. C., Lauvaux, T., Lavoie, T., Lyon, D., Newberger, T., Pétron, G., Rella, C., Smith, M., Wolter, S., Yacovitch, T. I. and Tans, P.: Aircraft-Based Estimate of Total Methane Emissions from the Barnett Shale Region, Environ. Sci. Technol., 49(13), 8124–8131, doi:10.1021/acs.est.5b00217, 2015.

Kim, S. W., Heckel, A., Frost, G. J., Richter, A., Gleason, J., Burrows, J. P., McKeen, S., Hsie, E. Y., Granier, C. and Trainer, M.: NO2 columns in the western United States observed from space and simulated by a regional chemistry model and their implications for NOx emissions, J. Geophys. Res. Atmos., 114(11), 1–29, doi:10.1029/2008JD011343, 2009.

Levi, M.: Climate consequences of natural gas as a bridge fuel, Clim. Change, 118(3–4), 609–623,

doi:10.1007/s10584-012-0658-3, 2013.

Lyon, D. R.: Methane Emissions from the Natural Gas Supply Chain, in Environmental and Health Issues in Unconventional Oil and Gas Development, pp. 33–48, Elsevier Inc., 2015.

McDuffie, E. E., Edwards, P. M., Gilman, J. B., Lerner, B. M., Dube, W. P., Trainer, M., Wolfe, D. E., Angevine, W. M., DeGouw, J., Williams, E. J., Tevlin, A. G., Murphy, J. G., Fischer, E. V., McKeen, S., Ryerson, T. B., Peischl, J., Holloway, J. S., Aikin, K., Langfor, A. O., Sneff, C. J., Alvarez II, R. J., Hall, S. R., Ullmann, K., Lantz, K. O. and Brown, S. S.: Influence of oil and gas emissions on summertime ozone in the Colorado Northen Front Range, J. Geophys. Res., 1–19, doi:doi:10.1002/2016JD025265., 2016.

McJeon, H., Edmonds, J., Bauer, N., Clarke, L., Fisher, B., Flannery, B. P., Hilaire, J., Krey, V., Marangoni, G., Mi, R., Riahi, K., Rogner, H. and Tavoni, M.: Limited impact on decadal-scale climate change from increased use of natural gas, Nature, 514(7523), 482–485, doi:10.1038/nature13837, 2014.

McKenzie, L. M., Witter, R. Z., Newman, L. S. and Adgate, J. L.: Human health risk assessment of air emissions from development of unconventional natural gas resources, Sci. Total Environ., 424, 79–87, doi:10.1016/j.scitotenv.2012.02.018, 2012.

Nakanishi, M. and Niino, H.: Development of an Improved Turbulence Closure Model for the Atmospheric Boundary Layer, J. Meteorol. Soc. Japan, 87(5), 895–912, doi:10.2151/jmsj.87.895, 2009.

Natarajan, M., Pierce, R. B., Schaack, T. K., Lenzen, A. J., Al-Saadi, J. A., Soja, A. J., Charlock, T. P., Rose, F. G., Winker, D. M. and Worden, J. R.: Radiative forcing due to enhancements in tropospheric ozone and carbonaceous aerosols caused by Asian fires during spring 2008, J. Geophys. Res. Atmos., 117(6), 1–18, doi:10.1029/2011JD016584, 2012.

National Centers for Environmental Prediction, National Weather Service, NOAA, U. S. D. of C.: NCEP FNL Operational Model Global Tropospheric Analyses, continuing from July 1999, , doi:10.5065/D6M043C6, 2000.

Nielsen-Gammon, J. W., Powell, C. A., Mahoney, M. J., Angevine, W. M., Senff, C., White, A., Berkowitz, C., Doran, C. and Knupp, K.: Multisensor Estimation of Mixing Heights over a Coastal City, J. Appl. Meteorol. Climatol., 27–43, doi:10.1175/2007JAMC1503.1, 2008.

Olaguer, E. P.: The potential near-source ozone impacts of upstream oil and gas industry emissions, J. Air Waste Manag. Assoc., 62(8), 966–977, doi:10.1080/10962247.2012.688923, 2012.

Peischl, J., Karion, A., Sweeney, C., Kort, E. A., Smith, M. L., Brandt, A. R., Yeskoo, T., Aikin, K. C., Conley, S. A., Gvakharia, A., Trainer, M., Wolter, S. and Ryerson, T. B.: Quantifying atmospheric methane emissions from oil and natural gas production in the Bakken shale region of North Dakota, J. Geophys. Res. Atmos., 121, 6101–6111, doi:10.1002/2015JD024631, 2016.

Pétron, G., Frost, G., Miller, B. R., Hirsch, A. I., Montzka, S. A., Karion, A., Trainer, M., Sweeney, C., Andrews, A. E., Miller, L., Kofler, J., Bar-Ilan, A., Dlugokencky, E. J., Patrick, L., Moore, C. T., Ryerson, T. B., Siso, C., Kolodzey, W., Lang, P. M., Conway, T., Novelli, P., Masarie, K., Hall, B., Guenther, D., Kitzis, D., Miller, J., Welsh, D., Wolfe, D., Neff, W. and Tans, P.: Hydrocarbon emissions characterization in the Colorado Front Range: A pilot study, J. Geophys. Res. Atmos.,

117(4), 1–19, doi:10.1029/2011JD016360, 2012.

Pétron, G., Karion, A., Sweeney, C., Miller, B. R., Montzka, S. A., Frost, G. J., Trainer, M., Tans, P., Andrews, A., Kofler, J., Helmig, D., Guenther, D., Dlugokencky, E., Lang, P., Newberger, T., Wolter, S., Hall, B., Novelli, P., Brewer, A., Conley, S., Hardesty, M., Banta, R., White, A., Noone, D., Wolfe, D. and Schnell, R.: A new look at methane and nonmethane hydrocarbon emissions from oil and natural gas operations in the Colorado Denver-Julesburg Basin, J. Geophys. Res. Atmos., 119(10), 5787–5805, doi:https://doi.org/10.1002/2013JD021272, 2014.

Pfister, G., Flocke, F., Hornbrook, R., Orlando, J. and Lee, S.: Process-Based and Regional Source Impact Analysis for FRAPPÉ and DISCOVER-AQ 2014. [online] Available from: https://www.colorado.gov/airquality/tech_doc_repository.aspx?action=open&file=FRAPPE-NCAR_Final_Report_July2017.pdf, 2017a.

Pfister, G. G., Reddy, P. J., Barth, M. C., Flocke, F. F., Fried, A., Herndon, S. C., Sive, B. C., Sullivan, J. T., Thompson, A. M., Yacovitch, T. I., Weinheimer, A. J. and Wisthaler, A.: Using Observations and Source-Specific Model Tracers to Characterize Pollutant Transport During FRAPPÉ and DISCOVER-AQ, J. Geophys. Res. Atmos., 122(19), 10510–10538, doi:10.1002/2017JD027257, 2017b.

Pierce, R. B., Schaack, T., Al-Saadi, J. A., Fairlie, T. D., Kittaka, C., Lingenfelser, G. S., Natarajan, M., Olson, J. R., Soja, A. J., Zapotocny, T., Lenzen, A., Stobie, J., Johnson, D., Avery, M. A., Sachse, G. W., Thompson, A., Cohen, R., Dibb, J. E., Crawford, J. H., Rault, D. F., Martin, R., Szykman, J. and Fishman, J.: Chemical data assimilation estimates of continental U.S. ozone and nitrogen budgets during the Intercontinental Chemical Transport Experiment-North America, J. Geophys. Res. Atmos., 112(12), doi:10.1029/2006JD007722, 2007.

Richter, D., Weibring, P., Walega, J. G., Fried, A., Spuler, S. M. and Taubman, M. S.: Compact highly sensitive multi-species airborne mid-IR spectrometer, Appl. Phys. B Lasers Opt., 119(1), 119–131, doi:10.1007/s00340-015-6038-8, 2015.

Saide, P. E., Carmichael, G. R., Spak, S. N., Gallardo, L., Osses, A. E., Mena-Carrasco, M. A. and Pagowski, M.: Forecasting urban PM10 and PM2.5 pollution episodes in very stable nocturnal conditions and complex terrain using WRF-Chem CO tracer model, Atmos. Environ., 45(16), 2769–2780, doi:10.1016/j.atmosenv.2011.02.001, 2011.

Skamarock, W. C., Klemp, J. B., Dudhia, J., O., G. D. and Barker, D. M.: A description of the Advanced Research WRF version 3. NCAR Tech. Note NCAR/TN-4751STR, 2008.

Smith, M. L., Kort, E. A., Karion, A., Sweeney, C., Herndon, S. C. and Yacovitch, T. I.: Airborne Ethane Observations in the Barnett Shale: Quantification of Ethane Flux and Attribution of Methane Emissions, Environ. Sci. Technol., 49(13), 8158–8166, doi:10.1021/acs.est.5b00219, 2015.

Stockwell, W. R., Middleton, P., Chang, J. S. and Tang, X.: The second generation regional acid deposition model chemical mechanism for regional air quality modeling, J. Geophys. Res., 95(D10), 16343, doi:10.1029/JD095iD10p16343, 1990.

Stockwell, W. R., Kirchner, F., Kuhn, M. and Seefeld, S.: A new mechanism for regional atmospheric chemistry

modeling, J. Geophys. Res., 102(D22), 25847, doi:10.1029/97JD00849, 1997.

Stull, R. B.: An introduction to boundary layer meteorology, Springer Science & Business Media., 1988.

Thompson, C. R., Hueber, J. and Helmig, D.: Influence of oil and gas emissions on ambient atmospheric non-methane hydrocarbons in residential areas of Northeastern Colorado, Elem. Sci. Anthr., 2, 000035, doi:10.12952/journal.elementa.000035, 2014.

U.S. Energy Information Administration: International Energy Outlook 2016-Electricity, in International Energy Outlook, pp. 81–100. [online] Available from: http://www.eia.gov/forecasts/ieo/pdf/0484(2016).pdf, 2016.

U.S. Environmental Protection Agency: 2011 National Emissions Inventory, version 2 Technical Support Document. [online] Available from: https://www.epa.gov/sites/production/files/2015-10/documents/nei2011v2_tsd_14aug2015.pdf, 2015.

UCAR/NCAR/CISL/TDD: The NCAR Command Language (Version 6.4.0) [Software]., 2017.

Valerino, M. J., Johnson, J. J., Izumi, J., Orozco, D., Hoff, R. M., Delgado, R. and Hennigan, C. J.: Sources and composition of PM2.5 in the Colorado Front Range during the DISCOVER-AQ study, J. Geophys. Res. Atmos., 122(1), 566–582, doi:10.1002/2016JD025830, 2017.

Vu, K. T., Dingle, J. H., Bahreini, R., Reddy, P. J., Campos, T. L., Diskin, G. S., Fried, A., Herndon, S. C., Hornbrook, R. S., Huey, G., Kaser, L., Montzka, D. D., Nowak, J. B., Richter, D., Roscioli, J. R., Shertz, S., Stell, M., Tanner, D., Tyndall, G., Walega, J., Weibring, P., Weinheimer, A. J., Pfister, G. and Flocke, F.: Impacts of the Denver Cyclone on Regional Air Quality and Aerosol Formation in the Colorado Front Range during FRAPPÉ 2014, Atmos. Chem. Phys. Discuss., (3), 1–40, doi:10.5194/acp-2016-532, 2016.

Xiao, Y., Logan, J. A., Jacob, D. J., Hudman, R. C., Yantosca, R. and Blake, D. R.: Global budget of ethane and regional constraints on U.S. sources, J. Geophys. Res. Atmos., 113(21), 1–13, doi:10.1029/2007JD009415, 2008.

Yacovitch, T. I., Herndon, S. C., Roscioli, J. R., Floerchinger, C., McGovern, R. M., Agnese, M., Pétron, G., Kofler, J., Sweeney, C., Karion, A., Conley, S. A., Kort, E. A., Nähle, L., Fischer, M., Hildebrandt, L., Koeth, J., McManus, J. B., Nelson, D. D., Zahniser, M. S. and Kolb, C. E.: Demonstration of an ethane spectrometer for methane source identification, Environ. Sci. Technol., 48(14), 8028–8034, doi:10.1021/es501475q, 2014.

Zavala-Araiza, D., Lyon, D. R., Alvarez, R. A., Davis, K. J., Harriss, R., Herndon, S. C., Karion, A., Kort, E. A., Lamb, B. K., Lan, X., Marchese, A. J., Pacala, S. W., Robinson, A. L., Shepson, P. B., Sweeney, C., Talbot, R., Townsend-Small, A., Yacovitch, T. I., Zimmerle, D. J. and Hamburg, S. P.: Reconciling divergent estimates of oil and gas methane emissions, Proc. Natl. Acad. Sci., 112(51), 15597–15602, doi:10.1073/pnas.1522126112, 2015.

**Table 1. Summary of basic WRF-Chem configuration**

| Category | Selected option |
|---|---|
| **Horizontal resolution** | 12km and 4km |
| **Vertical resolution** | 53 layers (11 within the lowest 1km) |
| **Microphysics** | Morrison double-moment scheme |
| **Land Surface** | 5-layer thermal diffusion |
| **Shortwave radiation** | Goddard shortwave |
| **longwave radiation** | RRTMG scheme |
| **Cumulus parametrization** | Grell-Freitas scheme |
| **Gas-phase chemistry** | RACM-ESRL |
| **Biogenic emission** | MEGAN |

**Table 2. Summary of WRF-Chem configurations for sensitivity tests designed for this study**

| Test | Sim. ID | Sim. Name | PBL Scheme | Met IC & BC | Chem IC & BC | Init. | Emiss. |
|---|---|---|---|---|---|---|---|
| PBL | PBL1 | 1-YFM | YSU (Y) | NCEP-FNL (F) | MACC (M) | Free run | NEI2011 |
| | PBL2 | 2-MjFM | MYJ (Mj) | NCEP-FNL (F) | MACC (M) | Free run | NEI2011 |
| | PBL3 | 3-MnFM | MYNN3 (Mn) | NCEP-FNL (F) | MACC (M) | Free run | NEI2011 |
| Initialization | Init4 | 4-MnER | MYNN3 (Mn) | ERA-interim (E) | RAQMS (R) | Free run | NEI2011 |
| | Init5 | 5-MnERi | MYNN3 (Mn) | ERA-interim (E) | RAQMS (R) | re-init (i) | NEI2011 |
| Met IC & BC | Met5 | 5-MnERi | MYNN3 (Mn) | ERA-interim (E) | RAQMS (R) | re-init (i) | NEI2011 |
| | Met6 | 6-MnFRi | MYNN3 (Mn) | NCEP-FNL (F) | RAQMS (R) | re-init (i) | NEI2011 |
| Horizontal resolution | Hor5 | 5-MnERi | MYNN3 (Mn) | ERA-interim (E) | RAQMS (R) | re-init (i) | NEI2011 |
| | Hor5-12km | 5-MnERi-12km | MYNN3 (Mn) | ERA-interim (E) | RAQMS (R) | re-init (i) | NEI2011 |
| Emission Inventory | Em7 | 5-MnERiMeg | MYNN3 (Mn) | ERA-interim (E) | RAQMS (R) | re-init (i) | NEI2011 + Megan |
| | Em8 | 7-MnERiMeg-2OnG | MYNN3 (Mn) | ERA-interim (E) | RAQMS (R) | re-init (i) | NEI2011 (doubled oil & NG) + Megan |

**Table 3. Summary of model performance in capturing temperature (T) and Relative Humidity (RH) at BAO 100m during 1 to 15 August 2014.**

| 100m | | PBL | | | Met IC and BC | | Initialization | | Horizontal resolution | |
|---|---|---|---|---|---|---|---|---|---|---|
| **T(C)** | **OBS** | **PBL1** | **PBL2** | **PBL3** | **Met5** | **Met6** | **Init4** | **Init5** | **Hor5** | **Hor5-12km** |
| **Mean** | 22.01 | 22.18 | 21.15 | 21.52 | 23.92 | 23.20 | 20.70 | 23.92 | 23.92 | 23.90 |
| **R** | | 0.85 | 0.83 | 0.81 | 0.81 | 0.84 | 0.63 | 0.81 | 0.81 | 0.82 |
| **RMSE** | | 1.86 | 2.07 | 2.01 | 2.74 | 2.17 | 3.07 | 2.74 | 2.74 | 2.72 |
| **MAE** | | 1.40 | 1.72 | 1.65 | 2.18 | 1.64 | 2.46 | 2.18 | 2.18 | 2.10 |
| **MB** | | 0.17 | -0.86 | -0.5 | 1.90 | 1.19 | -0.31 | 1.90 | 1.90 | 1.89 |
| **NMB(%)** | | 0.8 | -3.9 | -2.3 | 8.6 | 5.4 | -6.0 | 8.6 | 8.6 | 8.6 |
| **RH(%)** | **OBS** | **PBL1** | **PBL2** | **PBL3** | **Met5** | **Met6** | **Init4** | **Init5** | **Hor5** | **Hor5-12km** |
| **Mean** | 42.27 | 43.74 | 51.79 | 48.88 | 31.06 | 38.51 | 58.90 | 31.06 | 31.06 | 31.52 |
| **R** | | 0.69 | 0.59 | 0.53 | 0.52 | 0.52 | 0.44 | 0.52 | 0.52 | 0.58 |
| **RMSE** | | 11.90 | 16.33 | 14.67 | 16.69 | 13.63 | 25.90 | 16.69 | 16.69 | 16.00 |
| **MAE** | | 9.21 | 13.47 | 12.31 | 12.79 | 10.28 | 21.17 | 12.79 | 12.79 | 11.99 |
| **MB** | | 1.47 | 9.52 | 6.61 | -11.21 | -3.76 | 16.63 | -11.21 | -11.21 | -10.75 |
| **NMB(%)** | | 3.5 | 22.5 | 15.6 | -26.5 | -8.9 | 39.2 | -26.5 | -26.5 | -25.4 |

**Table 4. Summary of model performance in capturing wind speed and direction at BAO 100m during Aug 1-15, 2014**

| | | | PBL | | | Met IC & BC | | Initialization | | Horizontal Res. | |
|---|---|---|---|---|---|---|---|---|---|---|---|
| **Day - 100 m** | | **OBS** | **PBL1** | **PBL2** | **PBL3** | **Met5** | **Met6** | **Init4** | **Init5** | **Hor5** | **Hor5-12km** |
| **Wind Speed** | Mean | 3.22 | 3.84 | 3.40 | 2.70 | 2.87 | 3.19 | 3.77 | 2.87 | 2.87 | 2.76 |
| | STD | 2.02 | 2.14 | 2.26 | 1.57 | 1.57 | 1.80 | 2.86 | 1.57 | 1.57 | 1.45 |
| **Wind Direction** | Mean | 117.84 | 62.90 | 64.05 | 66.76 | 33.86 | 59.61 | 55.92 | 33.86 | 33.86 | 41.11 |
| | STD | 71.06 | 48.79 | 63.44 | 56.30 | 73.10 | 75.90 | 74.77 | 73.10 | 73.10 | 67.74 |
| **Night - 100 m** | | **OBS** | **PBL1** | **PBL2** | **PBL3** | **Met5** | **Met6** | **Init4** | **Init5** | **Hor5** | **Hor5-12km** |
| **Wind Speed** | Mean | 3.42 | 4.69 | 4.06 | 3.57 | 4.02 | 4.41 | 4.87 | 4.02 | 4.02 | 4.73 |
| | STD | 1.81 | 2.34 | 2.78 | 2.47 | 2.45 | 2.32 | 2.88 | 2.45 | 2.45 | 3.15 |
| **Wind Direction** | Mean | 233.09 | 114.12 | 268.45 | 349.75 | 331.38 | 292.24 | 155.59 | 331.38 | 331.38 | 303.89 |
| | STD | 70.62 | 97.13 | 89.35 | 86.75 | 87.28 | 77.12 | 85.20 | 87.28 | 87.28 | 85.11 |

**Table 5. Ethane mean, NMB, and NMB variability from C130 and P3 BAO and PAO airborne measurements below 2000m and the corresponding model values**

| | | | C130 - NFR | | P3 - BAO | | P3- PAO | |
|---|---|---|---|---|---|---|---|---|
| | | | AM | PM | AM | PM | AM | PM |
| | OBS | Mean (ppb) | 5.22 | 3.49 | 12.39 | 4.90 | 18.56 | 8.66 |
| PBL | PBL1 | Mean (ppb) | 2.97 | 1.83 | 8.51 | 3.85 | 7.79 | 2.62 |
| | | NMB (%) | -43.1 | -47.6 | -31.3 | -21.4 | -58.0 | -69.7 |
| | PBL2 | Mean (ppb) | 2.97 | 2.36 | 9.11 | 4.53 | 7.93 | 5.43 |
| | | NMB (%) | -43.1 | -32.4 | -26.5 | -7.6 | -57.3 | -37.3 |
| | PBL3 | Mean (ppb) | 2.76 | 2.46 | 8.67 | 4.90 | 10.40 | 4.20 |
| | | NMB (%) | -47.1 | -29.5 | -30 | 0 | -44.0 | -51.5 |
| | All PBL | NMB var. (%) | 4.0 | 18.1 | 4.8 | 21.4 | 14.1 | 32.4 |
| Init. | Init4 | Mean (ppb) | 1.93 | 2.17 | 5.23 | 2.66 | 3.62 | 2.35 |
| | | NMB (%) | -63.0 | -37.8 | -57.8 | -45.7 | -80.5 | -72.9 |
| | Init5 | Mean (ppb) | 2.72 | 2.09 | 7.46 | 5.47 | 8.68 | 6.06 |
| | | NMB (%) | -47.9 | -40.1 | -39.7 | 11.6 | -53.2 | -30.0 |
| | All Init | NMB var. (%) | 15.1 | 2.3 | 18.0 | 57.3 | 27.3 | 42.8 |
| Met IC & BC | Met5 | Mean (ppb) | 2.72 | 2.09 | 7.46 | 5.47 | 8.68 | 6.06 |
| | | NMB (%) | -47.9 | -40.1 | -39.7 | 11.6 | -53.2 | -30.0 |
| | Met6 | Mean (ppb) | 3.03 | 1.92 | 7.00 | 4.46 | 7.90 | 3.99 |
| | | NMB (%) | -42.0 | -45.0 | -43.5 | -9.0 | -57.3 | -53.9 |
| | All Met | NMB var. (%) | 5.9 | 4.9 | 3.7 | 20.6 | 4.2 | 23.9 |
| Hor. Res | Hor5 | Mean (ppb) | 2.72 | 2.09 | 7.46 | 5.47 | 8.68 | 6.06 |
| | | NMB (%) | -47.9 | -40.1 | -39.7 | 11.6 | -53.2 | -30.0 |
| | Hor5-12km | Mean (ppb) | 2.60 | 1.98 | 5.67 | 3.84 | 5.68 | 3.89 |
| | | NMB (%) | -50.2 | -43.3 | -54.2 | -21.6 | -69.4 | -55.1 |
| | All res. | NMB var. (%) | 2.3 | 3.2 | 14.4 | 33.3 | 16.2 | 25.1 |
| Emiss | Em7 | Mean (ppb) | 2.76 | 2.16 | 7.59 | 5.26 | 9.13 | 5.96 |
| | | NMB (%) | -47.1 | -38.1 | -38.6 | 7.3 | -50.8 | -31.2 |
| | Em8 | Mean (ppb) | 5.07 | 3.90 | 14.57 | 10.1 | 17.54 | 11.41 |
| | | NMB (%) | -2.9 | 11.7 | 17.6 | 106.1 | -5.5 | 31.8 |
| | All emiss | NMB var. (%) | 44.3 | 49.9 | 56.3 | 98.9 | 45.3 | 62.9 |

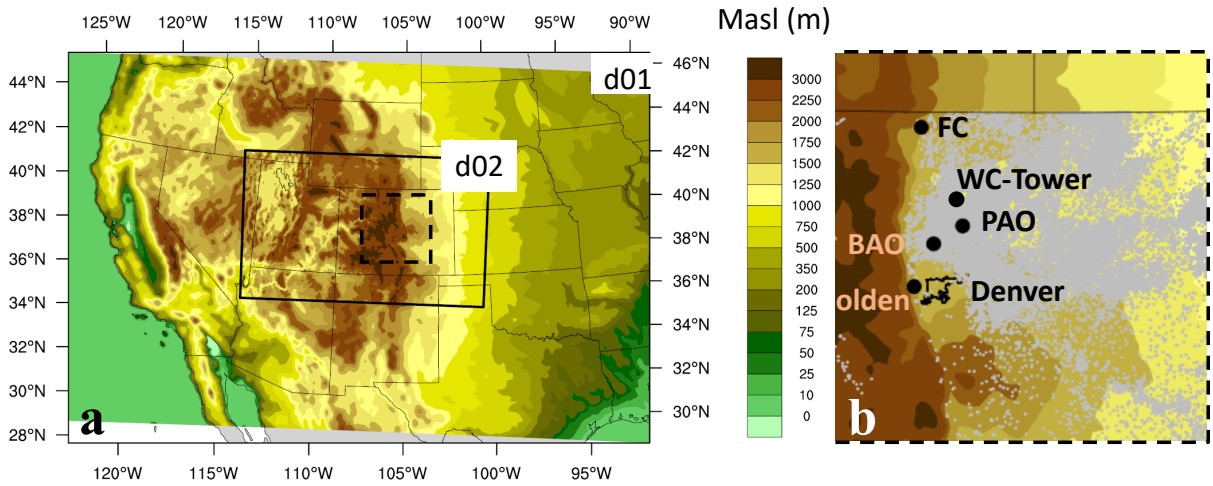


**Figure 1. Terrain map of the WRF-Chem outer domain (d01) and inner domains (d02) and location of observation sites. a) shows the two nested domains designed for this study. b) shows the zoomed in map of domain 2 with the location of several sites. Grey dots show the location of permitted wells (http://cogcc.state.co.us/)**

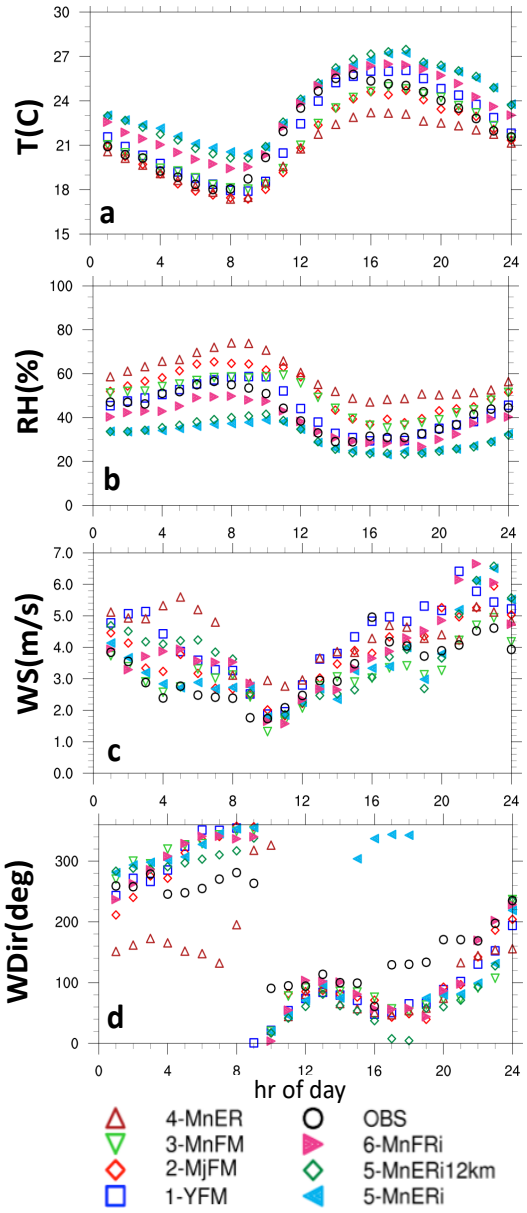


**Figure 2. Average diurnal cycle of temperature (a), relative humidity (b), wind speed (c) and wind direction (d) for all tests and observation at BAO 100m. Averages are calculated for Aug 1 to 15, 2014.**

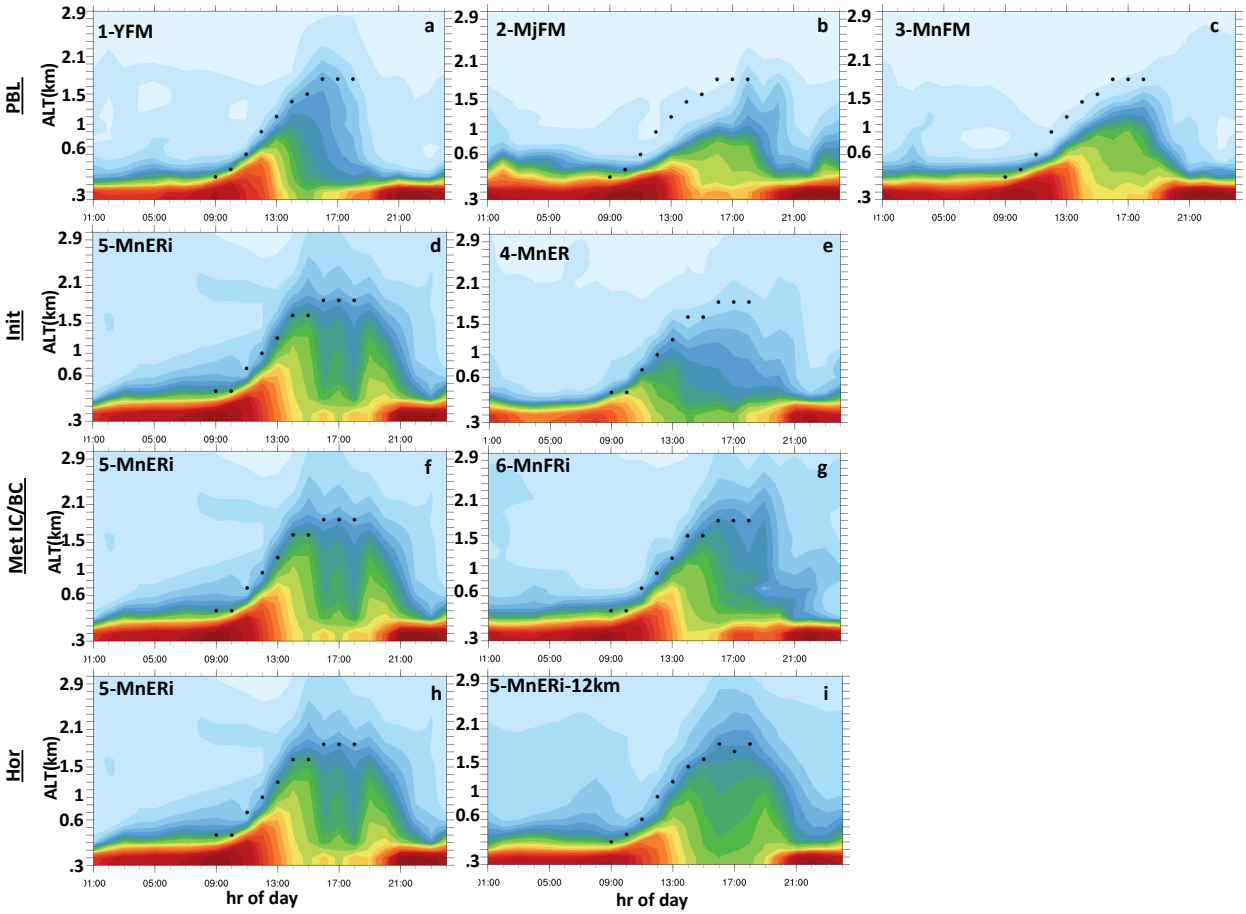


**Figure 3 Cross section of modeled ethane at PAO and measured PBL height (black dots) averaged from August 1 to 10, 2014 (a to i). j, k, and l show diurnal evolution of PBL in all simulations at PAO (j), Fort Collins (k), and Golden-NREL (l) sites and measured PBLH (during daytime).**

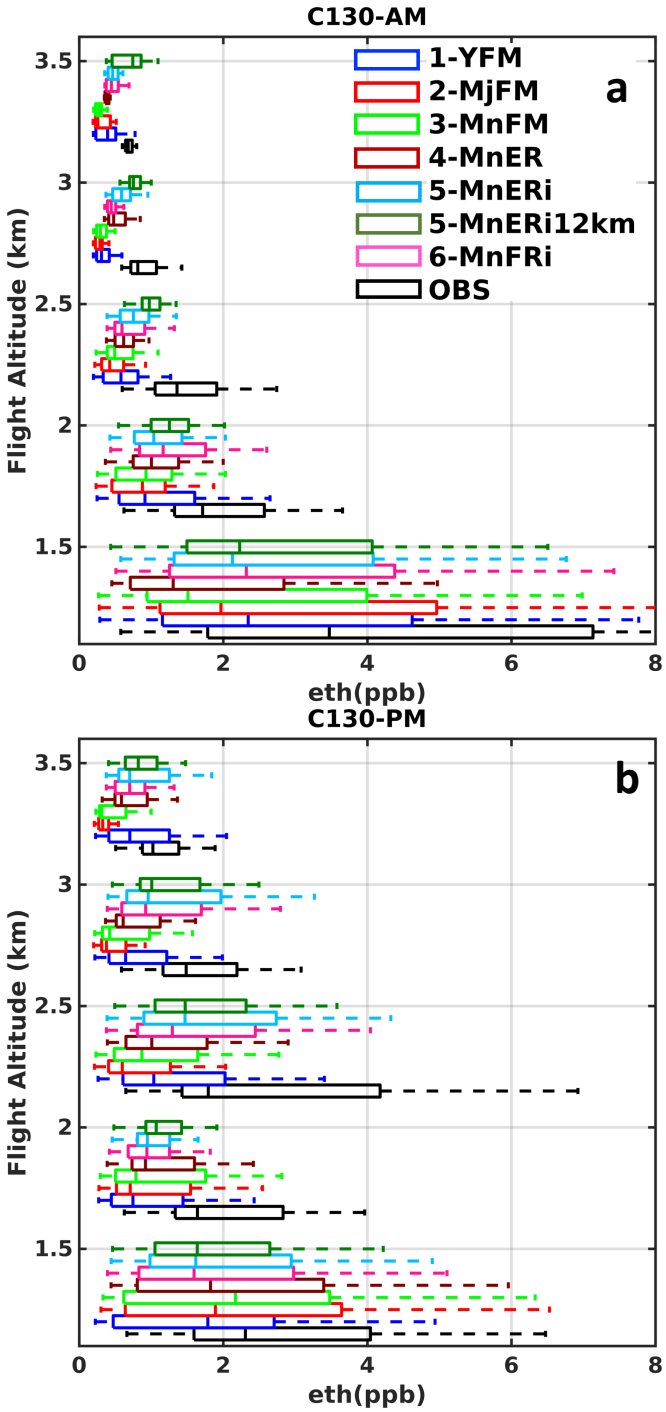


**Figure 4. Vertical distribution of simulated and measured ethane in the NFR area separated by the flight time. (a) C130-AM 9am to noon observation and the corresponding model values. (b) C130-PM noon to 6pm observation and the corresponding model values.**

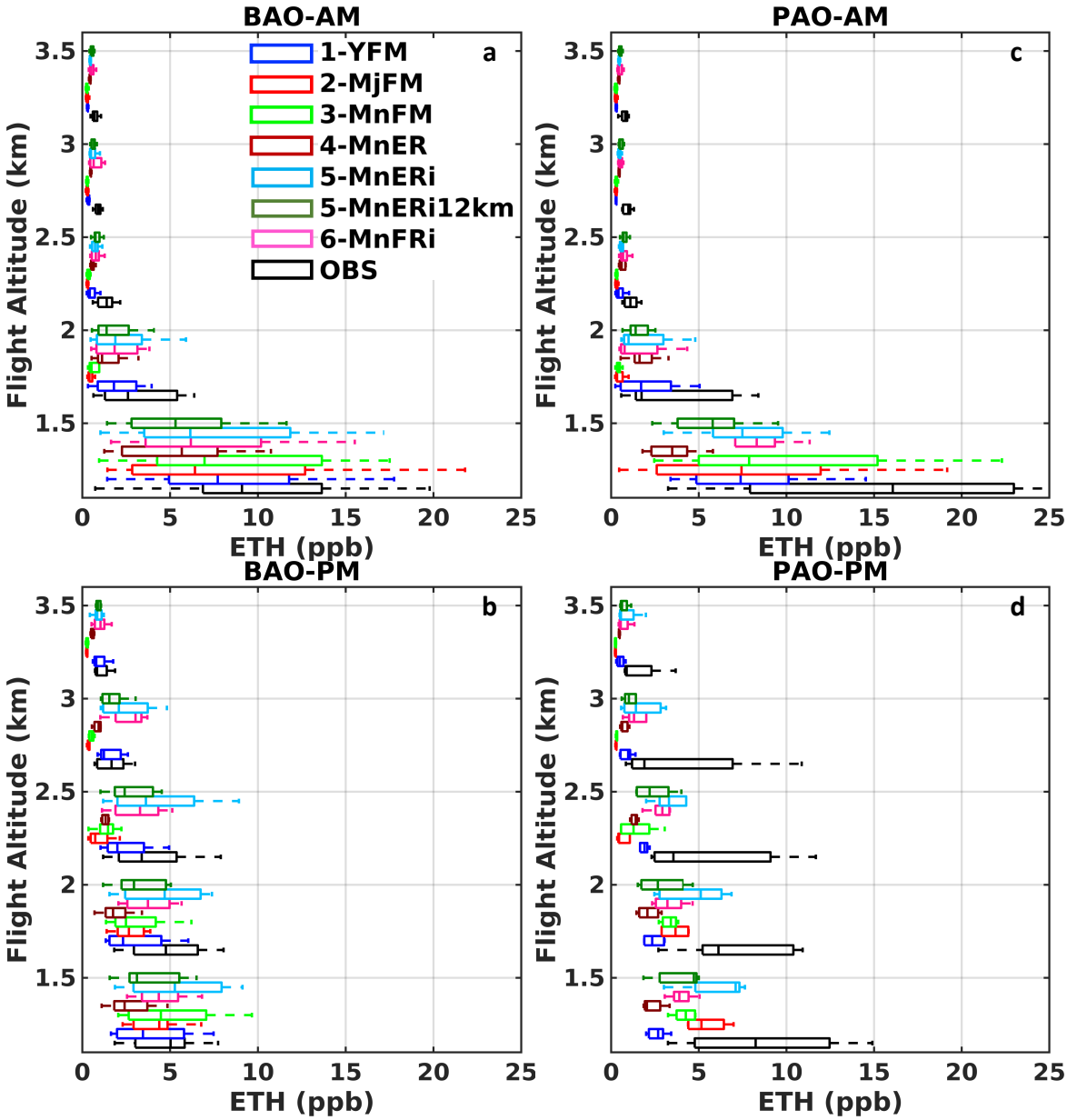


**Figure 5. Vertical distribution of ethane at PAO (a and b) and BAO (c and d) site measured during P3 spiral flights and the corresponding model values. Flights are separated by the flight time. a and c show P3-AM that include 9am to noon observation and the corresponding model values. b and d show P3-PM that include noon to 6pm observation and the corresponding model values.**

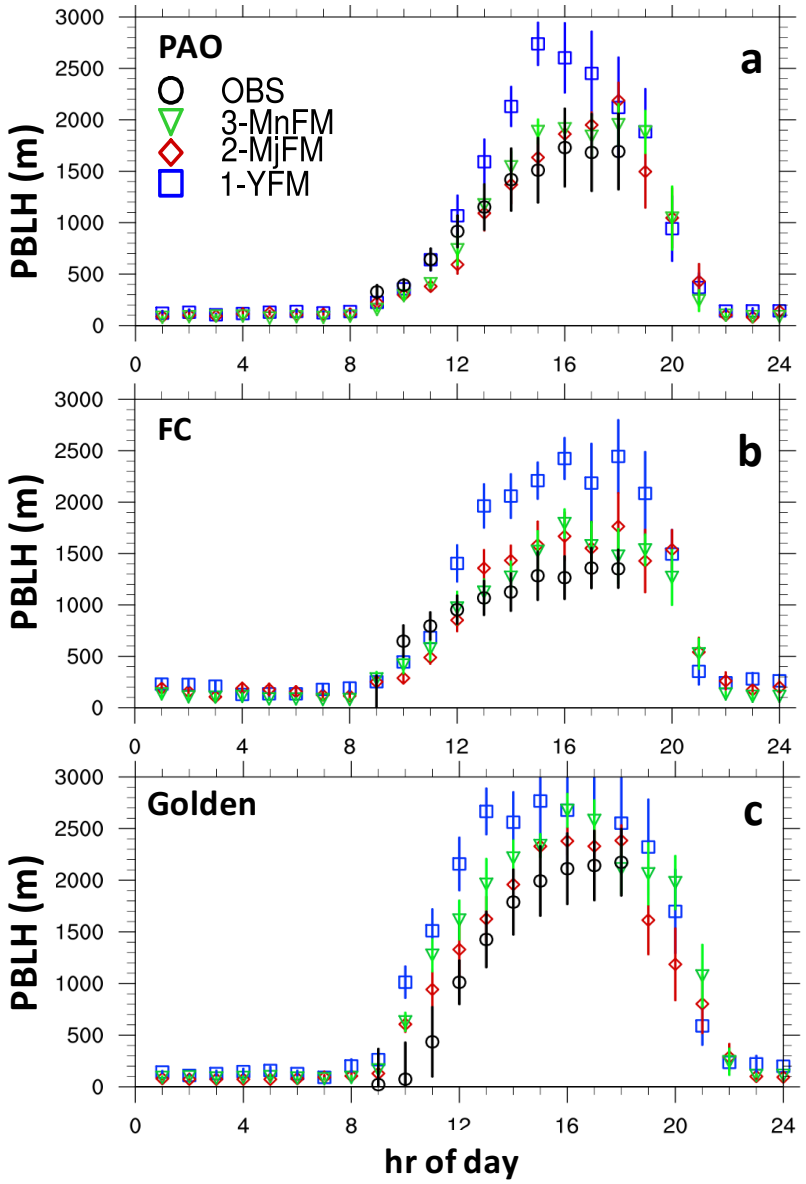


**Figure 6. Diurnal evolution of PBL in MYJ, MYNN3, and YSU schemes at PAO (a), Fort Collins (b), and Golden-NREL (c) sites. PBLH was measured using micro-pulse Lidar backscatter profiles during the daytime. Error bars represent the standard error.**

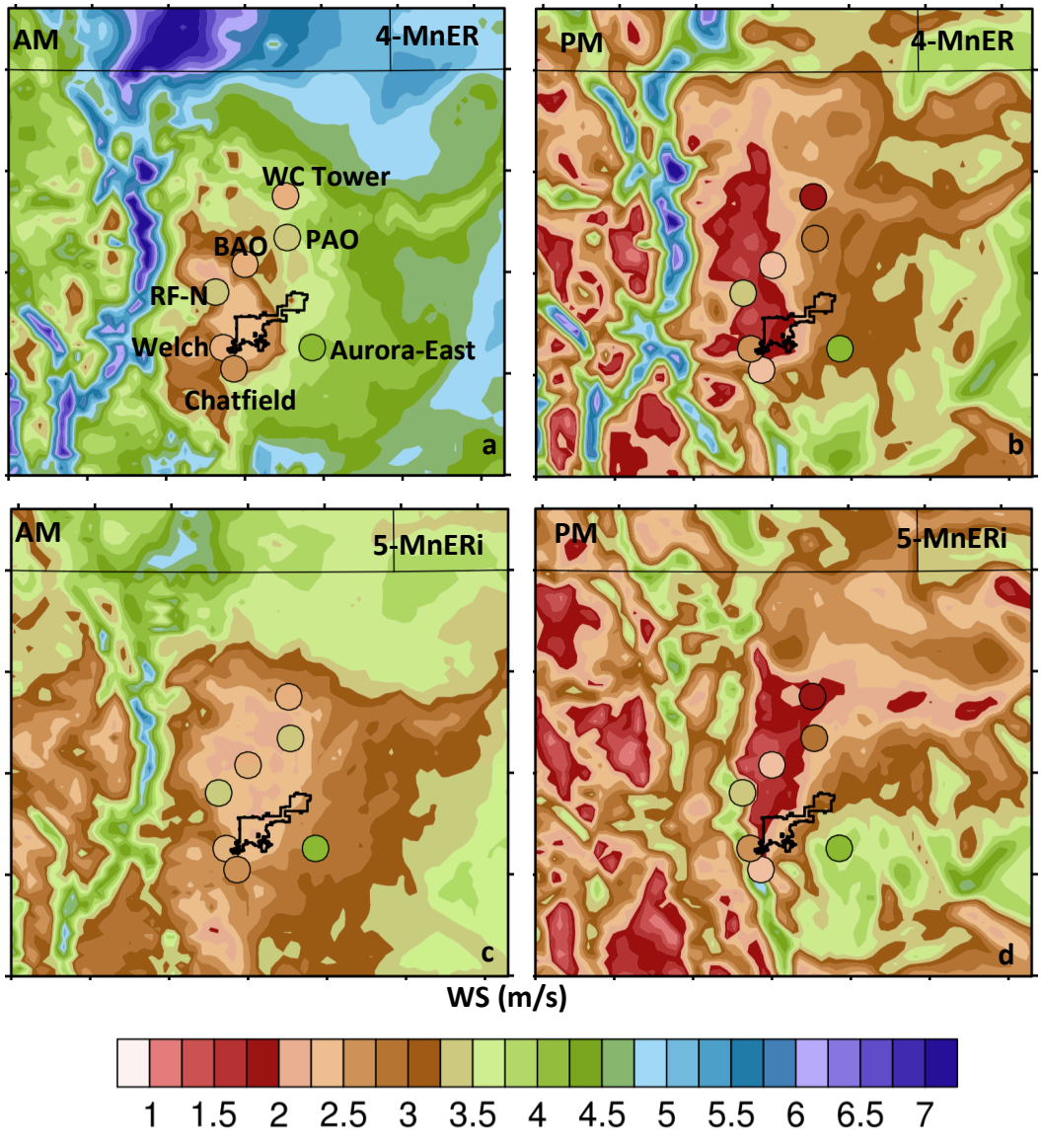


**Figure 7 Measured (circles) and modeled (color contour) wind speed at 10m captured by Init4 (a and b) and Init5 (c and d) from Aug 1 to 11, 2014 and separated by daytime vs nighttime.**

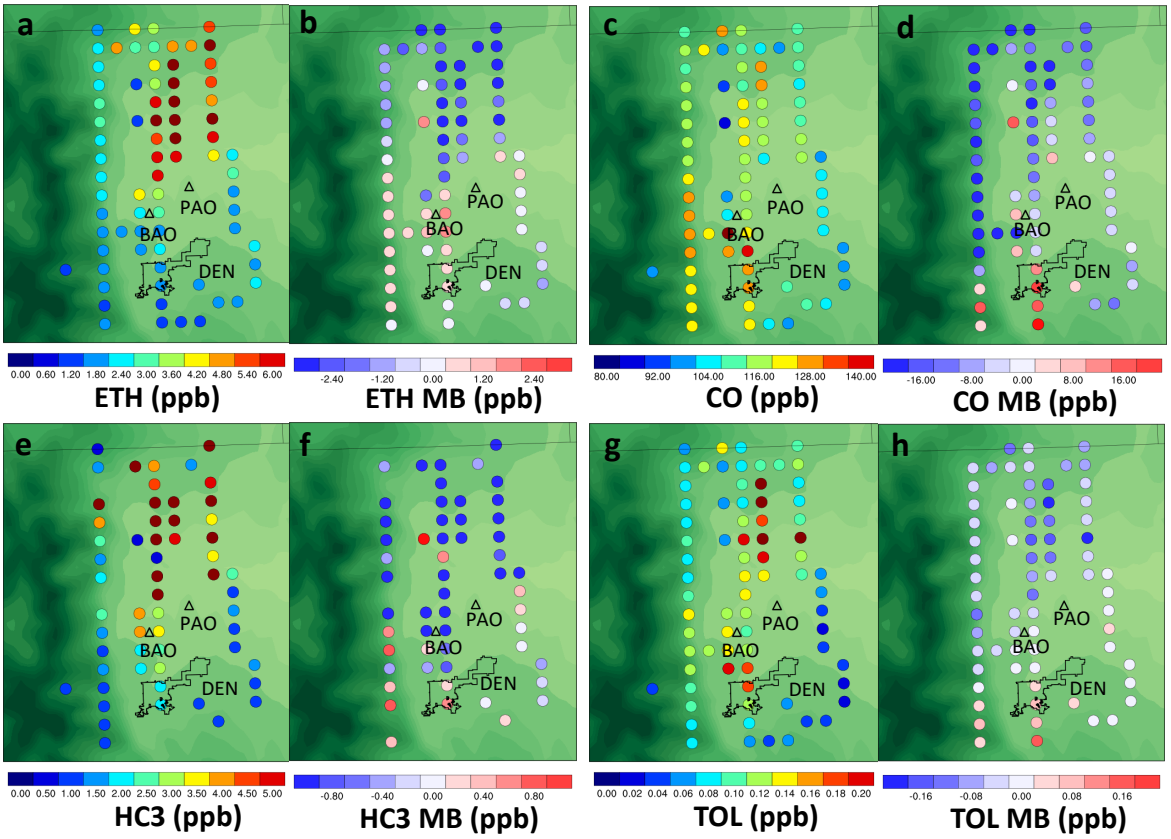


**Figure 8. Mean and mean bias ethane concentration (a and b), CO (c and d), HC3 (e and f), and TOL (g and h) along the C130 PM flights are limited to measurements below 2000m agl and grids with more than 4 measurement points. The outline of Denver county and the locations of BAO and PAO are marked on the underlying terrain map.**

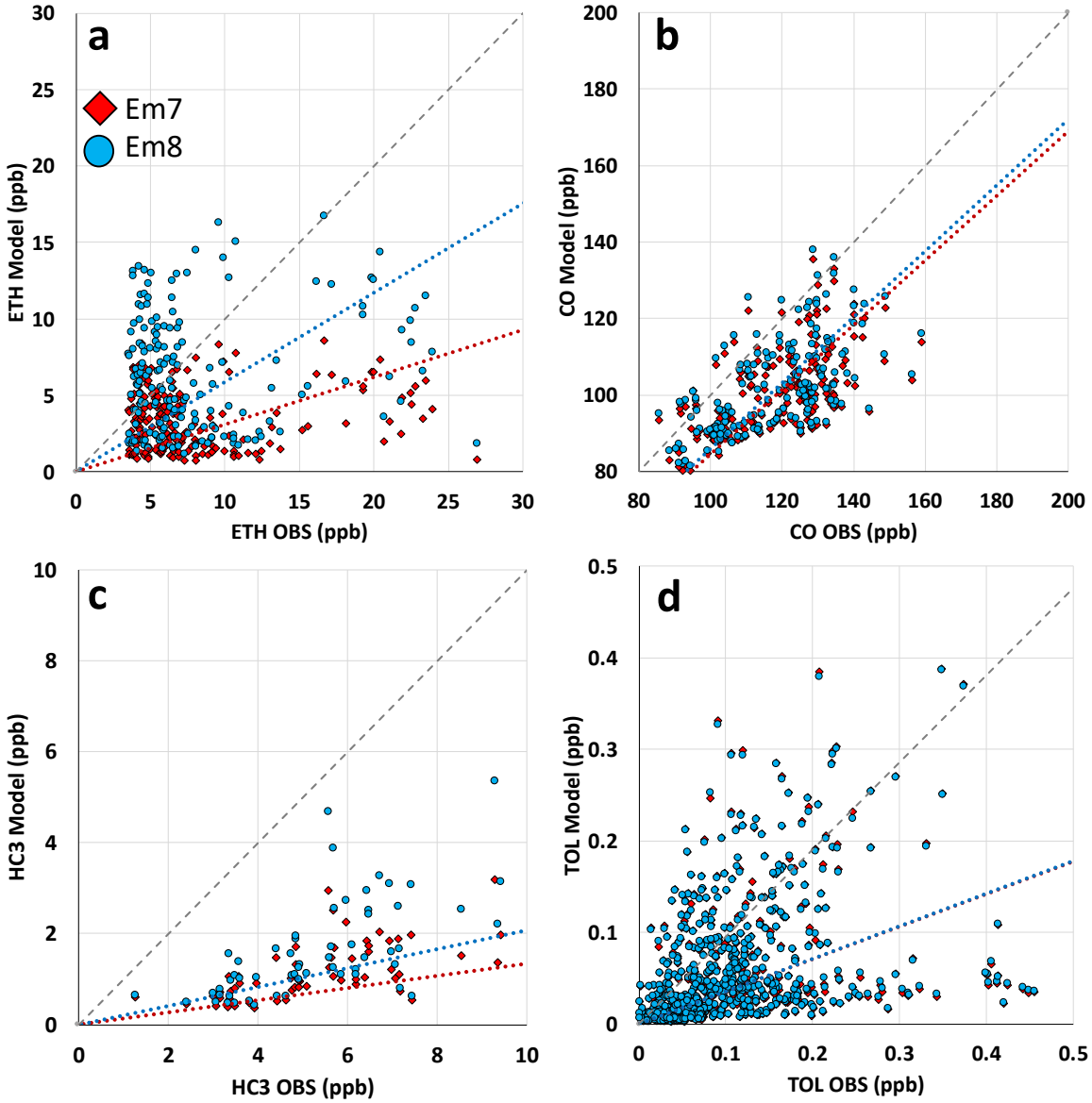


**Figure 9. Scatter plot of measured vs. corresponding model values of ethane (a), CO (b), HC3 (c), and TOL (d) along the C130 PM flights limited to measurements in the NFR and below 2000m. Red diamonds represent the Em7 (base emissions) and blue circles represent Em8 (perturbed emissions). Red and Blue lines show the best fit using least square linear regression method for Em7 and Em8, respectively.**

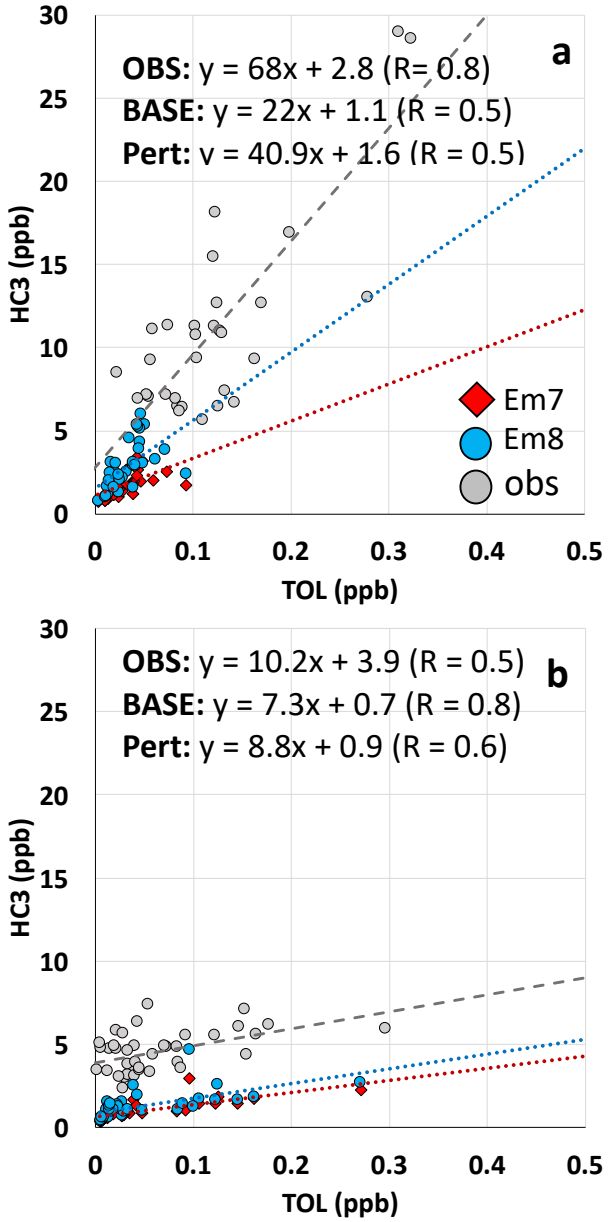


**Figure 10.Sscatter plot of HC3 vs. TOL concentrations along the C130 PM flights limited to measurements in the NFR and below 2000m altitude. Plot (a) shows HC3 vs. TOL (when measured ethane is greater than 2ppb) for measurements and the corresponding model values. Plot (b) shows HC3 vs. TOL (when measured ethane is less than 2ppb) for measurements and the corresponding model values. Grey circles represent measurements, red diamonds represent the Em7 (base emissions), and blue circles represent Em8 (perturbed emissions). Grey, Red and Blue lines show the best fit using least square linear regression method for observations, Em7 and Em8, respectively.**

S1. Definition of statistical measures

For quantitative comparison between the simulations we used statistical measures including correlation coefficient (R), root mean square error (RMSE), mean absolute error (MAE), mean bias (MB), and normalized mean bias (NMB). Definitions of these metrics can be found below:

$$R = \frac{\overline{(C_o - \overline{C_o})(C_p - \overline{C_p})}}{\sigma_{Cp}\sigma_{Co}} \tag{1}$$

$$RMSE = \sqrt{\frac{\sum_{i=1}^{n}\left(C_{p_i} - C_{o_i}\right)^2}{n}} \tag{2}$$

$$MAE = \frac{1}{n}\sum_{i=1}^{n}\left|C_{p_i} - C_{o_i}\right| \tag{3}$$

$$MB = \frac{1}{n}\sum_{i=1}^{n}\left(C_{p_i} - C_{o_i}\right) \tag{4}$$

$$NMB = \frac{\left(\overline{C_p} - \overline{C_o}\right)}{\overline{C_o}} \times 100\% \tag{5}$$

Where $C_o$ is the observation value, $C_p$ is the model value, σ is the standard deviation, $\bar{C}$ is the mean value, and n is total number of observation points

Table SM 1 Conversion table used to map species from NEI-2011 emission inventory to RACM chemical mechanism in and MADE/SORGAM aerosol module

| Emission inventory name | WRF-Chem name | Weight | Species name |
|---|---|---|---|
| CO | e_co | 1.00 | Carbon monoxide |
| NOX | e_no | 1.00 | Nitrogen Oxides (NO or NO2) |
| SO2 | e_so2 | 1.00 | Sulfur dioxide |
| NH3 | e_nh3 | 1.00 | Ammonia |
| HC01 | e_ch4 | 1.00 | Methane |
| HC02 | e_eth | 1.00 | Ethane kOH<500 /ppm/min |
| HC03 | e_hc3 | 1.00 | Alkane 500<kOH<2500 exclude(C3H8,C2H2,ethanol,acids) |
| HC04 | e_hc3 | 1.11 | Alkane 2500<kOH<5000 exlude(butanes) |
| HC05 | e_hc5 | 0.97 | Alkane 5000<kOH<10000 exlude(pentanes) |
| HC06 | e_hc8 | 1.00 | Alkane kOH>10000 exclude(ethylene glycol) |
| HC07 | e_ol2 | 1.00 | Ethylene |
| HC08 | e_olt | 1.00 | Alkene kOH <20000 /ppm/min |
| HC09 | e_oli | 1.00 | Alkene kOH >20000 /ppm/min exclude(dienes,styrenes) |
| HC10 | e_iso | 1.00 | Isoprene |
| HC12 | e_tol | 1.00 | Aromatic kOH <20000 /ppm/min exclude(benzene and toluene) |
| HC13 | e_xyl | 1.00 | Aromatic kOH >20000 /ppm/min exclude(xylenes) |
| HC14 | e_hcho | 1.00 | Formaldehyde |
| HC15 | e_ald | 1.00 | Acetaldehyde |
| HC16 | e_ald | 1.00 | Higher aldehydes |
| HC17 | e_ald | 1.00 | Benzaldehyde |
| HC18 | e_ket | 0.33 | Acetone |
| HC19 | e_ket | 1.61 | Methylethyl ketone |
| HC20 | e_ket | 1.61 | PRD2 SAPRAC species (aromatic ketones) |
| HC21 | e_hc3 | 0.40 | Methanol |
| HC22 | e_ald | 1.00 | Glyoxal |
| HC23 | e_ald | 1.00 | Methylglyoxal |
| HC24 | e_ald | 1.00 | Biacetyl |
| HC25 | e_csl | 1.00 | Phenols |
| HC26 | e_csl | 1.00 | Cresols |
| HC27 | e_ald | 0.50 | Methacrolein |
| HC27 | e_olt | 0.50 | Methacrolein |
| HC28 | e_ket | 0.50 | Methylvinyl ketone |

| | | | |
|---|---|---|---|
| HC28 | e_olt | 0.50 | Methylvinyl ketone |
| HC29 | e_ket | 1.00 | IPRD SAPRAC species (>C4 unsaturated aldehydes) |
| HC31 | e_ora2 | 1.00 | Acetic Acid |
| HC32 | e_ora2 | 1.00 | >C2 Acids (SAPRC PACD species) |
| HC33 | e_csl | 1.00 | Xylenols (SAPRC-11 species) |
| HC34 | e_csl | 1.00 | Catechols (SAPRC-11 species) |
| HC36 | e_olt | 1.00 | Propylene |
| HC37 | e_hc3 | 0.40 | Acetylene |
| HC38 | e_tol | 0.29 | Benzene |
| HC39 | e_hc3 | 1.11 | Butanes |
| HC40 | e_hc5 | 0.97 | Pentanes |
| HC41 | e_tol | 1.00 | Toluene |
| HC42 | e_xyl | 1.00 | m-Xylene |
| HC43 | e_xyl | 1.00 | p-Xylene |
| HC44 | e_xyl | 1.00 | o-Xylene |
| HC45 | e_hc3 | 0.57 | Propane |
| HC46 | e_oli | 1.00 | Dienes |
| HC47 | e_olt | 1.00 | Styrenes |
| HC47 | e_tol | 1.00 | Styrenes |
| HC48 | e_hc3 | 1.20 | Ethanol |
| HC49 | e_hc8 | 1.14 | Ethylene Glycol |
| PM01 | e_pm25i | 0.20 | Unspeciated primary PM2.5 - nuclei mode |
| PM01 | e_pm25j | 0.80 | Unspeciated primary PM2.5 - accumulation mode |
| PM02 | e_so4i | 0.20 | Sulfate PM2.5 - nuclei mode |
| PM02 | e_so4j | 0.80 | Sulfate PM2.5 - accumulation mode |
| PM03 | e_no3i | 0.20 | Nitrate PM2.5 - nuclei mode |
| PM03 | e_no3j | 0.80 | Nitrate PM2.5 - accumulation mode |
| PM04 | e_orgi | 0.20 | Organic Carbon PM2.5 - nuclei mode |
| PM04 | e_orgj | 0.80 | Organic Carbon PM2.5 - accumulation mode |
| PM05 | e_eci | 0.20 | Elemental Carbon PM2.5 - nuclei mode |
| PM05 | e_ecj | 0.80 | Elemental Carbon PM2.5 - accumulation mode |
| PM10-PRI | e_pm10 | 1.00 | Unspeciated Primary PM10 |

Table SM 2. Summary of model performance in capturing temperature at BAO 10m and 300m during Aug 1-15, 2014

| **T (C) - 10m** | **OBS** | **PBL** | | | **Met IC and BC** | | **Initialization** | | **Horizontal resolution** | |
|---|---|---|---|---|---|---|---|---|---|---|
| | | **PBL1** | **PBL2** | **PBL3** | **Met5** | **Met6** | **Init4** | **Init5** | **Hor5** | **Hor5-12km** |
| **Mean** | 21.67 | 22.40 | 20.95 | 21.20 | 24.06 | 23.44 | 21.59 | 24.06 | 24.06 | 24.08 |
| **R** | | 0.89 | 0.89 | 0.89 | 0.86 | 0.89 | 0.71 | 0.86 | 0.86 | 0.88 |
| **RMSE** | | 2.05 | 2.03 | 2.01 | 3.25 | 2.63 | 2.99 | 3.25 | 3.25 | 3.18 |
| **MAE** | | 1.56 | 1.62 | 1.59 | 2.60 | 2.05 | 2.30 | 2.60 | 2.60 | 2.53 |
| **MB** | | 0.74 | -0.72 | -0.46 | 2.40 | 1.77 | -0.08 | 2.40 | 2.40 | 2.41 |
| **NMB** | | 3.4% | -3.3% | -2.1% | 11.1% | 8.2% | -0.4% | 11.1% | 11.1% | 11.1% |
| **T (C) - 300m** | **OBS** | **PBL1** | **PBL2** | **PBL3** | **Met5** | **Met6** | **Init4** | **Init5** | **Hor5** | **Hor5-12km** |
| **Mean** | | 21.91 | 20.95 | 21.30 | 23.58 | 22.89 | 20.31 | 23.58 | 23.58 | 23.52 |
| **R** | | 0.76 | 0.75 | 0.72 | 0.74 | 0.78 | 0.57 | 0.74 | 0.74 | 0.75 |
| **RMSE** | | 2.16 | 2.14 | 2.10 | 2.79 | 2.27 | 3.09 | 2.79 | 2.79 | 2.80 |
| **MAE** | | 1.69 | 1.73 | 1.68 | 2.24 | 1.76 | 2.45 | 2.24 | 2.24 | 2.21 |
| **MB** | | 0.23 | -0.73 | -0.38 | 1.90 | 1.22 | -1.37 | 1.90 | 1.90 | 1.85 |
| **NMB** | | 1.1% | -3.4% | -1.8% | 8.8% | 5.6% | -6.3% | 8.8% | 8.8% | 8.5% |

Table SM 3. Summary of model performance in capturing relative humidity (RH) at BAO 10m and 300m during Aug 1-15, 2014

| RH (%)-10m | OBS | PBL | | | Met IC and BC | | Initialization | | Horizontal resolution | |
|---|---|---|---|---|---|---|---|---|---|---|
| | | **PBL1** | **PBL2** | **PBL3** | **Met5** | **Met6** | **Init4** | **Init5** | **Hor5** | **Hor5-12km** |
| **Mean** | 46.47 | 46.85 | 57.59 | 55.78 | 32.65 | 39.87 | 59.36 | 32.65 | 32.65 | 32.89 |
| **R** | | 0.78 | 0.69 | 0.73 | 0.63 | 0.64 | 0.53 | 0.63 | 0.63 | 0.71 |
| **RMSE** | | 10.89 | 16.90 | 15.13 | 19.13 | 14.95 | 22.33 | 19.13 | 19.13 | 18.15 |
| **MAE** | | 8.45 | 14.38 | 12.86 | 15.01 | 11.31 | 18.10 | 15.01 | 15.01 | 14.43 |
| **MB** | | 0.38 | 11.12 | 9.31 | -13.81 | -6.60 | 12.90 | -13.51 | -13.51 | -13.58 |
| **NMB** | | 0.8% | 23.9% | 20.0% | -29.7% | -14.2% | 27.7% | -29.7% | -29.7% | -29.2% |
| **RH (%)-300m** | **OBS** | **PBL1** | **PBL2** | **PBL3** | **Met5** | **Met6** | **Init4** | **Init5** | **Hor5** | **Hor5-12km** |
| **Mean** | 38.70 | 43.63 | 51.45 | 48.25 | 31.27 | 38.55 | 59.06 | 31.27 | 31.27 | 31.94 |
| **R** | | 0.64 | 0.59 | 0.48 | 0.53 | 0.52 | 0.41 | 0.53 | 0.53 | 0.57 |
| **RMSE** | | 13.06 | 17.92 | 15.25 | 12.66 | 11.14 | 28.39 | 12.66 | 12.66 | 12.11 |
| **MAE** | | 9.92 | 14.78 | 12.77 | 9.73 | 8.60 | 23.19 | 9.73 | 9.73 | 9.29 |
| **MB** | | 4.93 | 12.75 | 9.55 | -7.43 | -0.15 | 20.36 | -7.43 | -7.43 | -6.76 |
| **NMB** | | 12.7% | 32.9% | 24.7% | -19.2% | -0.4% | 52.6% | -19.2% | -19.2% | -17.5% |

Table SM 4 Summary of model performance in capturing wind speed and direction at BAO 10m during Aug 1-15, 2014

| | | | PBL | | | Met | | Init | | Horizontal Res. | |
|---|---|---|---|---|---|---|---|---|---|---|---|
| **Day - 10 m** | | **OBS** | **PBL1** | **PBL2** | **PBL3** | **Met5** | **Met6** | **Init4** | **Init5** | **Hor5** | **Hor5-12km** |
| Wind Speed | **Mean** | 2.46 | 2.99 | 2.68 | 2.20 | 2.63 | 2.83 | 3.30 | 2.63 | 2.63 | 2.58 |
| | **STD** | 1.25 | 1.47 | 1.55 | 1.27 | 1.41 | 1.51 | 2.02 | 1.41 | 1.41 | 1.33 |
| Wind Direction | **Mean** | 123.38 | 64.31 | 71.92 | 74.85 | 38.63 | 70.83 | 61.40 | 38.63 | 38.63 | 45.08 |
| | **STD** | 66.06 | 45.40 | 62.30 | 54.02 | 73.77 | 75.30 | 75.65 | 73.77 | 73.77 | 66.18 |
| **Night - 10 m** | | **OBS** | **PBL1** | **PBL2** | **PBL3** | **Met5** | **Met6** | **Init4** | **Init5** | **Hor5** | **Hor5-12km** |
| Wind Speed | **Mean** | 2.25 | 2.81 | 2.58 | 2.18 | 2.51 | 2.72 | 2.91 | 2.51 | 2.51 | 2.66 |
| | **STD** | 0.96 | 1.41 | 0.94 | 0.96 | 1.35 | 1.43 | 1.40 | 1.35 | 1.35 | 1.41 |
| Wind Direction | **Mean** | 222.98 | 244.07 | 243.95 | 263.07 | 226.97 | 230.93 | 160.02 | 226.97 | 226.97 | 295.43 |
| | **STD** | 50.01 | 90.68 | 69.52 | 74.66 | 83.89 | 69.81 | 87.15 | 83.89 | 83.89 | 87.30 |

Table SM 5 Summary of model performance in capturing wind speed and direction at BAO 300m during Aug 1-15, 2014

| | | | PBL | | | Met | | init | | Horizontal Res. | |
|---|---|---|---|---|---|---|---|---|---|---|---|
| **Day - 300 m** | | **OBS** | **PBL1** | **PBL2** | **PBL3** | **Met5** | **Met6** | **Init4** | **Init5** | **Hor5** | **Hor5-12km** |
| Wind Speed | Mean | 3.23 | 3.89 | 3.51 | 2.78 | 2.88 | 3.22 | 3.83 | 2.88 | 2.88 | 2.77 |
| | STD | 2.24 | 2.15 | 2.39 | 1.61 | 1.58 | 1.81 | 2.93 | 1.58 | 1.58 | 1.47 |
| Wind Direction | Mean | 117.31 | 62.69 | 62.42 | 64.05 | 32.91 | 57.67 | 56.71 | 32.91 | 32.91 | 39.52 |
| | STD | 74.56 | 51.99 | 63.89 | 59.84 | 75.14 | 76.03 | 74.32 | 75.14 | 75.14 | 69.43 |
| **Night - 300 m** | | | **PBL1** | **PBL2** | **PBL3** | **Met5** | **Met6** | **Init4** | **Init5** | **Hor5** | **Hor5-12km** |
| Wind Speed | Mean | 3.42 | 5.00 | 4.34 | 3.80 | 4.21 | 4.60 | 5.07 | 4.21 | 4.21 | 4.89 |
| | STD | 2.59 | 2.68 | 2.95 | 2.64 | 2.64 | 2.47 | 3.07 | 2.64 | 2.64 | 3.29 |
| Wind Direction | Mean Model | 213.59 | 141.12 | 223.36 | 355.95 | 326.05 | 294.02 | 156.88 | 326.05 | 326.05 | 306.58 |
| | STD Model | 72.73 | 98.36 | 93.80 | 91.39 | 91.33 | 77.67 | 84.60 | 91.33 | 91.33 | 88.31 |

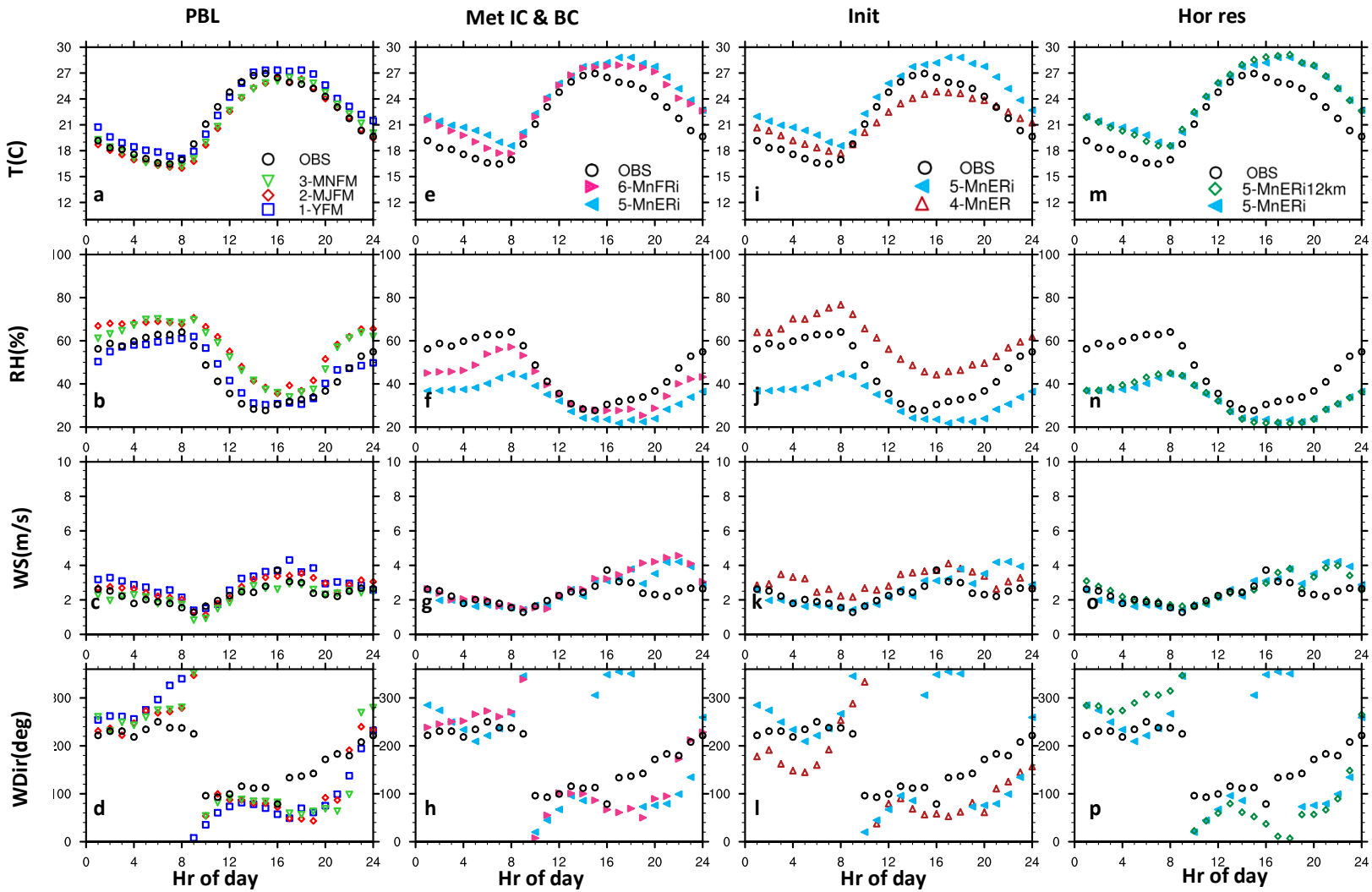


Figure SM 1 Average diurnal cycle of temperature, relative humidity, wind speed, and wind direction for all test sets and observation at BAO 10m. Averages are calculated for Aug 1 to 15, 2014

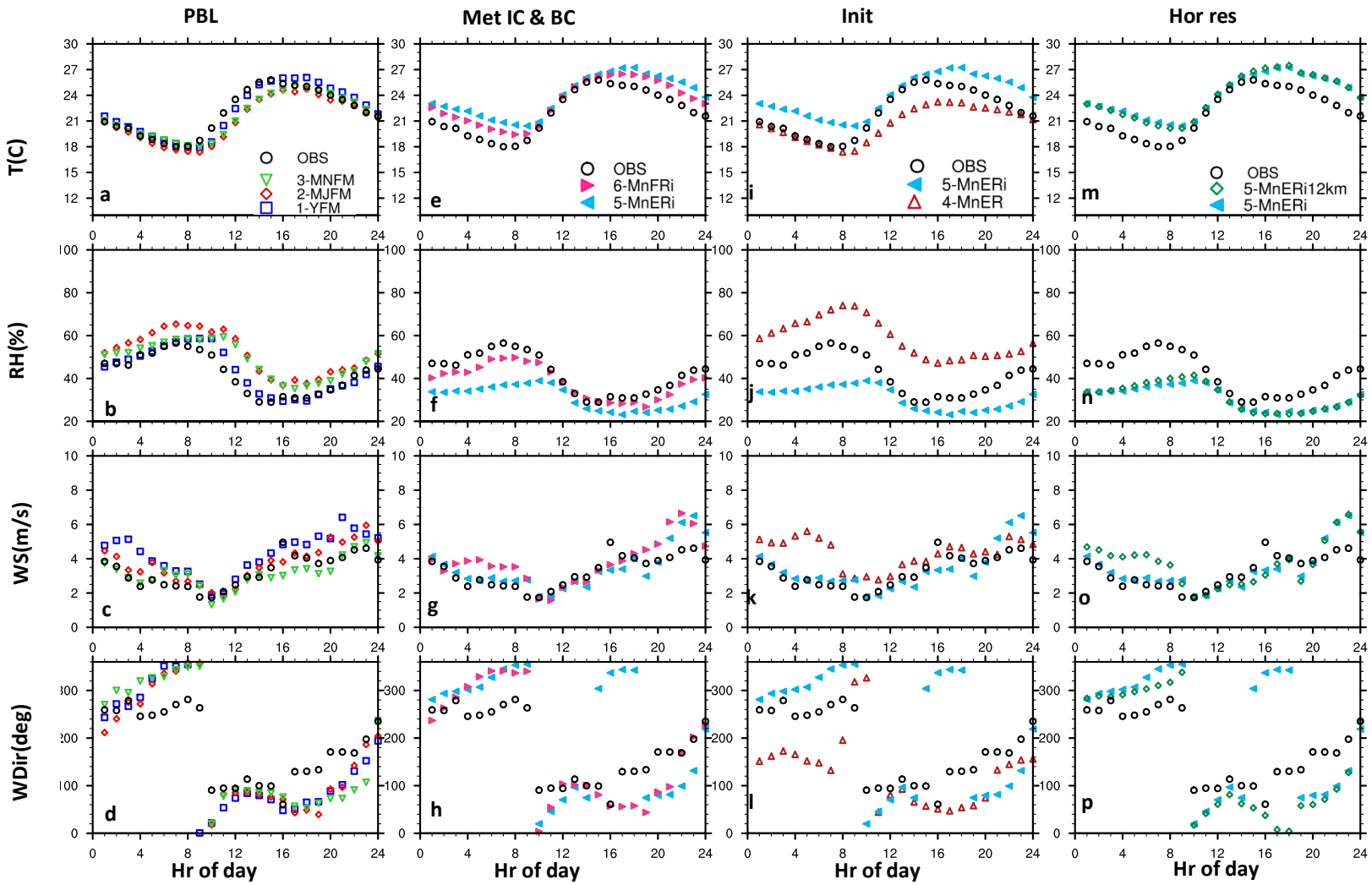


Figure SM 2 Average diurnal cycle of temperature, relative humidity, wind speed, and wind direction for all test sets and observation at BAO 100m. Averages are calculated for Aug 1 to 15, 2014

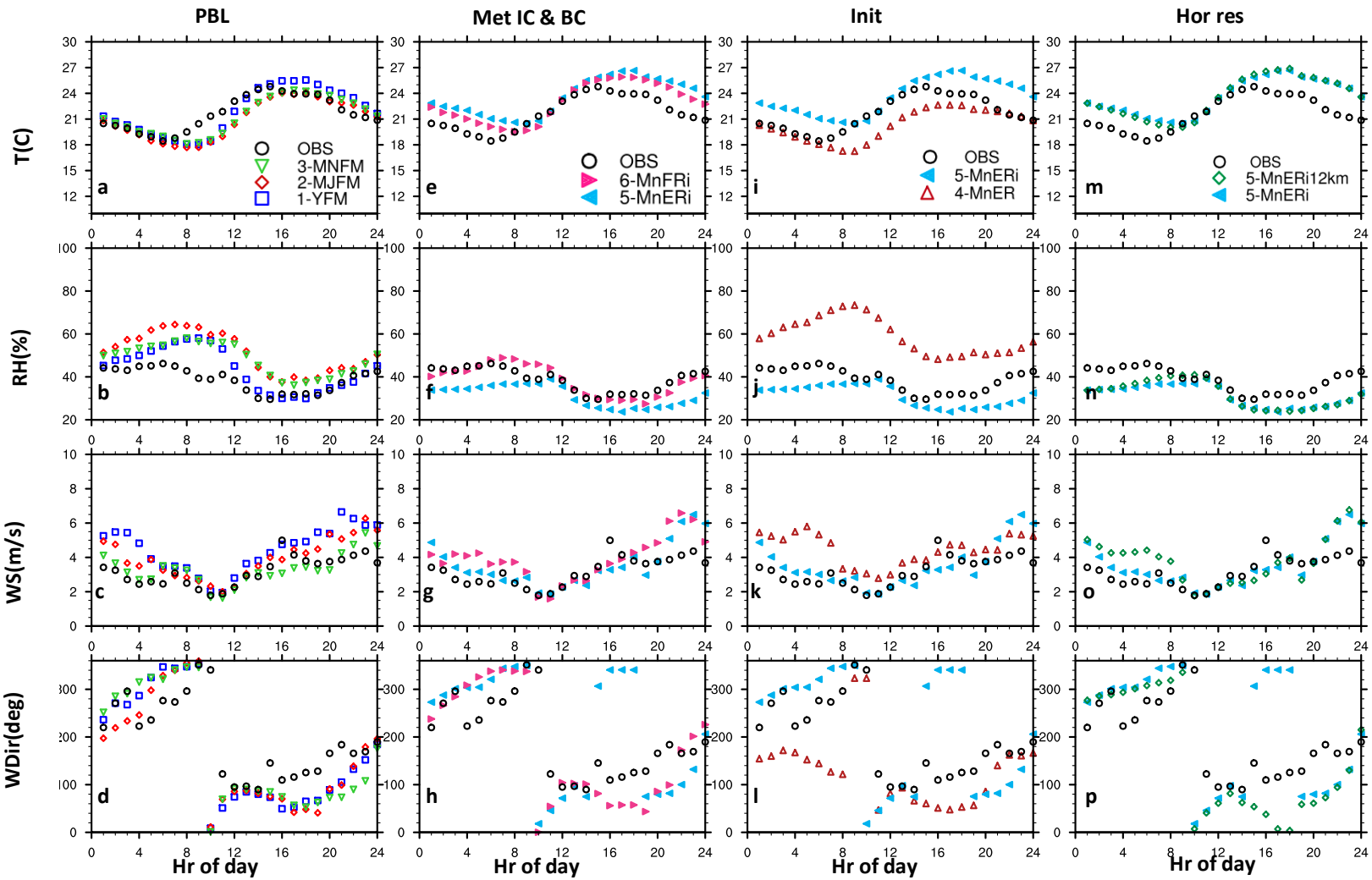


Figure SM 3 Average diurnal cycle of temperature, relative humidity, wind speed, and wind direction for all test sets and observation at BAO 300m. Averages are calculated for Aug 1 to 15, 2014

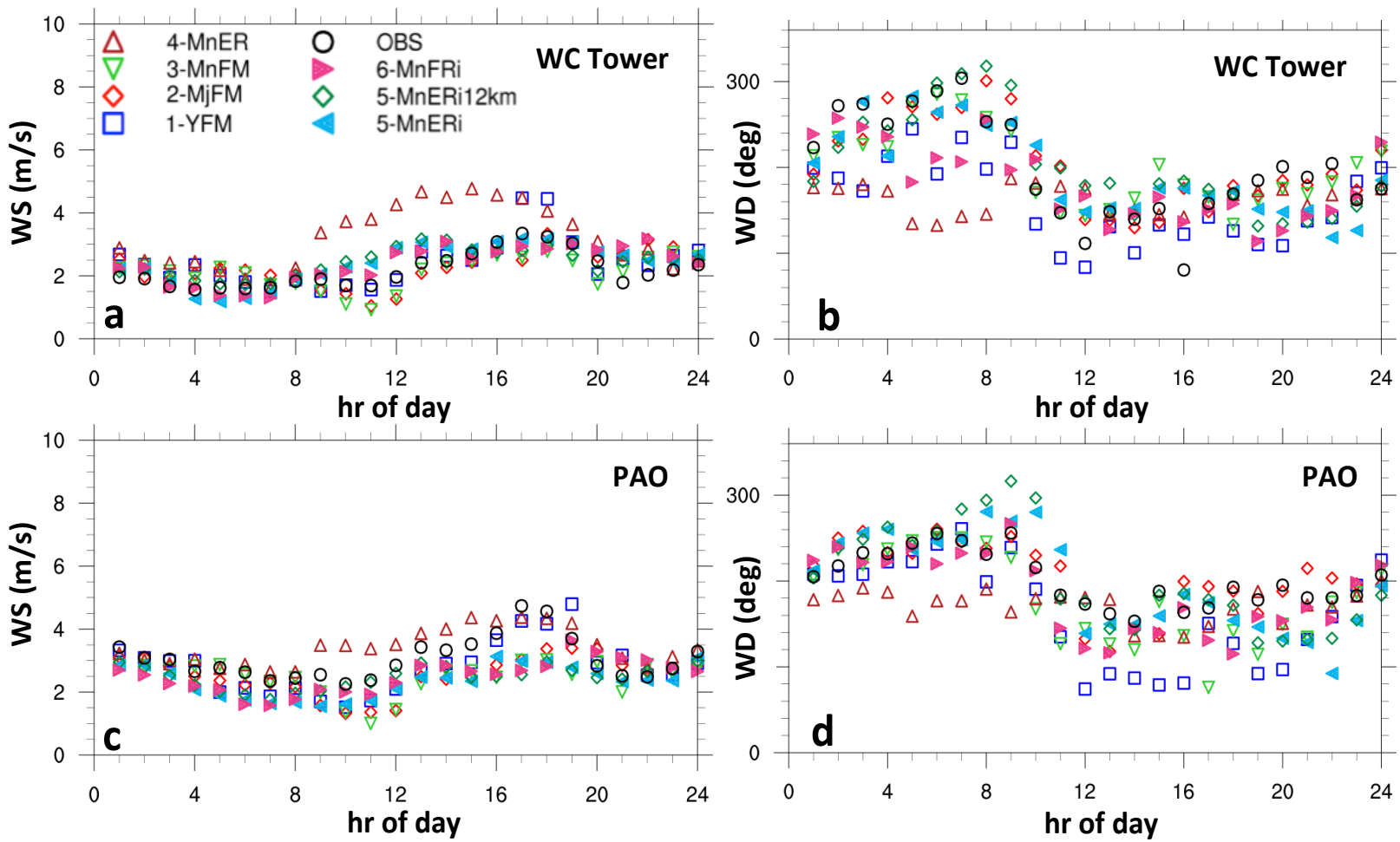


Figure SM 4. Average diurnal cycle of wind speed (WS) and direction (WD) at WC Tower and PAO sites. Averages are calculated for August 1 to 11, 2014

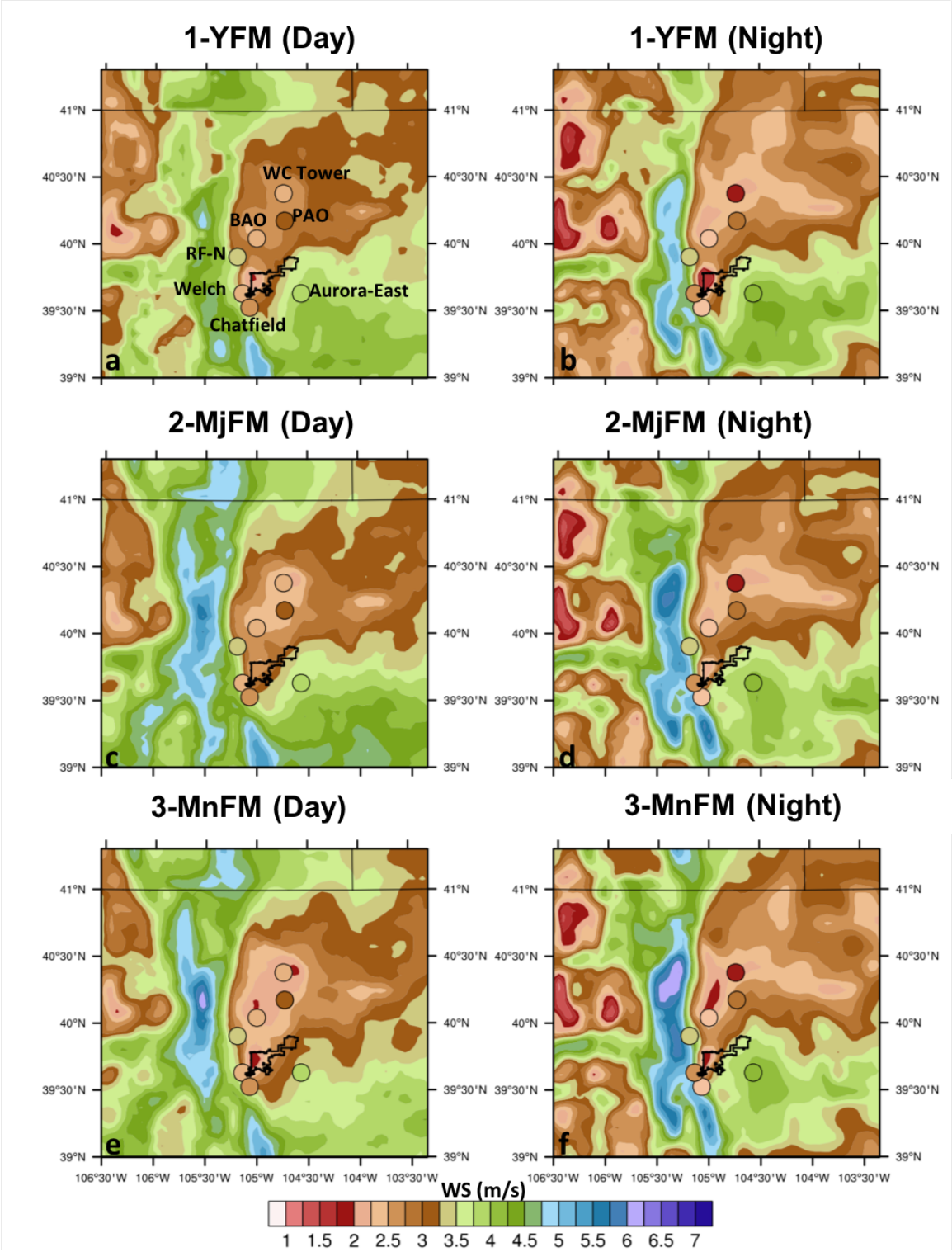


Figure SM 5 Wind speed at 10m captured by different PBL schemes. averaged from 1-August to 11-August 2014

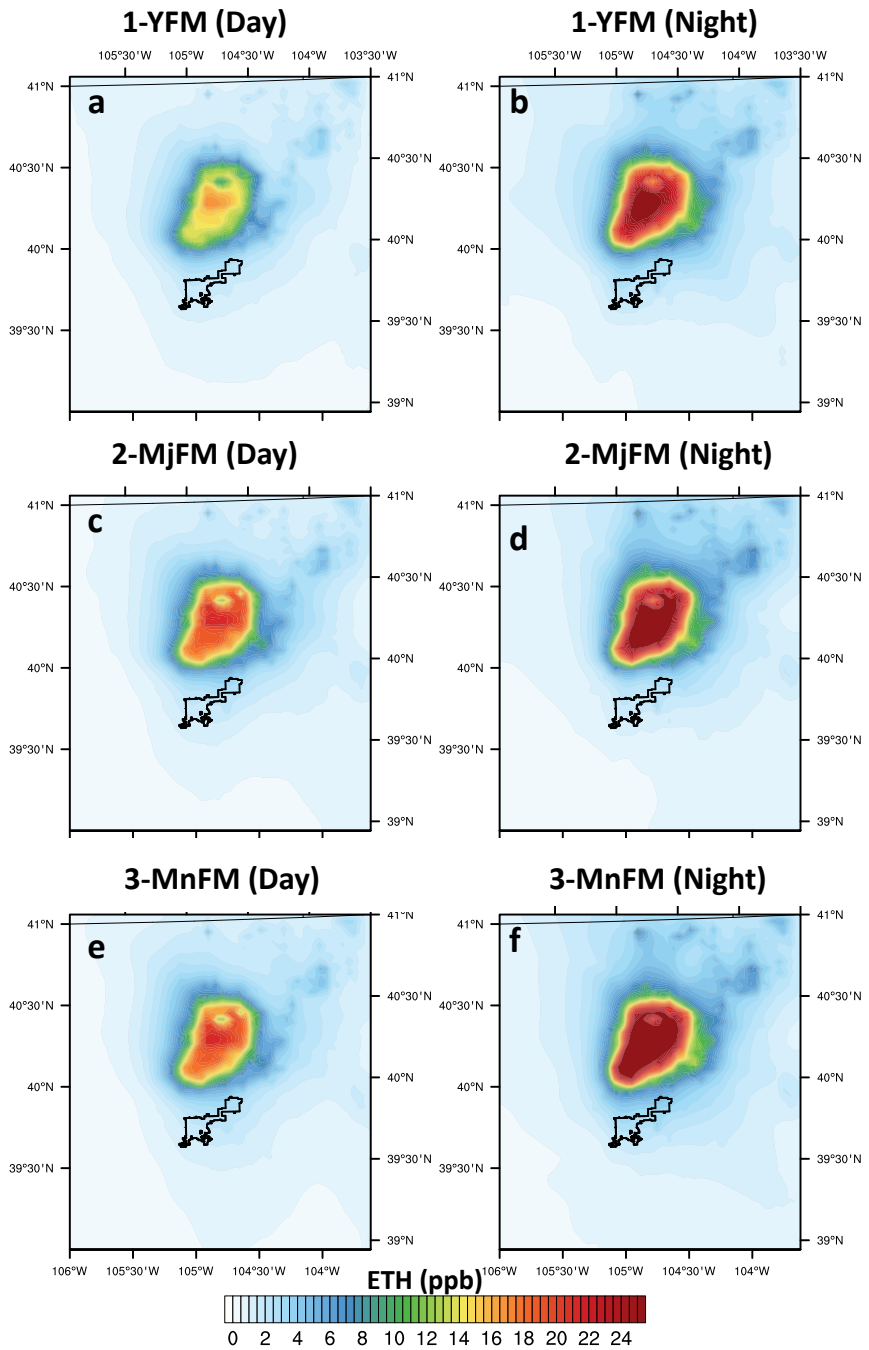


Figure SM 6. Surface ethane in sim 1 (1-YFM), sim 2 (2-MjFM), sim 3 (3-MnFm) averaged from August 1 to 15, 2014

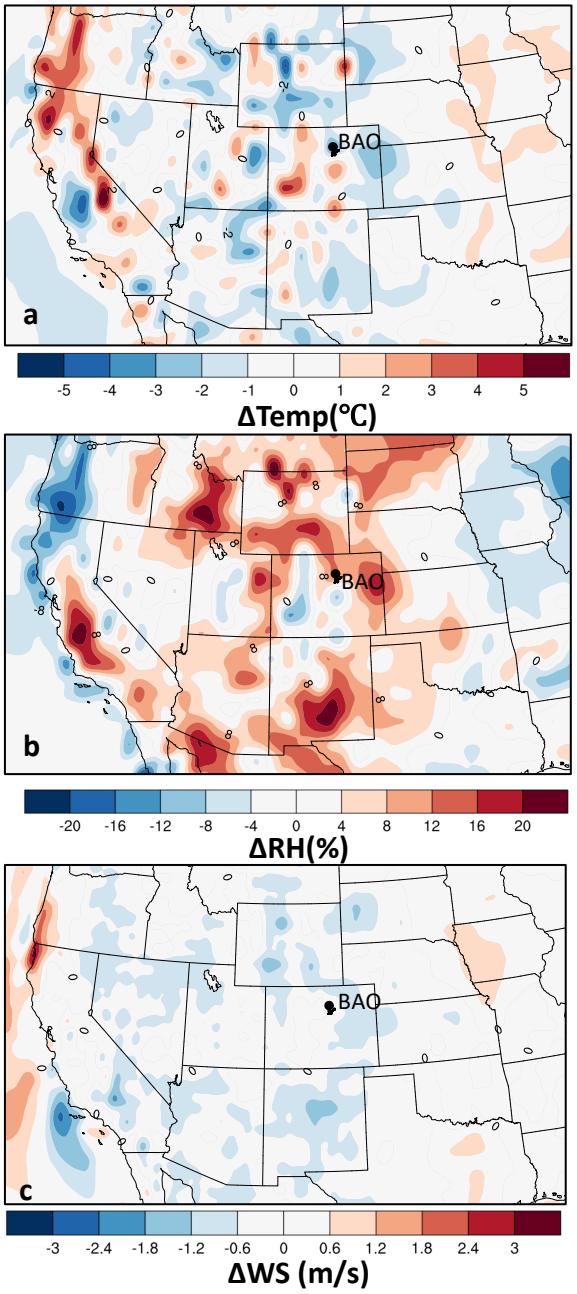


Figure SM 7 Differences in temperature (a), relative humidity (b), and wind speed (c) between ERA-interim and NCEP-FNL global models (Δx = X(ERA-interim) – X(NCEP-FNL)) averaged from Aug 1 to 15, 2014 using 6-hourly data

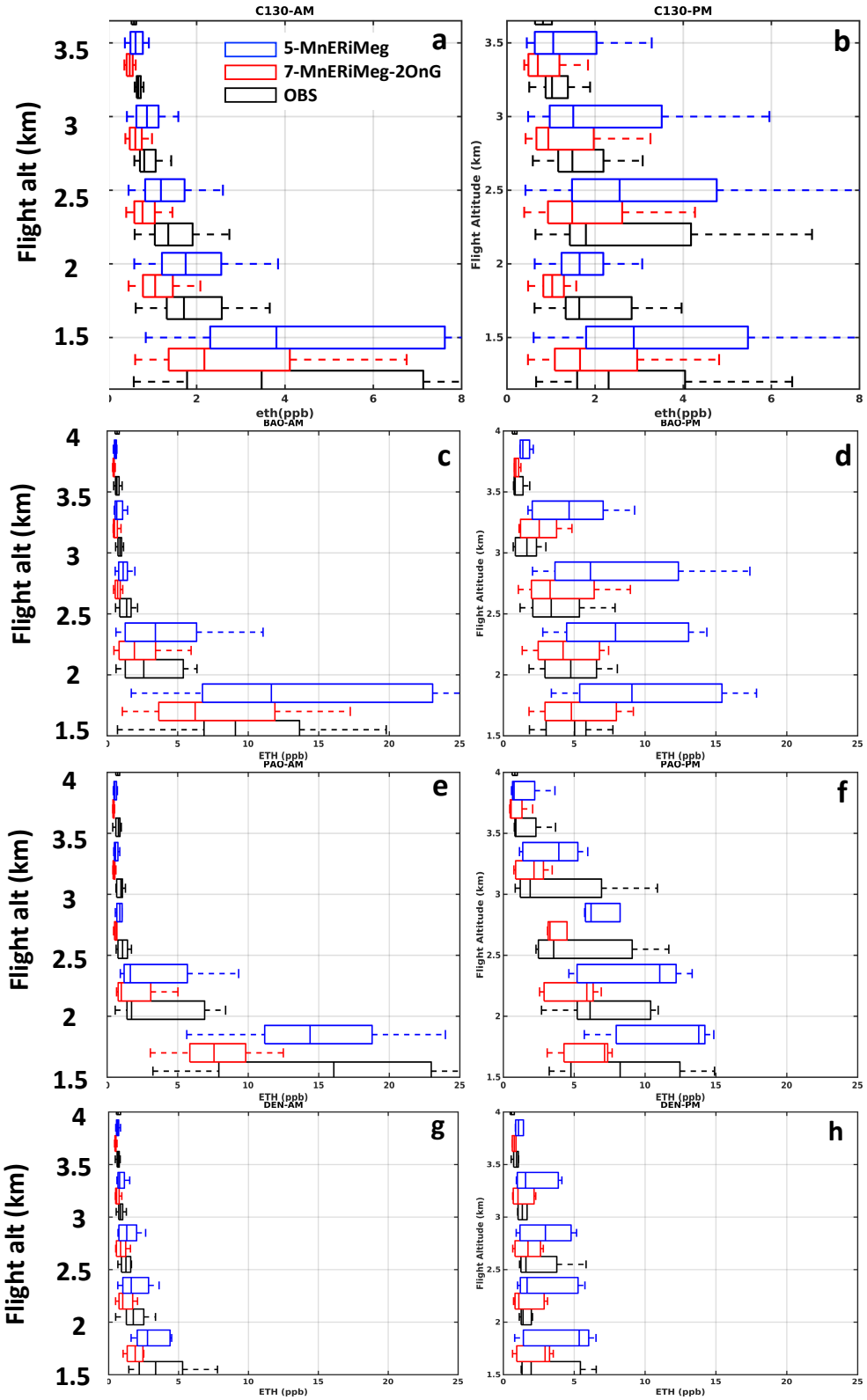


Figure SM 8. Sensitivity of ethane to oil and NG emission during C130-AM (a), C130-PM (b), P3-PAO AM (d), P3-PAO PM (c), P3-BAO AM (e), P3-BAO PM (f) averaged for August flights